COASTAL ENGINEERING IN JAPAN

VOL. 2

1959

COMMITTEE OF COASTAL ENGINEERING,
JAPAN SOCIETY OF CIVIL ENGINEERS

Price ¥ 300. (including domestic mail fare)

PREFACE

The year of 1959 marked an epoch to be remembered by the coastal engineers in Japan for a new record of storm surge damage took place in the central part of the Japanese coast. The significance of coast protection was again manifested to this country where the coastal regions are highly utilized for industries and other productive activities as well as habitation. Thus numerous new subjects have been added to the field of coastal engineering which has only a short history in this country.

Our intention in publishing the series of "Coastal Engineering in Japan" is to promote the researches and practices of this field of engineering through discussions from overseas and to reinforce exchange of knowledge between Japan and foreign countries.

This volume contains the papers published in 1957 to 1958.

Masashi Hom-ma

Chairman
Committee of Coastal Engineering
Japan Society of Civil Engineers
Tokyo, Japan

November, 1959

TABLE OF CONTENTS

PAGE

ON THE OCEAN WAVES DUE TO TROPICAL CYCLONES.
By S. Unoki. 1

THE POSSIBLE HIGHEST GRAVITY WAVES IN SHALLOW WATER.
By T. Kishi. 9

FIELD INVESTIGATION OF WAVE FORCES ON BREAKWATER.
By T. Kuribayashi, Y. Muraki and G. Udai 17

LABORATORY STUDY OF SAND MOVEMENT AND EQUILIBRIUM PROFILES OF BEACHES.
By K. Shinohara and T. Tsubaki 29

FUNDAMENTAL STUDIES ON THE DYNAMICS OF SAND DRIFTS (Report 1 and 2).
By T. Ishihara, T. Sawaragi and T. Amano 35

FIELD INVESTIGATION OF SUSPENDED SEDIMENT BY THE USE OF BAMBOO SAMPLERS.
By H. Fukushima and M. Kashiwamura 53

THE MEASUREMENT OF LITTORAL DRIFT AT SHORELINE HARBORS.
By N. Shiraishi 59

SHAPES OF SHORE STRUCTURES (DIKES) AND ITS DAMPING EFFECT FOR WAVE FORCES.
By J. Kato 73

THE EFFECTS OF COASTAL STRUCTURES ON THE LITTORAL SAND DRIFTS.
By S. Adachi, T. Sawaragi and A. Ogo 85

ARRANGEMENT OF GROINS ON A SANDY BEACH.
By S. Nagai. 99

MOTION OF SAND PARTICLES BETWEEN GROINS.
By S. Nagai and H. Kubo. 99

THE SHOCK PRESSURES EXERTED BY BREAKING WAVES ON BREAKWATERS.
By S. Nagai. 100

AN EXPERIMENTAL STUDY ON THE SUBMERGED BREAKWATER.
By M. Hom-ma and T. Sakou 103

THE CONSTRUCTION OF A LIGHTED BEACON ON A REEF IN THE OPEN SEA.
By Y. Fujino 111

ON THE OCEAN WAVES DUE TO TROPICAL CYCLONES

Sanae Unoki, Dr. Sc., Oceanographical Laboratory,
Meteorological Research Institute, Tokyo

1. Preface

An attempt to clarify the structure of ocean waves in tropical cyclones such as typhoons and hurricanes has seldom been made because it is extremely difficult to take an exact and systematic wave-observation over an extensive sea covered by mountaineous waves. In the meanwhile, the theory of ocean wave forecast has made considerable progress recently, but it is not yet satisfactorily powerful for our problems, in which the speed and direction of wind change rapidly with time and place.

Under such circumstances, the present author has investigated the distribution of wave height, period and other elements in typhoons on the basis of plentiful wave materials obtained by visual observations from weather ships and military planes for about one hundred typhoons. In this paper, however, the outline of the results will be given since the full discussion was already made in other journals (see references). Moreover, it is hoped that these results will be amended with further accumulation of exact data, because both quality and quantity of our wave materials remain still insufficient, particularly in the vicinity of the storm center. The wave height and period observed are those of prevailing waves which may correspond roughly to significant waves.

2. Distribution of wave height

Fig-1 shows an example of mean distribution of wave heights. The most remarkable feature is the asymmetry of height - distribution to the storm center, that is, the wave height is greatest in the right rear quadrant of the storm as pointed out by Cline (1926) and other investigators and smallest in the left front quadrant. This is attributed to the following conditions: (1) Winds blow with greater velocity in the right or dangerous semi-circle than in the left or navigable semi-circle. (2) In the right semi-circle waves move in a direction near to that of movement of the storm, therefore, the fetch and

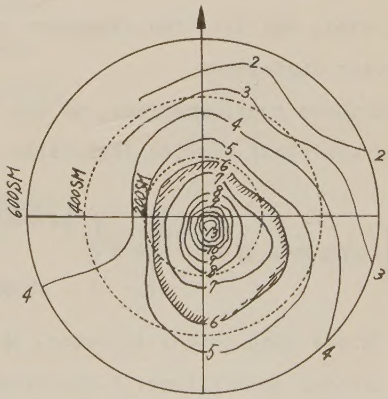

Fig-1 Mean distribution map of wave height (in meter) due to a typhoon whose central pressure is 940 ~ 960 mb.

duration of winds become longer than in the left semi-circle. (3) In the rear semi-circle we can usually find remarkable swells which were originated in the front semi-circle and were left behind, consequently, wind waves generated in the rear are superposed on and raised by these swells.

On the other hand, the distribution of waves depends remarkably on the speed of typhoon (C). Hereafter, the term "wave velocity" is always used in a sense of "group velocity" because it could be ascertained that swells sent out from a typhoon travel with the group velocity of deep water wave as theory demands. When the storm is slower than the usual wave (Fig-2a, $C < 20$ km/hr), the area of rough sea is wider in the right semi-circle than in the left semi-circle. On the contrary, when the storm is faster than the wave (Fig-2c, $C > 40$ km/hr), the wave is remarkably rougher in the rear semi-circle than in the front semi-circle since the wave arisen in the latter region is left in the former region. When the velocity of storm is near to that of wave (Fig-2b, C: 20~40 km/hr) the wave develops most conspicuously on account of the increase of duration and fetch of wind, and also the asymmetry of wave-height distribution diminishes.

From these considerations, we may construct the following empirical formula applicable in the range of $r > \varepsilon$:

$$H = a\left\{1 + n\cos(\theta - \alpha)\right\}\frac{1 + \frac{\varepsilon}{r_0}}{1 + \frac{r}{r_0}} \times \begin{cases} \frac{1}{7}(1030 - P_0); & 1000 > P_0 > 950 \\ 11.43 \quad ; & P_0 < 950 \end{cases}$$

where H is the wave height in meter, P_0 the central pressure of typhoon in millibar, r the distance from the storm center in nautical mile and θ the angle measured clockwise from a line showing the direction of movement of storm center. ε means the distance from the storm center to the region where the highest waves are raised, and a, n, α and r_0 are constants which depend on the

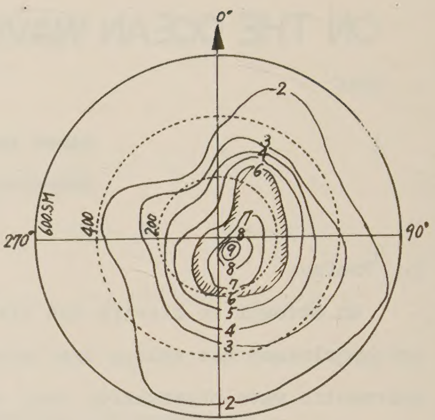

(a) C: 0~20 Km/hr

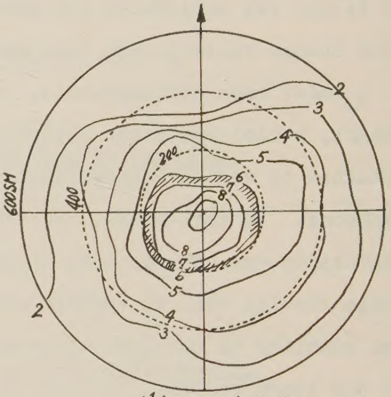

(b) C: 20~40 Km/hr

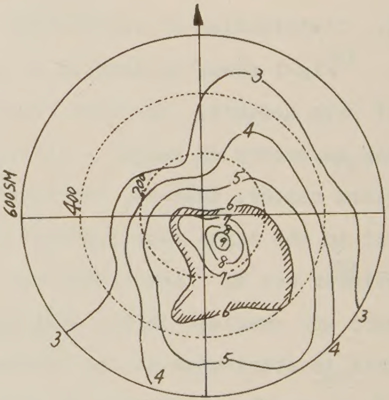

(c) C > 40 Km/hr

Fig-2 Mean distribution maps of wave height (in meter) due to typhoons whose central pressures are 960~980 mb in either case but whose speeds (C) differ.

speed of storm, though we have $a = 1.02$, $n = 0.20$, and $\alpha = 135°$ on the average. A calculation diagram based on this formula was already published. In the range of $r < \varepsilon$, sufficient knowledge to construct an empirical formula has not been obtained yet, but qualitative discussion will be made in section 5.

Moreover, it must be kept in mind that, out of typhoon too, we can generally find swells with greater size and length in the rear than in the front as well as within the storm being contrary to what is usually believed.

3. Distribution of wave period

The distribution of period of prevailing waves is represented in Fig-3. Waves with great length are more frequently raised in the rear semi-circle than in the front semi-circle, and the wave period decreases on the whole as the distance from the storm center increases and as the central pressure of storm becomes high. The wave period frequently observed in typhoon is 7∼11 sec, and this is somewhat smaller than the observed one in shallow water near a land. Moreover, the wave period in the front semicircle is likely to decrease as the speed of storm increases.

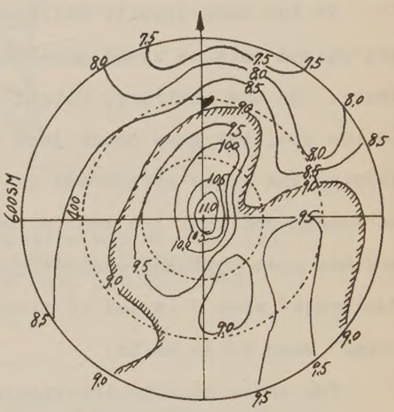

Fig-3 Mean distribution map of wave period (in sec) due to a typhoon whose central pressure is 940∼960 mb.

In conclusion, we may say that the distribution of wave period is generally similar to that of wave height, although the former is more complicated and more confused. If we neglect the difference of wave period among quadrants and the effect of speed of typhoon, the distribution of period of prevailing waves is given approximately by

$$\overline{T} = 48.5 - \frac{p}{25} - \frac{r}{250}$$

However, it should be impressed that actual seas constitute complicated spectra including waves with various periods as shown in section 7.

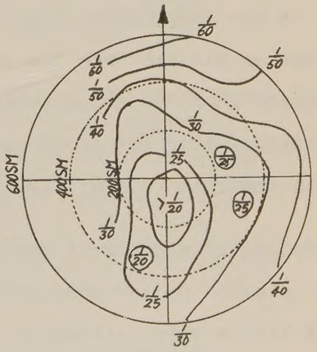

Fig-4 Distribution map of wave steepness in typhoon whose central pressure is 940∼960 mb.

4. Distribution of wave steepness and wave age

The wave is the steepest in the vicinity of the storm center with the steepness more than 1/20, and it becomes more gentle as the distance from the center increases (Fig-4). Moreover, the wave is steeper in the rear than in the front. The steepness observed frequently in typhoon is 1/15∼1/30, and the steepness more than

1/10 is very rare.

The wave age decreases usually as the distance from the storm center diminishes. For example, in typhoon with 960∿980 mb the average of wave age is 0.60, 0.81 and 0.95 at the places whose distance from the center is 0∿100, 100∼200 and 200∼300 sea miles, respectively. Any wave whose age is less than 0.4 or longer than 1.4 ($=\beta_m$) was not reported as a prevailing wave in question. The wave steepness for a given wave age is generally smaller than the value given semi-theoretically by Sverdrup and Munk (1947).

5. State of the sea in the eye of a tropical cyclone

It has been usually believed that in the eye of typhoon or hurricane pyramidal waves are raised because waves penetrate into this place from all directions and collide each other. On the contrary, Ootani (1941) suggested that pyramidal waves would not be raised in the eye, but they occur just behind the storm center. Then, the author collected data showing the state of the sea in the eye observed from ships or planes. From them it could be recognized that the sea in the eye is less confused when the typhoon moves slowly, and becomes more confused according as it moves faster. For instance, the sea in the eye was "moderate" when C (speed of storm) = 7 km/hr, "confused" when C = 20 km/hr and "very confused" when C = 36 km/hr.

The cause of this interesting phenomenon can be made clear by considering geometrical conditions necessary for the penetration of developed swells into the eye and also by considering the effect of wind on these swells. Thus, the sea condition in the eye of tropical cyclone is expected as follows:

less confused when $C < V$,

very confused when $C \sim V$,

rather confused when $C > V$,

where V is the group velocity of wave (usually 20∼40 km/hr). Particularly, in the rear region not so distant from the storm center, "mountaineous and pyramidal waves" are apt to be raised when the storm progresses with a speed larger than V, because the remarkable swell originated in the front semi-circle collides at great angles with the wind wave generated in the rear (confer Fig-6).

6. Direction of wind waves and swell

In relation to the presumption of the location of tropical cyclone, it has been discussed a little which direction wind waves and swell in it take, but the discrepacies of opinions are found. Actually, the distribution of wave-direction is not so simple as stated formerly, but depends on the individualities of storm such as the speed, the track and the stage of development, etc.

Fig-5 represents a typhoon which has but just developed rapidly. We recognize that

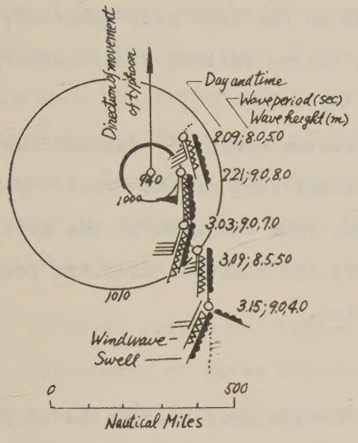

Fig-5 Composite map of wind, wind waves, swell, period and height of prevailing waves in Typhoon Jane of Sept. 2~3, 1950.

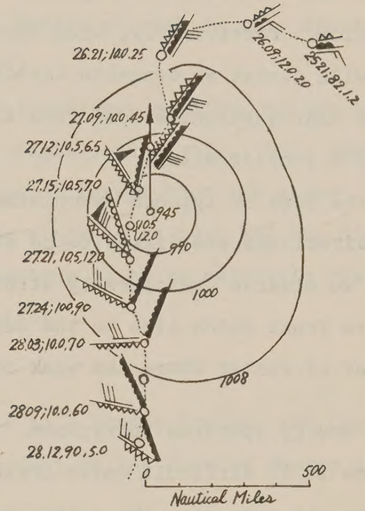

Fig-6 Composite map of wind and ocean waves due to Typhoon Patricia of Oct. 25~28, 1949.

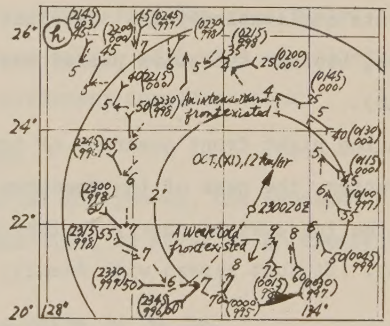

Fig-7 Composite map of wind and ocean waves due to typhoon of Oct. 1946. Small arrows with solid or broken lines indicate the direction of wind or swell, respectively. Numerals in the front or rear of the arrows give the scale of swell and the speed of wind (in knot), respectively.

i waves (or wind waves of swell type) prevail a the same direction as that of wind, since lls have not grown sufficiently yet. Fig-6 shows ase when the typhoon moved straight forward with speed of 50 km/hr which is greater than that of ll. In the front of center wind waves due to is at that place prevail, while in the rear of ter conspicuous swells which have been left be-i coexist with wind waves taking almost right les between them. When the storm advances slowly ;-7), swells with direction different from that vind waves are seen in the front of center as as in the rear. When the storm is changing its 'se the distribution of wave direction becomes plicated, and when the storm is located near a i the influence of being of land on the direction of waves is also recognized.

Further, observed values of angle between wind and swell can be explained quantitatively 'espective cases from a theoretical consideration. When the storm moves slowly the swell :h should appear in whole area deviates from the wind to the right (in the Northern Hemisere) as pointed out first by Tannehill (1936). As the speed of storm increases the deviation of swell from wind becomes small in the right section of storm and large in the left section. Particularly, when the speed of storm exceeds that of swell, we can find a swell with almost an opposite direction from the wind in the left rear quadrant, and in the right rear quadrant we can find a swell travelling to the left of wind contrary to Tannehill's consideration.

In the case of typhoon associated with a frontal system confused seas and swell with unusual directions are likely to be raised in the adjacent seas of the front. For example, in Fig-7 we observe considerably strong swells deviating from the wind to the left on intense warm front which lies to the left front of center, and confused seas are found to the right rear of center where the weak cold front is located.

7. Wave energy spectrum in typhoon

Since it is difficult under present conditions to obtain wave spectra in tropical cyclone on the open sea, the author intends to investigate the distribution of them on the basis of wave energy spectra that Ijima (1957) constructed by analysing wave records at the Port of Onahama. Fig-8a indicates the relative position of the port to the storm center at each observational time when the energy spectrum shown in Fig-8b and c could be traced. In this case, we may say that the variation of wave spectrum with time at the port represents qualitatively the distribution of it in the right semi-circle of typhoon on the open sea, because the storm passed west of Onahama and the speed of it is very great (60 ~ 90 km/hr).

In the right front quadrant of typhoon with great velocity, as it becomes near to the storm center, the peak of the spectrum moves rapidly towards the long period band resulting in the increase of energy in this band, while the energy of short period band remains constant. It just agrees with results given by the theory of wave generation. In the

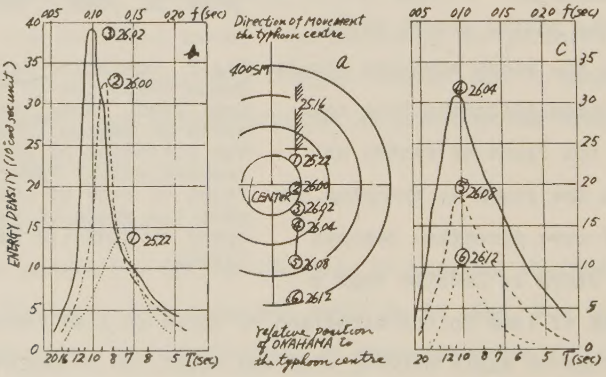

Fig-8b and c The time change of wave energy spectrum at the Port of Onahama during the passage of Typhoon Tess from Sept. 25 to 26, 1953.

ar region of the roughest waves, as the distance from the center becomes large, the ergy decreases gradually at every period keeping the period of peak in wave spectrum be constant because swells are prevailing (see Fig-6).

Moreover, on the open sea, it is also expected that the wave spectrum in the left mi-circle does not differ seriously from that in the right semi-circle. But, when a phoon moves slowly the change of wave spectum shall be different from the above-ntioned case. Consider, for example, a case when the storm is at rest and the distri-tion of wind is symmetrical about its center. The spectrum is to be naturally just the me for all quadrants, where wind waves and swell coexist.

Energy of waves raises in typhoon

The total energy of waves amounts to about 10^{24} erg in a strong typhoon and less than ^{23} erg in a weak one. It corresponds to about ten percent of the kinetic energy of the phoon itself.

If we assume that the state of the sea is steady and the dissipation of waves due to iction is neglected in accordance with Sverdrup and Munk (1947), the energy of waves nerated per unit time by wind in the storm must be equal to the flow of energy per unit me due to swells which go out from the storm. From such consideration, it is shown at several percent of the wind energy dissipated by surface friction goes toward increas-g and maintaining the energy of waves, and this agrees nearly with what was obtained for gnificant waves by Sverdrup and Munk from entirely different considerations.

Mean relation between wind velocity and wave height

When a certain velocity of wind (W, m/s) is observed in typhoon, the average of wave ights in all cases (H, m), to be observed at the same time, is given by an empirical rmula

$$H = 0.31 W$$

shown in Fig-9. Such linear equation is similar to those given by Cornish (1934) and hers, but our coefficient 0.31 is naturally smal-r than those in the latter, since they are related the highest waves. In Fig-9, we recognize that e wave height in the Atlantic given by Roll (1954) almost always smaller a little than that in ty-oon though they are parallel, and also that the obable wave height (recommended by the World Me-orological Organization) is smaller when the wind weak and larger when the wind is strong than the ight in the typhoon and in the Atlantic.

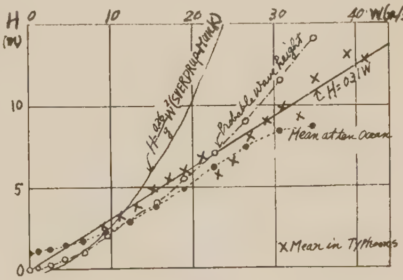

Fig-9 Mean relation between the wind velocity and the wave height in typhoons.

Besides, when the wind velocity is increasing continuously the wave height is usually lower than that calculated by this formula, and on the contrary, when the wind velocity is decreasing continuously the wave height is usually higher than the calculated one. This can be interpreted by the fact that in the former case the weather ship is located in the fr semi-circle of storm and in the latter case in the rear semi-circle, therefcre, the waves are lower in the former than in the latter (Fig-1). The mean relation between wind velocity and wave period is omitted here.

References

(The present paper is the outline of the following ones.)

Unoki, S. (1956) : On the speed, travel time and direction of ocean waves due to tropical cyclones, Journ. Meteor. Soc. Japan, Vol.34, No. 6, 354 - 363.

Unoki, S. (1957) : On the ocean waves due to tropical cyclones (2nd paper), Distribution of waves viewed from geometric consideration and typhoon reconnaissance by aircrafts, ibid, Vol. 35, No. 2, 78 - 87.

Unoki, S. (1957) : On the ocean waves due to tropical cyclones (3rd paper), Mean distibution of wave heights and periods, ibid, Vol. 35, No. 5, 297 - 309.

Unoki, S. (1957) : On the ocean waves due to tropical cyclones (4th paper), Energy of waves and some other subjects, ibid, Vol. 35, No. 6, 350 -361.

THE POSSIBLE HIGHEST GRAVITY WAVES IN SHALLOW WATER

Tsutomu Kishi, Dr. Engineering

Assistant Prof. of Hydraulics, Hokkaido University

: When we design seashore structures, for examples, groins, breakwaters and sea
c., it is often essential to consider the possible highest clapotis and progressive
shallow water.

present paper is an abstract of two papers published by the author in Japanese dur-
and 1955, and consists of two parts. In the first part the clapotis of finite height
he second the progressive wave of finite height are respectively discussed.
criterion of the highest clapotis is based on the vertical acceleration of water
, while that of the progressive wave is based on the horizontal velocity of water
.

possible highest clapotis in shallow water.

ution of the clapotis of finite height in shallow water.

x-axis be horizontal and y-axis vertically upwards. Velocity potential φ and wave
$\eta(x,y,t)=0$ are assumed to be expanded in the following infinite series :

$$\varphi = \sum_{n=0}^{\infty} \alpha_n(t) \cosh nk(y+d) \cos nkx, \tag{1}$$

$$\eta(x,y,t) = -y + \frac{1}{2} a_0(t) + \sum_{n=1}^{\infty} a_n(t) \cos nkx = 0. \tag{2}$$

bove expressions, $\alpha_n(t)$ and $a_n(t)$ are unknown functions of time t and k is the wave
Equation (1) must satisfy the condition of continuity. Namely,

$$\frac{\partial^2 \varphi}{\partial x^2} + \frac{\partial^2 \varphi}{\partial y^2} = 0. \tag{3}$$

the wall surface the horizontal velocity u is always zero so that

$$u = -\frac{\partial \varphi}{\partial x} = 0 \qquad \text{at } x = 0 \quad \text{for all } t. \tag{4}$$

resent problem, the water is of uniform depth d. And the vertical velocity will
at y = - d, i.e.

$$v = -\frac{\partial \varphi}{\partial y} = 0 \qquad \text{at } y = 0 \quad \text{for all } t. \tag{5}$$

itions of eqs. (4) and (5) are satisfied by the potential assumed as eq. (1).
m the condition of pressure p = 0 at the free surface, one has

$$-gy+\frac{\partial\varphi}{\partial t}-\frac{1}{2}\left\{\left(\frac{\partial\varphi}{\partial x}\right)^2+\left(\frac{\partial\varphi}{\partial y}\right)^2\right\}=0 \qquad \text{on} \quad \eta(x,y,t)=0 . \tag{6}$$

At the free surface a fluid element must move so that its velocity component normal to t surface is the same as the normal velocity of the surface itself. Hence the function η must satisfy the condition

$$\frac{\partial\eta}{\partial t}+u\frac{\partial\eta}{\partial x}+v\frac{\partial\eta}{\partial y}=0 \qquad \text{on} \quad \eta(x,y,t)=0 . \tag{7}$$

Therefore, the problem is reduced to the determination of the unknown functions $\alpha_n(t)$ a $a_n(t)$ under the conditions given by eqs. (6) and (7).

By substituting eqs. (1) and (2) into eqs. (6) and (7) and equating the sum of the respective terms of $\cos n/kx$ to zero, following equations are obtained:

from condition (6),

$$\begin{aligned}
&-\frac{1}{2}ga_0+\dot\alpha_0+\frac{k}{2}\Big(\dot\alpha_1 a_1\sinh kd+\frac{k}{2}\dot\alpha_1 a_0a_1\cosh kd+2\dot\alpha_2a_2\sinh 2kd\\
&+2k\dot\alpha_2a_0a_2\cosh 2kd+3\alpha_3a_3\sinh 3kd+\frac{9}{2}k\dot\alpha_3a_0a_3\cosh 3kd\Big)\\
&-\frac{k^2}{4}\left(\alpha_1^2\cosh 2kd+k\alpha_1^2a_0\sinh 2kd\right)=0\\[6pt]
&-ga_1+\dot\alpha_1\cosh kd+\frac{k}{2}\dot\alpha_1a_0\sinh kd+\frac{k^2}{8}\dot\alpha_1a_0^2\cosh kd+\frac{k}{2}\dot\alpha_1a_2\sinh kd\\
&+\frac{k^2}{2}\dot\alpha_1a_0a_2\cos kd+k\dot\alpha_2a_1\sin 2kd+k^2\dot\alpha_2a_0a_1\cos 2kd-k^2\alpha_2\alpha_1\cosh 3kd=0\\
&-ga_2+\dot\alpha_2\cos 2kd+k\dot\alpha_2a_0\sinh 2kd+\frac{k}{2}\dot\alpha_1a_1\sinh kd+\frac{k^2}{2}\dot\alpha_1a_0a_1\cos kd\\
&+\frac{k}{2}\dot\alpha_1a_3\sinh kd+\frac{k^2}{4}\dot\alpha_1a_0a_3\cosh kd+\frac{k^2}{2}\dot\alpha_2a_0^2\cos 2kd+\frac{3}{2}k\dot\alpha_3a_0\sin 3kd+\frac{1}{4}k^2\alpha_1^2=0\\[6pt]
&-ga_3+\dot\alpha_3\cos 3kd+3k\dot\alpha_3a_0\sinh 3kd+\frac{9}{8}k^2\dot\alpha_0\cosh 3kd\\
&+\frac{k}{2}\dot\alpha_1a_2\sinh kd+\frac{k^2}{4}\dot\alpha_1a_0a_2\cosh kd+k\dot\alpha_2a_1\sinh 2kd\\
&+k^2\dot\alpha_2a_0a_1\cosh 2kd+k^2\alpha_2\alpha_1\cosh kd=0\\
&- - - - - - - - - - - - - - - -
\end{aligned} \tag{8}$$

and from condition (7),

$$\begin{aligned}
&\frac{1}{2}\dot a_0-\frac{k^2}{2}\Big(\alpha_1a_1\cosh kd+\frac{k}{2}\alpha_1a_0a_1\sinh kd+9\alpha_3a_1\cosh 3kd\\
&+\frac{27}{2}k\alpha_3a_0a_1\sinh 3kd+4\alpha_2a_2\cosh 2kd+4k\alpha_2a_0a_2\sinh 2kd\Big)=0\\[6pt]
&\dot a_1+k\alpha_1\sinh kd+\frac{k^2}{2}\alpha_1a_0\cosh kd-k^2\Big(\alpha_1a_2\cosh kd+\frac{k}{2}\alpha_1a_0a_2\sinh kd\\
&+\alpha_2\dot a_1\cosh 2kd+k\alpha_2a_0a_1\sinh 2kd\Big)=0\\[6pt]
&a_2+2k\alpha_2\sinh 2kd+k^2\alpha_1a_1\cosh kd+2k^2\alpha_2a_0\cosh 2kd\\
&+\frac{k^2}{2}\Big(\frac{k}{2}\alpha_1a_0a_1\sinh kd+4\alpha_2a_2\cosh 2kd+4k\alpha_2a_0a_2\sinh 2kd
\end{aligned} \tag{9}$$

$$+ 9\alpha_3 a_1 \cosh 3kd + \frac{27}{2} k^2 \alpha_3 a_0 a_1 \sinh 3kd) = 0$$

$$\dot{a}_3 + 3k\alpha_3 \sinh 3kd + \frac{9}{2} k^2 \alpha_3 a_0 \cosh 3kd + k^2 (\alpha_1 a_2 \cosh kd$$

$$+ \frac{k}{2} \alpha_1 a_0 a_2 \sinh kd + \alpha_2 a_1 \cosh 2kd + k\alpha_2 a_0 a_1 \sinh 2kd) = 0$$

. . . .

cessive calculations give the following results:

$$\begin{aligned}
\alpha_0 &= \frac{1}{2} gC - \frac{1}{2} A^2 \sigma^2 \sin^2 \sigma t + \frac{k}{4} A^2 \sigma^2 \frac{\cosh 2kd}{\sinh^2 k\alpha} \cos^2 \sigma t \\
\alpha_1 &= - \frac{A\sigma}{k \sinh kd} \cos \sigma t \\
\alpha_2 &= - \frac{3A^2 \sigma \sin 2\sigma t}{2 \sinh 4kd (2 \tanh kd - \tanh 2kd)} \\
a_0 &= C \\
a_1 &= A \sin \sigma t \\
a_2 &= \frac{kA^2 \tanh kd}{2} \sin^2 \sigma t + \frac{kA^2 \tanh kd}{4 \sin^2 kd} \cos^2 \sigma t \\
&\quad - \frac{3kA^2 \tanh kd}{2 \sinh 2kd (2 \tanh kd - \tanh 2kd)} \cos 2\sigma t \\
\sigma^2 &= gk \tanh kd \left(1 - \frac{kC}{2} \tanh kd + \frac{k^2 C^2}{4} \tanh^2 kd + \cdots\cdots \right) \\
&\text{where} \quad A = \text{const.}, \quad C = \text{const.},
\end{aligned} \tag{10}$$

e physical interpretation of the first constant A is easily obtained by considering itude of this wave.

$$\begin{aligned}
\eta_{max} &= A + \frac{kA^2}{2} \tanh kd \left\{ 1 + \frac{3}{\sinh 2kd (2 \tanh kd - \tanh 2kd} \right\}, \\
\eta_{min} &= -A + \frac{kA^2}{2} \tanh kd \left\{ 1 + \frac{3}{\sinh 2kd (2 \tanh kd - \tanh 2kd)} \right\}.
\end{aligned} \tag{11}$$

means the half of the wave height of clapotis. Second constant C indicates the f the height of the still water level above x-axis. Referring to the Sainflou's , the author assumed the value of C as

$$C = \frac{1}{2} kA^2 \coth kd. \tag{12}$$

e profile given by eq, (10) has been examined by the author to show a good agreement e experimental results reported by F. Suquet and A. Wallet.1)

e highest clapotis.

the perfect liquid cannot bear the tensile stress, the condition of $\partial p / \partial y \leqq 0$ e satisfied at the free surface. The equation of motion related to y-axis is

$$\frac{\partial v}{\partial t} + u \frac{\partial v}{\partial x} + v \frac{\partial v}{\partial y} = -g - \frac{1}{\rho} \frac{\partial p}{\partial y}, \tag{13}$$

$=0$ at the free surface when the wave is critical, the above equation becomes

$$\frac{\partial v}{\partial t} + g = - \frac{1}{\rho} \frac{\partial p}{\partial y} \leqq 0$$

W. G. Penny and A. T. Price[2] have proposed the following relation as the criterion of the highest clapotis in deep water:

$$\frac{\partial v}{\partial t} + g = 0 . \tag{14}$$

And the maximum height calculated by eq. (14) is

$$kA = 0.592 .$$

In the case of a shallow water, the maximum height will decrease as the water depth decreases. Then the generalized criterion of the highest clapotis in any water depth ca be expressed as

$$\frac{\partial v}{\partial t} + g\alpha = 0 , \qquad \alpha \text{ is a coefficient and } \leqq 1 . \tag{15}$$

The coefficient α in eq. (15) must satisfy the following condition:

1. $\lim\limits_{kd \to 0} \quad kA = 0$
2. $\lim\limits_{kd \to 0} \quad kA = 0.592$

The author assumes the coefficient α in the following form:

$$\alpha = \tanh^2 kd . \tag{16}$$

The relation (16) is one of the simplest relation that satisfies the above two conditions

Let the origin be on the wave crest and then $\partial v/\partial t$ becomes from eqs. (10) and (12) a

$$\frac{\partial v}{\partial t} = - \frac{\partial^2 \phi}{\partial y \partial t} = - gkA \tanh kd \left\{ 1 + kA \coth kd + O(k^2A^2) + \cdots\cdots \right\} . \tag{17}$$

Substitution of the above result into eq. (15) leads to

$$(kA \coth kd)^2 + (kA \coth kd) - 1 = 0 + O(k^3A^3) . \tag{18}$$

As the expression (17) is applicable only in the order of magnitude $O(k^2A^2)$, eq. (18) should be replaced by

$$(kA \coth kd)^2 + (kA \coth kd) - \beta = 0 \tag{19}$$

Where is a coefficient nearly equal to unity.

By determining the value of β in such a way that the solution of eq. (19) satisfies the condition 2, i.e., $\lim\limits_{kd \to \infty} kA = 0.592$, β = 0.940 and the solution

$$kA \coth kd = 0.592 \tag{20}$$

are obtained. The relation (20) is the general criterion of the highest clapotis in any depth.

In the case of a practical application, it is convenient to express d in relation (20) by the water depth H. When the wave is critical the relation between d and H becom

$$d = H - \frac{C}{2} = H - \frac{1}{4} kA^2 \coth kd = H - 0.148A . \tag{21}$$

Substitution of the relation (21) into the relation (20) gives the relation

$$kA = \frac{\sqrt{(\coth^2 kH + 0.350 \operatorname{cosech}^2 kH)} - \coth kH}{0.296 \operatorname{cosech}^2 kH} . \tag{22}$$

The relation (22) is compared with the experimental results of F. Suquet and A Wallet[3] in Fig. 1.

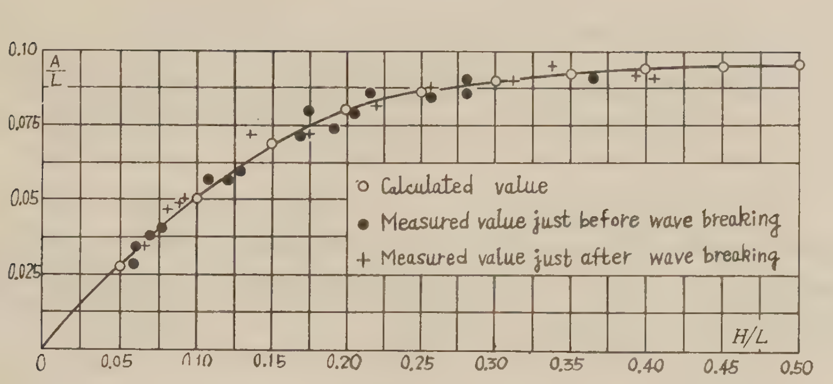

Fig. 1

rding to Fig. 1, the criterion of the highest clapotis given by the relation(20) or seems to be applicable.

The possible highest progressive wave in shallow water.

Solution of a progressive wave of finite height in shallow water.

In the author's method, the progressive wave with celerity c is superposed with a orm flow of equal velocity in the opposite direction by following the Rayleigh's method. resulting motion becomes a steady flow with a sinuous surface.

Let x-axis be horizontal being positive direction in the superposed flow and y-axis be ical upwards. The velocity potential ϕ and stream function ψ of the flow under consid-ion can be expressed as follows:

$$\phi = -cx + c\beta\cosh k(d+y)\sin kx, \quad (1)$$

$$\psi = -cy + c\beta\sinh k(d+y)\cos kx,$$

where

k = wave number = $2\pi/L$,

L = wave length,

c = wave celerity.

Stream lines $\psi = 0$ and $\psi = cd$ indicate the free surface and the bottom respectively. profile of the free surface given by S. Sato[4)] is

$$\eta = \frac{1}{2}ka^2\coth kd + a\cos kx + \frac{1}{2}ka^2\coth kd\cos 2kx + \frac{1}{4}k^2a^3\left(\coth kd + \frac{1}{2}\right)\cos 3kx. \quad (2)$$

where

η = displacement from the axis $y = 0$.

$$a = \beta\sinh kd\left\{1 + \frac{3}{4}k^2\beta^2\left(1 + \frac{3}{2}\sinh^2 kd\right)\right\}. \quad (3)$$

larly, the mean level y of the stream line $\psi = cd'$ $(d' < d)$ and profile of the stream line given by eqs. (4) and (5), respectively.

$$y = -\eta' + \frac{1}{2} k r^2 \coth k\,(d-d') \tag{4}$$

$$\eta' = \frac{1}{2} k r^2 \coth k\,(d-d') + r \cos kx + \frac{1}{2} k r^2 \coth k\,(d-d') \cos 2kx$$
$$+ \frac{1}{4} k^2 r^2 \left\{ \coth^2 k\,(d-d') + \frac{1}{2} \right\} \cos 3kx + \cdots\cdots \tag{5}$$

where
$$r = a \frac{\sinh k\,(d-d')}{\sinh kd} \tag{6}$$

These relations give the momentum contained in the domain of unit length bounded by the stream line $\psi = 0$ and $\psi = cd'$. The momentum m_s of the steady flow is given by

$$m_s = \int_{\psi=cd'}^{\psi=0} \rho u\, dy = -\rho \int_{\psi=cd'}^{\psi=0} \frac{\partial \psi}{\partial y}\, dy = \rho c d' \tag{7}$$

where ρ density of the fluid.

While, the momentum of the superposed uniform flow of velocity c contained in the same domain is given by

$$\int_{y}^{\eta} \rho c\, dy \tag{8}$$

Consequently, the momentum $m_{d'}$ of the progressive wave with the propagation velocity c is the difference of the above two expressions, that is

$$m_{d'} = \rho c (a - r) \cos kx + \rho c k \left\{ a^2 \coth kd - r^2 \coth k(d-d') \right\} \cos^2 kx$$
$$+ \frac{1}{4} \rho c k^2 \left[a^3 \left(\coth kd + \frac{1}{2} \right) - r^3 \left\{ \coth^3 k(d-d') + \frac{1}{2} \right\} \right] \cos^3 kx + \cdots \tag{9}$$

By putting d = d' in eq. (9) and by integrating over one wave length, the momentum of the progressive wave per one wave per one length can be obtained:

$$M = \frac{L}{2} \rho c k a^2 \coth kd = \pi \rho c a^2 \coth kd \tag{10}$$

Horizontal velocity $u_{d'}$ along the stream line $\psi = cd'$ can be calculated by differentiating $(m_{d'}/\rho)$ with respecting to d'.

$$u_{d'} = \frac{1}{\rho} \frac{\partial m_{d'}}{\partial d'} = cak \frac{\cosh k(d-d')}{\sinh kd} \cos kx + ca^2k^2 \frac{\cosh 2k(d-d')}{\sinh^2 kd} \cos^2 kx$$
$$+ \frac{1}{4} c a^3 k^3 \frac{\cosh k(d-d') \left\{ \cosh^2 k(d-d') + \frac{7}{2} \sinh^2 k(d-d') \right\}}{\sinh^3 kd} + \cdots, \tag{11}$$

when d' = 0 is substituted into eq. (11), the horizontal velocity along the free surface u_0 becomes

$$u_0 = cak \coth kd \cos kx + ca^2k^2 (\coth^2 kd + 1) \cos^2 kx + \frac{1}{4} ca^2k^3 \left(\coth^3 kd + \frac{7}{2} \coth kd \right) \cos 3kx + \cdots \tag{12}$$

The value of u_0 takes its maximum at the wave crest x = 0, i.e.,

$$u_{0max} = c \left\{ ak \coth kd + a^2k^2 (\coth^2 kd + 1) + \frac{1}{4} a^3k^3 \left(\coth^3 kd + \frac{7}{2} \coth kd \right) + \cdots\cdots \right\} \tag{13}$$

(2) The highest progressive wave

A wave attains its possible highest limit when the horizontal velocity of the fluid particle at the crest becomes equal to the wave celerity. The above fact gives the following criterion of the highest progressive wave:

$$ak \coth kd + a^2k^2 (\coth^2 kd + 1) + \frac{1}{4} a^3k^3 \left(\coth^3 kd + \frac{7}{2} \coth kd \right) = 1 \tag{14}$$

In order to examine the above relation by experiments, physical meanings of the two ameters "a" and "d" involved in eq. (14) must first be revealed. From eq. (2), it is ily seen that "a" and "d" are respectively related to the half wave height A and water th H by the following realtions:

$$\left.\begin{aligned} A &\fallingdotseq a \\ H &= h + \frac{1}{2} k a^2 \coth k d \end{aligned}\right\} \qquad (15)$$

The combination of the relations (14) and (15) gives the relation between steepness L and shallowness H/L of the highest progressive wave, which is shown in Fig. 2 by a id curve. The experimental rsults reported by F. Suquet and A. Wallet[5] are also ered in the same figure.

The calculated values agree paratively well with the experital values. Another examination eq. (14) is made by considering limiting case of deep water, ., kd = ∞ . When the condition = ∞ is introduced in eq. (14), ak= 60 or 2A/L = 0.146 = 1/6.8 is ulted. The above value of 2A/L rly coincides with the value of given by Michell.[6]

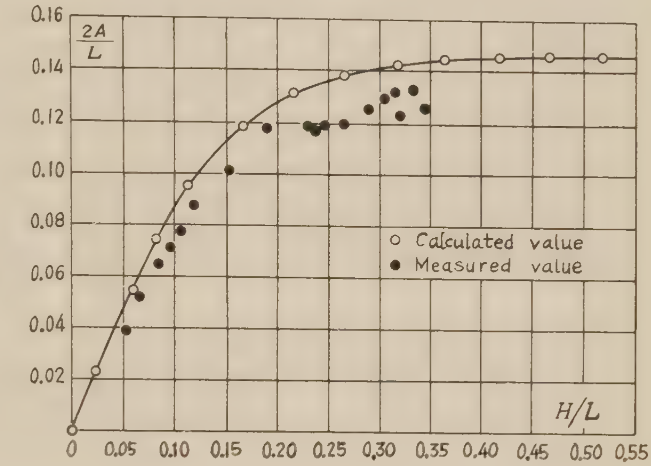

Fig. 2

clusion

In the present paper the author discussed the possible highest gravity wave in shallow er. The ciriterions of the highest waves, clapotis and progressive wave, proposed by author agree fairly well with the experimental results. However, he still has some stions from the mathematical point of view because the convergences of his solutions not verified.

References

F. Suquet and A. Wallet: "Basic experimental wave research". Proc. Minnesota Int. Hyd. Conv., Sep. 1953.

W. G. Penney and A. T. Price: "Finite periodic stationary gravity waves in a perfect liquid". Phil. Trans., Series A, Vol. 244, 1952.

Same as 1)

S. Sato: "Surface waves in shallow water". Journal of Research, Public Works Research Institute, Ministry of Construction, Vol. 1, July 1954

5) Same as

6) Michell: "On the highest wave in water ". Thorade, p.p. 33.

FIELD INVESTIGATION OF WAVE FORCES ON BREAKWATER

Takashi Kuribayashi, Hokkaido Development Bureau, Sapporo
Yoshio Muraki, Hokkaido Development Bureau, Sapporo
Goichi Udai, Hokkaido Development Bureau, Sapporo

ntroduction

Many theoretical studies and laboratory experiments on wave forces against breakwaters been made. However, it is usually very difficult to apply these results directly to natural sea because of the complexity of the actual phenomena.

The present investigation is intended to make a comparison between experimental results ined in laboratory and the data observed in the natural sea, and to determine a practimethod for designing economical and safe breakwaters. The practical observations of dimensions, wave pressures and breakwater vibrations have been made at Haboro Harbor e November, 1957.

This paper presents an outline of the experimental equipments and some of the experial results obtained -- the classification of wave pressures in shape, frequency of type pressure, some considerations on the maximum wave pressure and vibrations of the kwater.

escription of Haboro Harbor

Haboro is a small fishing harbor located he north-west coast of Hokkaido facing on Japan sea. This harbor was designed and t as a river-mouth-harbor in early time, now, the course of the river has already changed artificially as will be seen in 1. At present, the construction of new kwaters which are shown by the broken line ig-1, is going on under a new plan for the ose of preventing waves and drifting sands entering into the harbor.

This harbor has several convenient points investigating wave pressures:

) It is easy to set measuring instruments on the breakwater, because the new

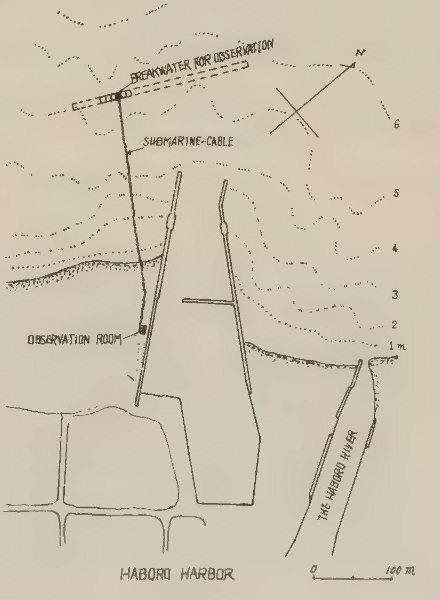

Fig-1

breakwaters are now being built.

2) Since violent stormy waves come to this sea region during the period from November to February, many available data for investigations can be expected.
3) Height of tidal wave is very small.
4) The direction of the breakwater which is used for the observation is perpendicular to the direction of the main wave.
5) As the foundation-mounds of the breakwaters are new, the up-lift pressure which acts against the bottom of the breakwater may be measured easily.
6) The obtained results can be used directly for the practical works of breakwaters at this harbor.

3. Equipments provided for the observations

The principal instruments provided for the measurements of wave heights, wave pressures and vibrations of the breakwater are as follows:

(1) Pressure type wave recorder

This wave recorder was designed by Transportation Technical Research Institute, Japan. The principle and mechanism are similar to California Mark III wave recorder. This wave recorder was provided for measuring the offshore wave heights.

(2) Transit type wave recorder

This wave recorder was designed by G. Udai, one of the authors. The principle of this wave recorder belongs to the optical method. First, a float which has a clear mark is set at the expected position of the sea. The motion of the float, which moves closely with the waves, is traced by the observer with the transit which is set in the observation room built at the higher place. The motion of the transit is transmitted to a recording chart through a magnifying lever mechanism, and the wave motion is recorded with pen on a chart. This instrument has some excellent points. The principle of this instrument is very simple, and it seldom be damaged. And, its cost is very low. But it can not be used when the weather is so bad, because the mark of the float can not be clearly seen. This wave recorder was also provided to measure the offshore wave heights. This apparatus is shown in Photo-1.

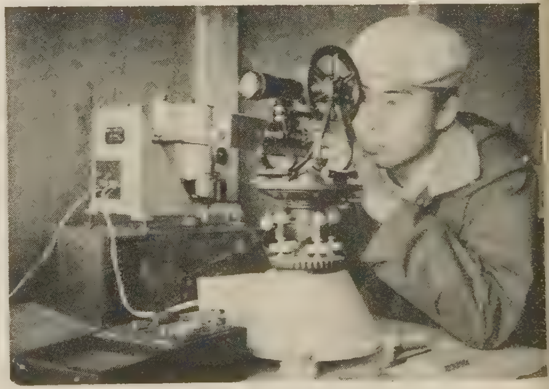

Photo-1

(3) Step type wave recorder

This wave recorder was used to measure the heights of the waves at the front position of the breakwater. This recorder was designed by Y. Muraki, one of the authors. Similar type wave recorder which has been used up to the present involves an inconvenient point --

:hough relatively clear steplike wave records can be obtained on a chart when the sea :e rises, the records show smooth curved without showing steplike shapes on account : electrical leakage through the sea water film of the electrodes (spark-plug) when ea surface falls. It means that the records accompany the time lag and do not show :tual wave motion.

Ir. Gerhrdt also noticed the same point in his report.[1)] He used the electrodes which oated with silicon grease in order to avoid the influence of this leakage, but it was 'ficient.

)ne of the authors solved this point by using magnet-relays, which have low electrical :ances, on the old type apparatus. The detailed explanation of this gage will be re- i in another paper. The diagram of this circuit is shown in Fig-2 and an example of ecords, which shows the very clear steplike shape from start to end, is shown in -2.

Iave pressure gage

Electric Resistance Strain Gage

Iave pressure gages are used in investigation. These were de- i by Transportation Technical :ch Institute, and made by Toyo K.K. The pick-up of pressure ie amplifying apparatus are in Photoes-3 and 4, respective-

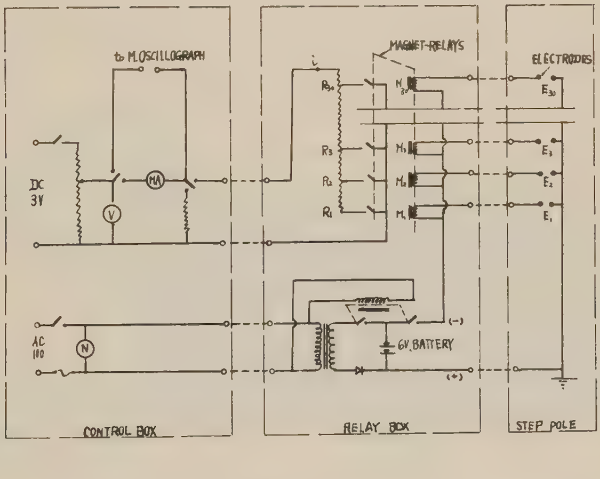

Fig-2

'ibrograph

:n order to investigate the mo- of the breakwater caused by wave ires, and accelerograph is set : breakwater. At first, the 's had an intention of measuring bration in displacement, but a ole displacement vibrograph was und. Therefore, a preliminary ation of only the period of the ion is performed with an accel- ph in the present investigation. celerograph used is Electric ance Strain Gage type which was

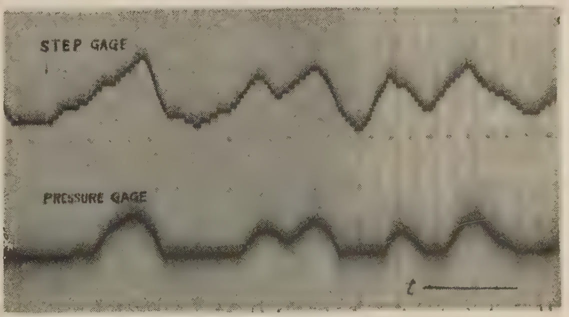

Photo-2

Photo-3

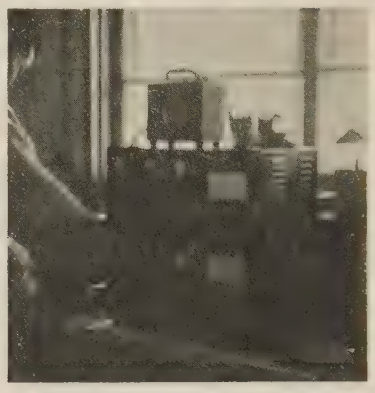

Photo-4

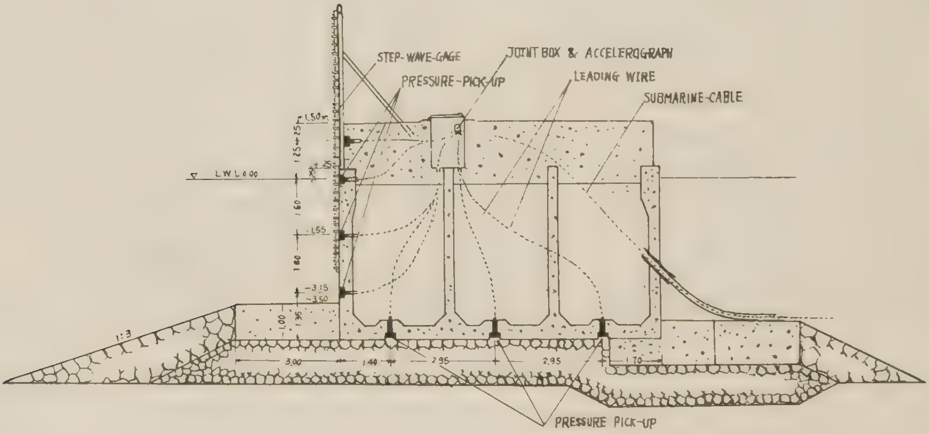

Fig-3

Photo-5

de by Kyowa Musen K. K. Its proper frequency is 22 c/s and the capacity is ± 1G.

These measuring instruments are set on one breakwater as shown in Fig-3 and Photo-5. ur pick-ups of pressure are set on the front vertical wall and three pick-ups of pressure e set on the bottom surface. The step wave gage, 6 m in length, is also set on the same ont wall and the accelerograph is fixed to the breakwater in the manhole.

There is a joint box in the manhole. Leading wires from each pick-up of pressure, tep wave gage and accelerograph are connected together in the box with a submarine-cable ich comes from the observation room 300 m apart from the breakwater.

. Types of wave pressure

) Classification of wave pressure in shape

The practical field observations were carried out for about three months from November, 957 to January, 1958. During this period, many stormy waves which involved wind waves and wells came to this coast. Therefore, many different kinds of wave pressure records, in agnitude and shape, were obtained. An example of their records is shown in Photo-6. Acording to the wave data obtained in past several years, it is evident that the season in ich our observations were made takes the largest frequency in the occurrence of violent aves through a year. Therefore, the results obtained in this observation seem to repreent the characteristics of the wave pressures, and the largest value of the observed ressures also seems to show an approximate alue of the maximum wave pressure to be exected at this harbor.

According to the records obtained, the ave pressures (at S. W. L.) take various apes. Of course, this variation depends on e characteristics of the wave, topography of e sea bottom, type of the structure and othrs. However, when the variation of the apes is considered, the obtained records eem to include the shapes of almost all the ind of pressures which would occur at any ther sea obstructed by a vertical breakwater.

The shapes of the obtained wave pressures ich act on the vertical wall at S. W. L. re classified as shown in Fig-4. Although is manner of classification is not always e generalized one, it is believed that all ave pressures in any other sea can also be

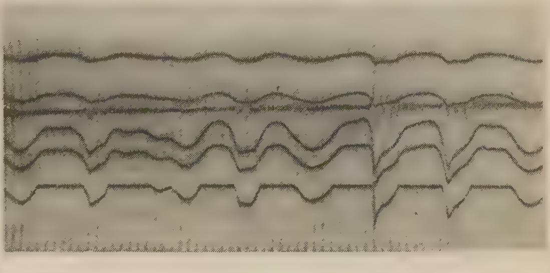

Photo-6

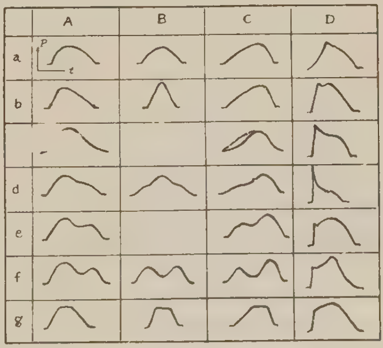

CLASSIFICATION OF WAVE PRESSURE SHAPE

Fig-4

classified by this manner.

As will be seen in Fig-4, the curves of any group of A, B and C are always smooth and simple, perhaps because they are caused by nonbreaking waves. On the other hand, the curve of group D has a sharp angle, which is perhaps caused by breaking waves. There are some differences among the groups of A, B and C. In type A, the curves incline ahead, in type B they are symmetrical, and in type C they incline behind. The shape of type A is usually caused by wind waves, type C by swells and type B by both. The wave pressure of type D, which is caused by breaking waves, has been studied in laboratory experiments. However, it has rarely been studied in the natural sea.

(2) Frequency of each type of wave pressures

In order to discuss the stability of the breakwater, it is very important to know the intensity of the wave pressure, but, it is also very important to know the frequency of each type of wave pressures in the natural sea.

The frequency of each type of wave pressures at Haboro Harbor is shown in Fig-5. The values of frequency are respectively 45 % in type A, 27 % in type B, 24 % in type C and 4 % in type D. It is noticed that type D, which is caused by breaking waves and considered to have particular characteristics, shows very small value. The detail of the frequency is shown in Fig-6. Fig-7 shows some relations between wave characteristics and the frequency of type D. It means that wave pressures of type D occur more easily when the wave period is about 8 sec, and the intensities of the wave pressures at that time are relatively large. From

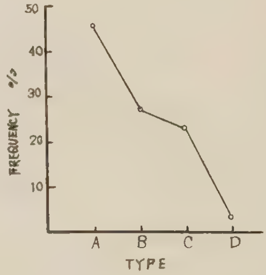

Fig-5

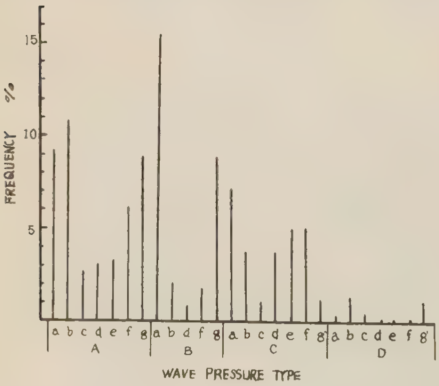

Fig-6

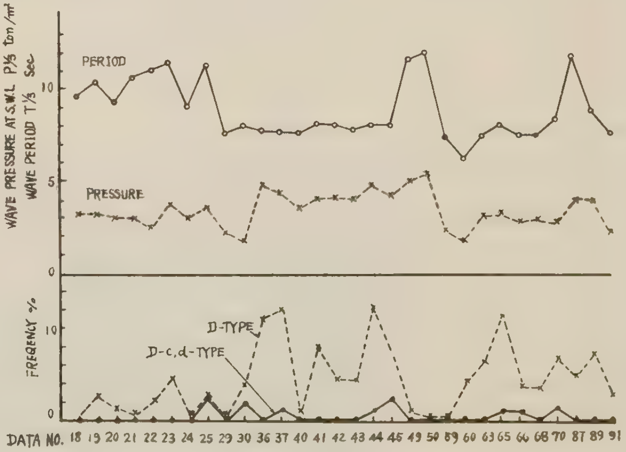

Fig-7

e facts, it may be said that wave pressures of type D would ly appear when some conditions concerning the wave character- cs, structure and topography are superposed at the same time.

The most typical pressure of shocking type observed is shown ig-8. The shape of this shocking pressure is almost same as one which is obtained in laboratory experiments.2)3) The time hock is 0.07 sec, the magnitude of the pressure is 11 ton/m^2 ifle and 3.2 ton/m^2 in bourrage. The numbers of such shocking sures observed are only 2 or 3 in our data. Although the uency of this shocking pressure is very small, the pressure his type can not be neglected, because such pressure shows lly the large value in magnitude.

The fact that laboratory tests and field observations showed me shocking type of wave pressure indicates the validity of similarity between the laboratory experiments and the natural omena.

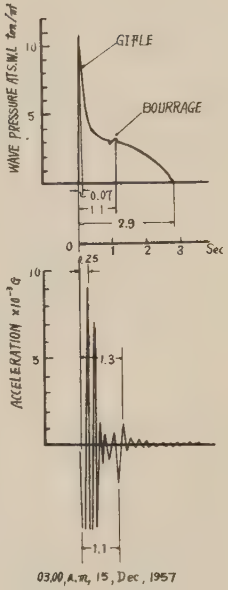

03,00, A.m, 15, Dec, 1957

Fig-8

The maximum wave pressure at Haboro Harbor

A great number of observed values of wave pressures are plot- against the wave period in Fig-9. This shows a relation among the wave period, wave sure and wave type. According to this figure, it can be understood that the largest pressure which is obtained in this observation was caused by the breaking wave which takes the period of about 7 sec. From this result, it may be predicted that the maximum wave pressure, which can occur at Haboro Harbor, will also be caused by such waves.

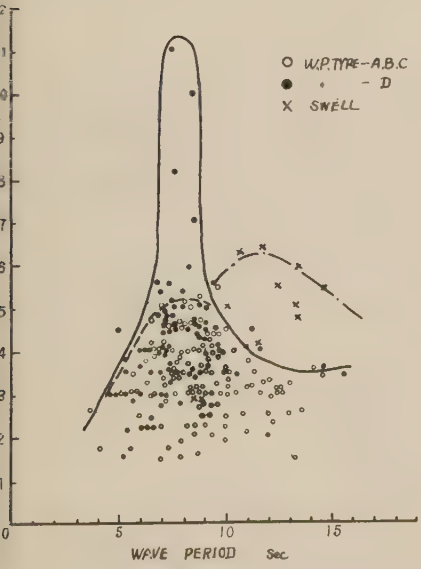

Fig-9

In Fig-10, wave pressures are plotted against the rising time, which means the time from the start to the first peak of each wave pressure curve. The upper limit of these plotted values is represented by one curve, which shows that the wave pressure increases steeply as the rising time becomes short. From this, it is considered that the maximum wave pressure will be caused by the breaking wave type which takes very short time of shock, and the value of the maximum wave pressure may be determined

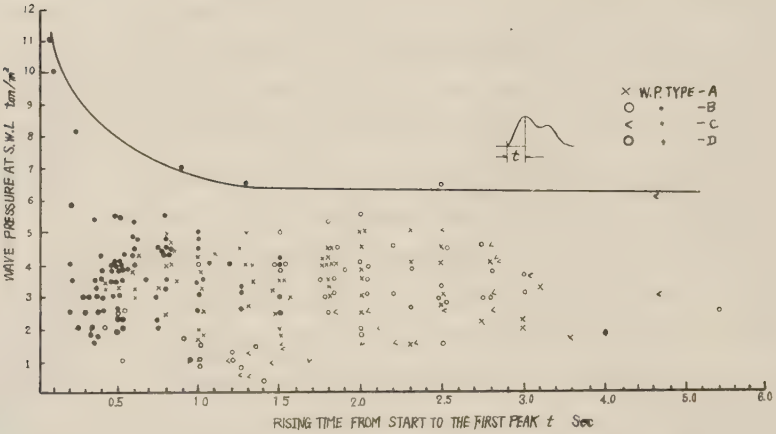

Fig-10

approximately by this empirical curve. From this figure, the value of the maximum pressure which can occur at this harbor can be read as 14～15 ton/m².

When this maximum value of wave pressure is taken, the wave height can be calculated as about 10 m by Hiroi's formula. When the past data of waves and the actual topography are considered, the wave of 10 m in height can not occur at this harbor. On the other hand, according to Minikin's formula[4)], the wave height becomes to be about 1.3 m, which is too small for the actual condition of the sea at that time. From the consideration described above, it can be seen that both formulas are not suitable for the prototype breakwater at Haboro Harbor.

6. Vibration of breakwaters

In order to study the stability of the breakwater, it is necessary to know not only the wave pressure but also the vibration of the breakwater caused by the wave pressure. But inspite of its importance, the measurement of the breakwater vibration has rarely been made up to the present. A similar measurement was once made at Algiers Harbor about 25 years ago. In that case, the three-components accelerograph of crystal type was used. According to that results, a proper frequency of the breakwater was not observed within 1～1000 c/sec, but the shake with the same period as the wave period was recognized.

In our observation, an Electric Resistance Strain Gage type of Accelerograph was used. Its proper frequency is 22 c/sec. The period of the breakwater vibration obtained in our observation is about 0.2 sec as shown in Fig-11. This result is different from the result obtained at Algiers Harbor mentioned above.

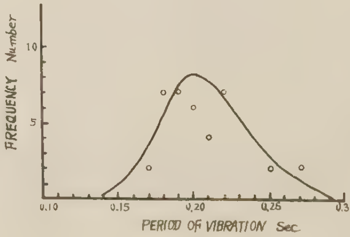

Fig-11

By comparing the observed period with the proper frequency of the accelerograph, it an be seen that the obtained records represent the acceleration and not the displacement. he displacement is more essential for studying the motion of the breakwater. But it was ot obtained. Only the existance of the vibration with the period of about 0.2 sec was ound in this observation.

The largest acceleration was caused by the largest wave pressure. The record is shown n Fig-8 with the largest pressure.

From the observation, two qualitative relations between the wave pressure and the reakwater vibration were obtained. The one is concerning the phase and the other is conerning the magnitude.

The vibration occurs at the regular positions against the one wave pressure curve as hown in Figs-12 and 13. In typical case, it occurs at each position corresponding to the tart, midway between the start and the peak, every peaks and the end of the wave pressure urve. There is one interesting phenomenon. In the case of a shock-type pressure, small ibrations of pressure almost always appear at the position of bourrage, corresponding to he vibrations of the breakwater, as shown in Fig-8.

The magnitude of the acceleration is plotted against the wave pressure at S. W. L. in igs-14~17. From these figures, it can be seen that the upper limit of the acceleration akes different value in each type. In A and D type, the limiting value increases linearly ith increase in wave pressure. Especially in type D, this trend of increase is remarkable.

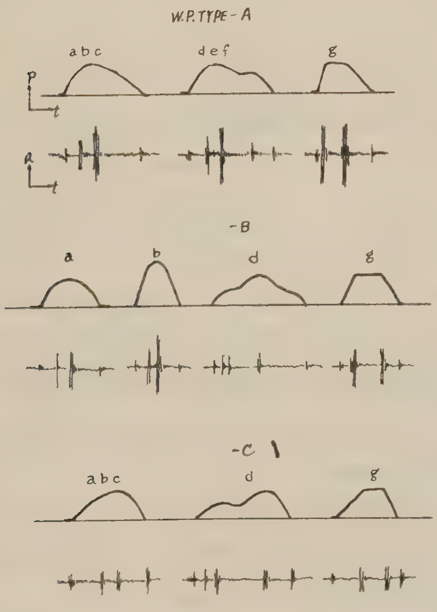

Fig-12

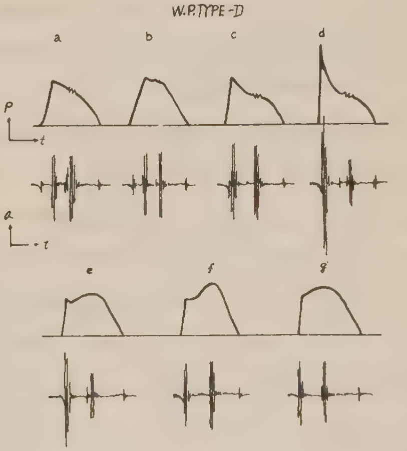

Fig-13

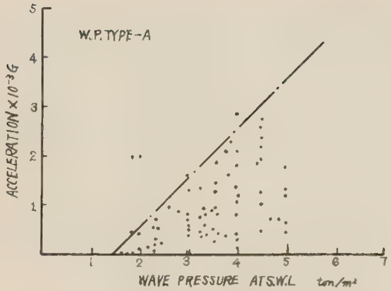

Fig-14

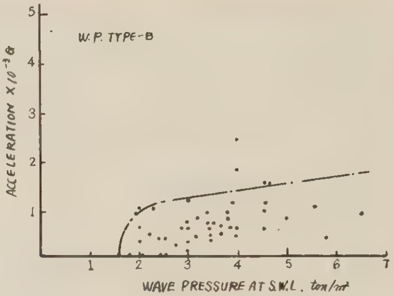

Fig-15

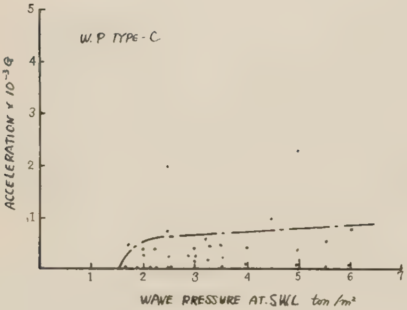

Fig-16

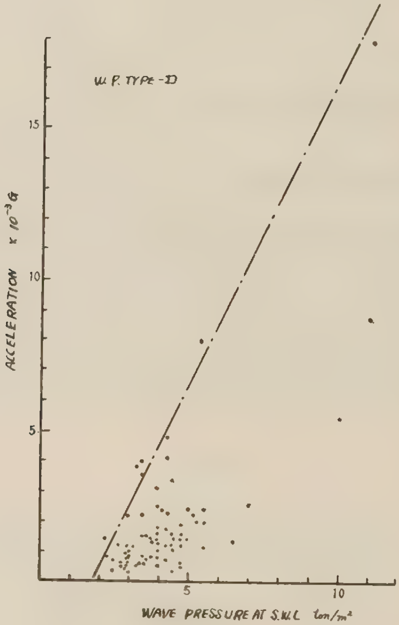

Fig-17

On the other hand, in B and C types, it increases little with increase in wave pressure.

7. Summary

In this paper, the authors discribed the purpose of this investigation, some explanations of measuring equipments used, and some results obtained in this observation. The pricipal qualitative results are as follows:

(1) Quite a wide variety of the shapes of wave pressure can occur, but they are classified into four types which are named by the symbols of A, B, C and D, in this paper. According to another way, they are classified into two types. The one is the nonbreaking wave type (steady wave type), which includes A, B, and C types, and the other is the breaking wave type, which is named by type D in the present paper.

(2) The values of frequency of each type A, B, C and D are 45, 27, 24, and 4 %, respectively. Although the breaking wave type D takes only 4 %, it should be noticed that the pressure of this type will easily occurs if some conditions are satisfied at the same time.

(3) The typical shocking type of wave pressure which was obtained in laboratory tests was

so observed in the natural sea.

) The maximum wave pressure at Haboro Harbor will be caused by the shocking type wave ich has the period of $7 \sim 9$ sec, and its magnitude will be $14 \sim 15$ ton/m^2.

) The maximum pressure is of the shocking type pressure. However, its acting time is ry short. Therefore, in order to investigate the stability of the breakwater, further vestigations should be made under the consideration of its acting time and influences on the breakwater.

) The observed period of the breakwater vibration which is caused by the wave pressure about 0.2 sec.

) The vibration of the breakwater occurs at regular positions of one wave pressure rve.

) D-type wave pressure causes larger acceleration of the breakwater vibration than the her types, and the value of its upper limit increases linearly with increase in wave essure.

At present, the further observations are to be continued. The available results con- rning the distribution of the wave pressure and the relations among the wave pressures, ve dimensions and breakwater vibration will also be obtained.

Acknowledgment

The authors wish to express their sincere thanks to Mr. N. Hiramatsu, Chief of Harbor vision, Hokkaido Development Bureau, and Mr. M. Ifukube, Chief of Civil Engineering search Institute, Hokkaido Development Bureau, for their guidance and suggestions.

References

1) J. R. Gerhardt, K. H. Jehn, and I. Katz: A comparison of step -, pressure -, and continuous-wire-gage wave recordings in the Golden Gate Channel, Trans. A.G.U. Vol.36, No.2, 1955.

2) T. Hamada and others: Wave forces against structure, A symposium of the council of coastal engineering, 1956 (in Japanese).

3) T. Hayashi and M. Hattori: Pressure of the breaker against a vertical wall, Coastal Engineering in Japan, Vol 1, 1958.

4) R. R. Minikin: Winds, Waves and Maritime Structures, 1950.

LABORATORY STUDY OF SAND MOVEMENT AND EQUILIBRIUM PROFILES OF BEACHES

K. Shinohara, Dr. Engineering
Professor of Hydraulics, Kyushu University, Fukuoka

T. Tsubaki, Dr. Engineering
Assistant Professor, Yamaguchi University, Ube

Introduction

When a sandy beach is subjected to attack for long hours by the uniform wave action efinite properties, the definite beach profile corresponding to the wave steepness will stablished. Since J. W. Johnson[1] has expressed this equilibrium profile as a dimension- form, a lot of researches on this profile have been reported. This profile is not influenced by initial wave steepness, but also by the size of bed materials and its inal profile. Among these factors, Y. Iwagaki and T. sawaragi[2] have recently reported t the effect of the size of bed materials. But the effect of the original profile is yet much clear, though it seems to be very important to make clear this effect when change of beach profile is studied from the standpoint of the equilibrium slope method. his paper the authors are to state some experimental results on the effects of the size ed materials and the original profile of beach upon the final equilibrium profile of h and sand movement.

Equipment and procedure

The experiment was carried out in a water tank of oreganic glass, stiffened with steel e works, 50 cm wide, 50 cm tall and 20 cm long. The methods of measurement of wave erties and collecting the sand transport are nearly the same as in the preceding paper.[3] experiment consists of following two parts.

riment 1. (Case 1)

Tests were conducted on beaches carefully molded to two different initial slopes, ly 1:10 and 1:20. Each beach was molded from two kinds of bed materials, whose median eters were 0.2 mm and 0.8 mm, and whose specific gravities were 2.66 and 2.65 respec- ly. The wave properties submitted to the experiment were 80 - 210 cm in wave length eep water, 2.1 - 7.1 cm in wave height and 0.0104 - 0.0790 in initial wave steepenss

Case 1-1. $D = 0.20$ mm, initial slope $I_0 = 1/10$, $\delta_0 = 0.0107 - 0.0672$

Case 1-2. $D = 0.20$ mm, initial slope $I_0 = 1/20$, $\delta_0 = 0.0108 - 0.0719$

Case 1-3. $D = 0.88$ mm, initial slope $I_0 = 1/10$, $\delta_0 = 0.0109 - 0.0613$

Case 1-4. $D = 0.88$ mm, initial slope $I_0 = 1/20$, $\delta_0 = 0.0104 - 0.0789$

The shape of beach profile was measured at every one hour in the case of 1:10 slope, and at every two hours in the case of 1:20 slope. The duration required for obtaining the equilibrium profile was ranged from 4 hours to 10 hours in the case of 1:10 slope and from 8 hours to 14 hours in the case of 1:20 slope.

Experiment 2. (Case 2)

In this experiment, the beach of 1:10 slope was molded, in the first place, from the sand whose median diameter was 0.2 mm, and then the beach was attacked by uniform wave action of a wave steepness δ_1. After the equilibrium profile was established by this wave action, this beach was attacked by uniform wave action of another steepness δ_2. New beach profile was measured at every one hour until the equilibrium profile was obtained. When the equilibrium profile was established, the shape of beach profile and the amount of change of shoreline were measured. The range of this experiment is as follows:

Case 2-1.	Initial slope 1:10,	$\delta_1 = 0.067$,	$H_1 = 5.33$,	$\delta_2 = 0.0104 - 0.0456$
Case 2-2.	〃	$\delta_1 = 0.011$,	$H_1 = 3.55$,	$\delta_2 = 0.0157 - 0.0666$
Case 2-3.	〃	$\delta_1 = 0.017$,	$H_1 = 3.98$,	$\delta_2 = 0.0101 - 0.0647$
Case 2-4.	〃	$\delta_1 = 0.022$,	$H_1 = 3.97$,	$\delta_2 = 0.0086 - 0.0598$
Case 2-5.	〃	$\delta_1 = 0.032$,	$H_1 = 5.02$,	$\delta_2 = 0.0090 - 0.0698$

3. The effect of the size of bed materials and the initial slope upon the equilibrium profile

Fig. 1a, 1b, 1c, 1d show dimensionless expression of the equilibrium profiles for the different wave steepness to make clear the effects of the size of bed materials and the initial slope of beach. The distribution of sand transport along the bed is also shown in this figure. From the figure we can see the difference in the location and the scale of longshore bar as the effect of the difference of the size of bed materials

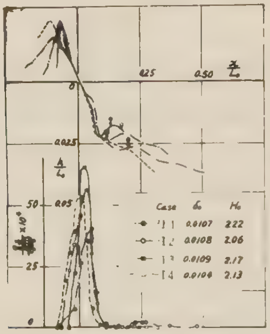

Fig. 1a

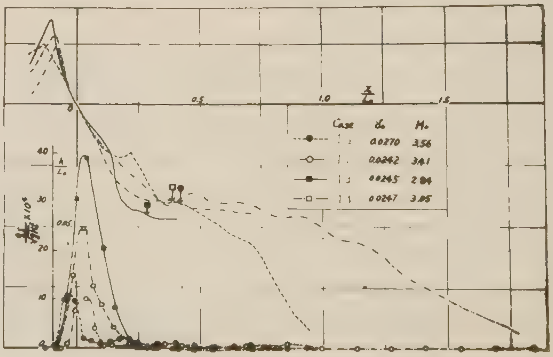

Fig. 1b

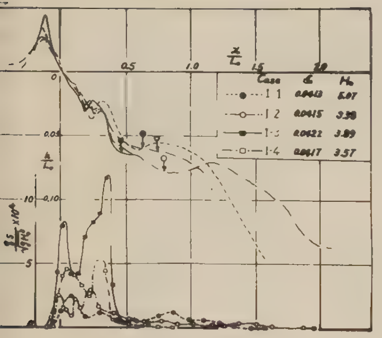

Fig. 1c

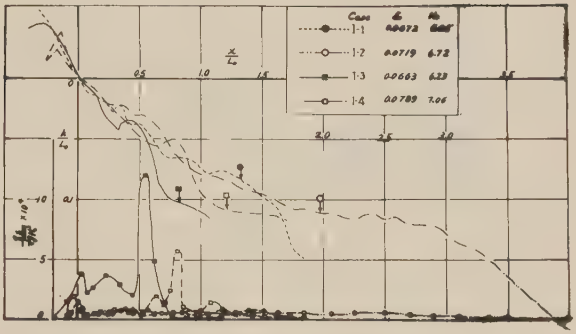

Fig. 1d

een 0.88 mm sand and 0.2 mm sand. Namely in the case of 0.2 mm sand, as the wave pness becomes steeper the suspended sand deposits in the offshore far from the break-point and forms large longshore bar. Local erosion and small bar are also seen near foam line. On the other hand, in the case of 0.88 mm sand, the range of sand movement imited in the parts between the shoreline and the breaking point. In the case of low steepness the amount of sand transport is concentrated near the shoreline. In the of large wave steepness, the distribution of sand transport of 0.2 mm sand is flat all range of movement, but that of 0.88 mm sand has two peaks, one is on the shore- and the other on the bar. These results agree with those of Iwagaki's experiment.

In the next place let us consider the effect of initial slope. In the case of 0.88 mm , the effect cannot be clearly conceived as the range of sand movement is limited be- the breaking point and the shoreline. In the case of 0.2 mm sand the beach profiles een the shoreline and the breaking point are nearly similar, but the profiles in the hore show some difference according to initial slope.

Fig. 2 shows the relation between the initial wave pness and the dimensionless expression of the amount and transport at the shoreline. From the figure we see the sand transport decreases rapidly as δ_0 becomes e.

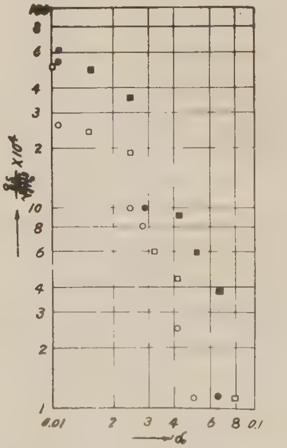

Fig. 2

Effect of the original beach profiles upon he equilibrium profiles

In this experiment the beach of 1:10 slope was molded the sand whose median diameter was 0.2 mm and then each was attacked by uniform wave action of a wave ness δ_0. After the equilibrium beach profile was lished by this wave action, this beach profile was

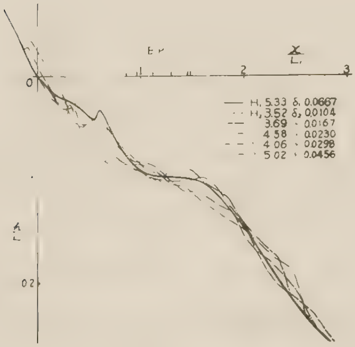

Fig. 3a

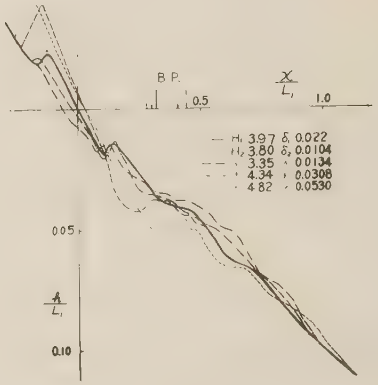

Fig. 3b

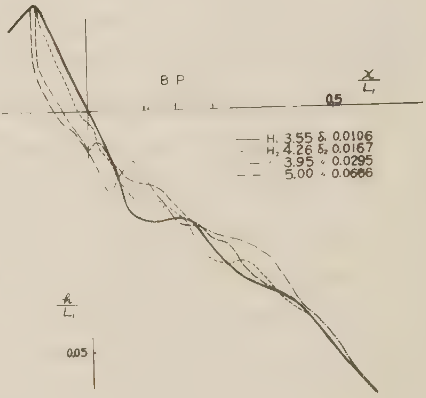

Fig. 3c

established by this wave action, this beach profile was attacked by uniform wave action of another steepness δ_2. Thus, the new equilibrium beach profile was established. Fig. 3a, 3b, 3c show these profiles.

In the Fig. 3a the original steepness of uniform wave action is 0.607 and the subsequent steepnesses are smaller than the original steepness, namely 0.01, 0.017, 0.023, 0.030 and 0.046. These are the case that the storm beach established by large steepness δ_1 is subjected to attack by wave action of smaller steepness than δ_1. From the figure, it will be seen that the sand drifts deposit near the shoreline, the shoreline moves towards the offshore and the longshore bar is eroded. The rate of this action is remarkable as the wave steepness becomes smaller. But, in the case of the wave steepness above 0.03, any changes in the shoreline or the foreshore are not seen. On the contrary, the surfzone is a little eroded and some deposits are found in the offshore. It seems that this comes from the movement of small bar made near the foam line of the original beach profile. We cannot see the remarkable change of the beach profile in this case.

In the Fig. 3b, the original steepness of uniform wave action is $\delta_1 = 0.022$ and this is such case that the beach lies between summer type and winter type. The subsequent wave steepnesses are 0.010 and 0.013 which are smaller than the original steepness δ_1, and 0.031 and 0.053 which are larger than the original steepness δ_1. In the case $\delta_2 < \delta_1$, we can see some deposits in the foreshore, movement of the shoreline towards the offshore and the erosion at the foam line and offshore part. When δ_2 is above 0.03 the erosion near the shoreline and the formation of bars in the offshore become remarkable.

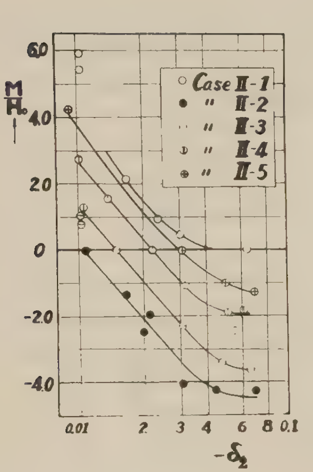

Fig. 4

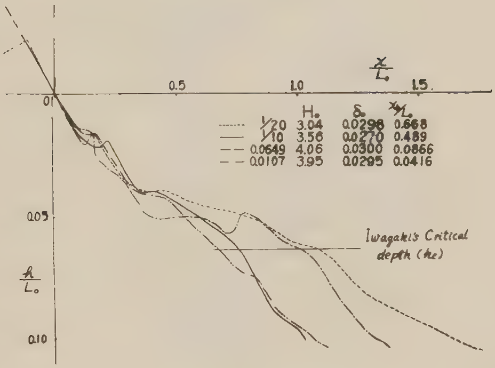

Fig. 5

Fig. 3c is the case that the beach established by the original wave steepness $\delta_1=0.01$ subjected to attack by waves of larger steepness δ_2 than δ_1. In this case we can see e erosion near the shoreline and the formation of bars in the foamline and offshore.

From these results, the relationships between the rate of change of shoreline M/H_0 the subsequent wave steepness δ_2 are shown in the Fig. 4 for the various original wave eepness δ_1. From the figure we can easily understand the shoreline moves towards offore or foreshore whether $\delta_2 \lessgtr \delta_1$. If δ_1 is given, M/H_0 varies directly proportional to δ_2 the range of $\delta_2 \leqq 0.03$, but it becomes approximately independent of δ_2 when $\delta_2 > 0.04$.

Fig. 5 shows the effect of the original profile upon the equilibrium profile. aches with initially different original profiles are subjected to attack by uniform wave tion of nearly equal steepness. From this figure we can see in the case $\delta_1 > \delta_2$ the original profiles still remain in the offshore part from the breaking point.

From these facts, it may be said that the equilibrium profile consists of two parts, mely, the part mainly established by wave steepness and the part subjected to the inuence of both wave steepness and the original profile. Thus, it comes that we cannot timate the equilibrium profile from the equilibrium slope method alone without any knowdge about the original profile.

Fig. 6 shows the relationship between wave run-up and wave steepness. In the figure ve run-up is expressed by dimensionless parameter R/H_0 and experimental results by R. P. vage[4] are also shown for the sake of comparison. From the figure we can see that wave n-up has the definite relation to the wave steepness, but it is independent of the orignal profile.

Fig. 7 shows the relationship between the slope of foreshore and the wave steepness. e figure includes also the results by Iwagaki. From the figure it may be clear that the

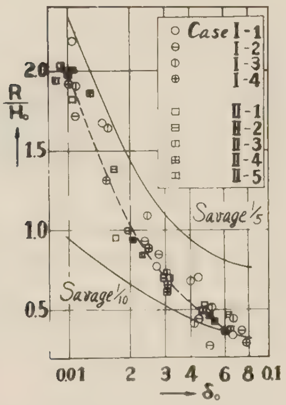

Fig. 6

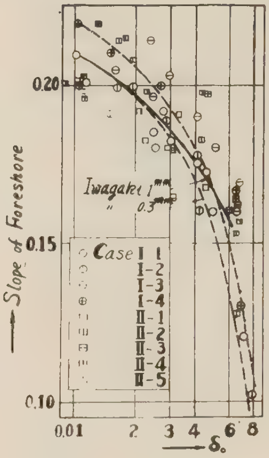

Fig. 7

slope of foreshore decreases as δ_0 becomes large and it is independent of the original prifile.

5. Conclusion

In this paper, the experimental results on the effects of grain size of bed materials and the original profile upon the equilibrium beach profile are reported and discussed. The following are the main conclusions.

(a) The equilibrium profile consists of two parts, namely the part established by wave steepness alone and the part subjected to the influence of the original profile. Generally speaking, the onshore profile from the breaking point is mainly subjected by the wave steepness and the offshore profile from the breaking point is subjected by both the wave steepness and the original profile.

(b) The wave run-up and the slope of foreshore change with the wave steepness and are independent of the original profile and grain size of bed materials.

References

1) J. W. Johnson : Scale Effect in Hydraulic Model Involving Wave Motion, Trans. A.G.U. Vol. 30, No. 4, 1949.

2) Y. Iwagaki and T. Sawaragi : Some Problems on the Equilibrium Slopes of Beaches, Dis. Pre. Res. Inst., Bulletin, Memo. Issue, 5th Anniversary, Nov., 1956.

3) K. Shinohara, T. Tsubaki, M. Yoshitaka and Ch. Agemori : Sand Transport along a Model Sandy Beach by Wave Action, Coastal Engineering in Japan, Vol. 1, 1958.

4) R. P. Savage : Wave Run-up on Roughened and Permeable Slopes, Proc. A.S.C.E., Paper 1640, 1958.

FUNDAMENTAL STUDIES ON THE DYNAMICS OF SAND DRIFTS

- Reports I and 2 -

Tojiro Ishihara, Dr. Eng., Professor of Hydraulic Eng., Kyoto University
Toru Sawaragi, Research Assistant, Kyoto University
Tetsuo Amano, Postgraduate Student, Kyoto University

Synopsis: The purpose of this study is to analyze theoretically and experimentally the motion of water particle near sea bed, especially in surf zone, in order to obtain the fundamental knowledge on the dynamics of sand drift. The current meter of unbonded gauge type is used for the experimental study. Furthermore, this study deals with the theory of net mass transport velocity of water particles in surf zone. Introducing the idea of bed load functions in alluvial channels, it is possible to explain the experimental results on equilibrium beach profile fairly well from the change of effective water particle velocity.

1. Introduction

It is one of the basic essentials to clarify the dynamic process of beach erosion by wave action for protection of beach and for pertient design of shore structures. Little literatures, however, have been published on the surf and bed material movement caused by wave action because of the complication in mechanism, and therefore no remarkable study has been done on this subject.

It is evident that the relationship between the characteristics of sand movement and the ones of waves, and the difference of the amount of sand movement depending on the above characteristics are of basic significance to reveal the beach process, and therefore the hydraulic behaviours described above has urged strongly the author's experimental project.1) The dynamical analysis for equilibrium bed profile and transport mechanisms of beach sand, however, have scarcely been analyzed for their complications. Since the changes of beach profile result from the movement of sand drift, it can be declared that this problem is solved only when the mechanics of movement and dynamical analysis on equilibrium bed profile are established.

There have not been remarkable studies on the mechanics of sand drift, but recently, Ippen and Eagleson 2),3) published several reports on the sorting of bed material, and the study on movement of water particles produced by the motion of oscillating plane is in its progress by Kalkanis[4]. In these studies, it is revealed that the gravity force and the dynamic forces like drag, lift and so on produced by the progression of waves take main parts as influential factors on the sediment particle. Furthermore, making the assumption taht the velocity change of water particle by wave action is sinusoidal at all points, they conclude that this velocity change determines the movement of sediment particles. Extrapolation of these studies for the flow on sloping beaches has not been made. It is not possible to analyze the mechanics of sand drift dynamically unless actual behaviours of fluid motion by wave are made clear, and consequently the author measured the movements of water particles at following five points on a model shore with smooth sloping bed by the use of the current meter of unbounded type[5].

1) Offshore on horizontal bottom, 2) Inshore, 3) Near breaking point, 4) Near plunging point, 5) Near shore line.

The measurement of spectra in velocity profiles by the oscillatory motion of wave were conducted at these points, and especially the following articles were investigated in details

(1) Changes in maximum particle velocity in the direction of depth: The data obtained will be useful to get the characteristics of wave and furthermore its characteristics, which used to be studied only in terms of its shape and celerity, will become more definite.

(2) Variations in maximumpparticle velocity along sea bottom: In this test, the transformation of incoming waves in their hydraulic characteristics is made, and the influence of wave transformation on the sorting action of sand is estimated.

(3) Change of water particle velocity in the course of time: With the sue of experimental data obtained, the time variation of particle velocity in classical theory of waves, which is still popular for engineering use, is investigated, and furthermore the contribution to analysis of sand drifts will be possible.

Using the spectra of velocity variation in wave flows the mass transport velocity of water, which will be largely related to the transport velocity of sediment particles verified by Ippen and Eagleson, is obtained, and the back currents near breaking point revealed from variations in mass transport velocity along sea bottom. With changes in effective water particle velocity along sea bottom, the authors will explain the fact, approved by several researchers, that the sediment transport depends on the steepness of deep water waves and the grain size of bed material, assuming that the amount of sand drift can be expressed by the same expression as in the bed load in river. Furthermore, the authors intend to take into some considerations of beach process based on the idea of critical steepness of es which has been proposed by S. Hayami.6)

Apparatus for experiments and procedures

Experimental flume used for tests.

The pictorial details of the ass walled flume at the Ujigawa raulic Laboratory, Disaster Preation Research Institute, Kyoto versity, are shown in Fig. 1. consists of steel framed channel 21.6 m long, 0.75 m wide and 2 m high, and the pneumatic ssure pump to generate the wave equiped. Steel bed of 5 m long 0.73 m wide with variable slope placed at one end of the flume, s forming a model beach. In this experiment, the slope of this steel bed was set at 06'. A by-pass valve is used for the pneumatic wave generator so that the pressure is othly adjusted, and thus waves generated in the flume varies their period from 0.7 to sec. The speed of revolution of the valve is regulated continuously by the Byer gover of 1/2 HP motor and the wave height can also be adjusted by the by-pass valve. This erator is capable of producing the maximum wave height of 0.2 m.

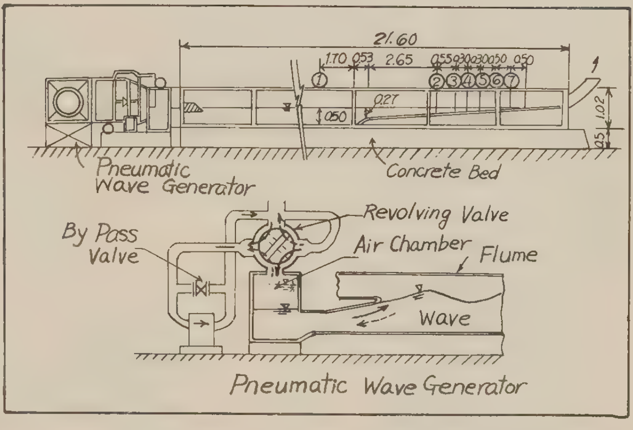

Fig. 1 Details of wave tank and wave generator

Current meter.

The measurement of velocity variation in wave motion was made by the current meter ch transformed the difference of dynamic to static pressures into the electrical difence of resistance. The actual velocity in wave motion is calculated by the output tage indicated in the meter. The capacitance gauge current meter has already been made M.I.T., whereas it seems to be unstable for measurements. Therefore, the meter is igned to transform the pressure difference into the change of electric resistance through strain gauge. The velocity changes are thus recorded in forms of continuous changes of ctrical resistance by the use of amplifiers and pen-oscillograph. The principles and uctures of the meter is explained in next paragraph, together with its characteristics.

This instrument transmits the strain of thin phosphor-bronze plate to unbonded type ge through a rod ⑧ set at the thin plate and the resulting strain is transformed into change in electrical resistance of unbonded gauge. The strain at the center of thin te which is subjected to pressure is expressed by the following equation which is an exssion for deflection at the center of flat circle plate fixed to the boundary under uniformly distributed load (Δp pressure difference in this case).

$$\delta_{max} = 3(1-\nu^2)\cdot \Delta p \cdot r^4/16Et^3 , \qquad \ldots\ldots\ldots (1)$$

where t: thickness of thin plate (mm), r: its radius, E: Youngs' modulus, ν: Poissons ratio, (t= 0.3 mm, r= 28 mm in this instrument).

Fig. 2 shows the details of the current meter of unbonded gauge. The portion of instrument described by ⑥ is interchangeable to either slender pitot tubes (3 mm diameter) or streamline headed flat type pitot tubes with slots (1 mm). depending on its purposes. Holes ⑨ and ⑩ are air outlet of the meter.

1	Diaphragm support
2	Cover
3	Support handle
4	Diaphragm
5	Cover
6	Pitot tube connector
7	Connecting rod
8	Connecting rod
9	Air outlet
10	Cap
11	Gauge box

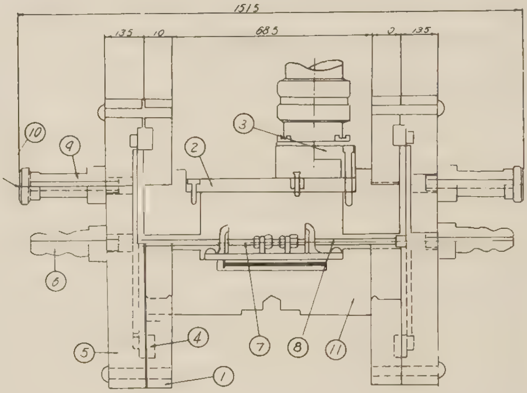

Fig. 2 Details of current meter of unbonded gauge type

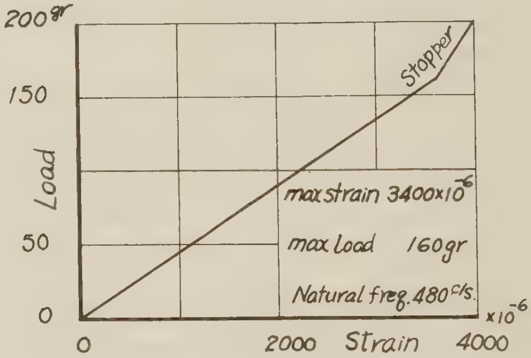

Fig. 3 Characteristic curve of U gauge of T-3 type

In all experimental runs, the pitot tubes of streamline headed type indicated good results for the measurements of water particle velocity in offshore zone where the pressure difference was small, and the slender pitot tubes demonstrated better results in the measurement of current velocity than the former tubes in onshore zone from breaking point where the pressure difference was so large that the irregular vibration caused by the surf gave much disturbances to the instrument. The U gauge of T-3 type was selected for this instrument because of its better linearity, sensitivity and stability than other types. Fig. 3 shows the characteristic curve of this gauge. The maximum input voltage is 5 V, in- and output resistances 128.1Ω, and natural frequency 480 c/s. The pressure load-strain relationship is shown in Fig. 4, and the maximum upper limit for measurement is

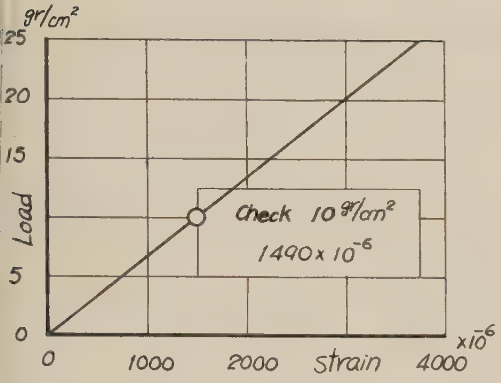

Fig. 4 Relation between strain and pressure

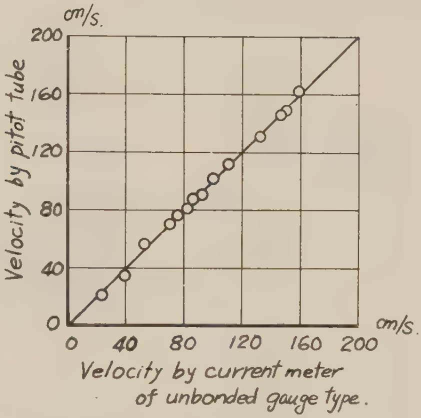

Fig. 5 Calibration curve of current meter

gr/cm^2. The strain at the check point of 10 gr/cm^2 (pressure difference) is 1490 x 10^{-6} /mm.

The calibration in velocities obtained by this instrument was made by comparison with ose obtained by the normal pitot tubes in the uniform open channel flows before conduc-ng the experiment.

Comparison of both velocities is indicated in Fig. 5, where the solid line indicates e perfect correlationship between two values. It is found that this instrument gives a ttle larger value than the normal pitot tubes and the difference is less than 2 %.

) Recording system and accuracy of measurements.

All records were taken by the amplifier system at Disaster Prevention Research Institute, oto University, and the system consists of pre-amplifier, D.C. amplifier and ink-oscillo-aph. The pre-amplifier contains an oscillator circuit, an amplifier and a phase discrimi-tor circuit, and amplifies 2,000 times the original input, while the D.C. amplifier ampli-es 400 times, so that the system gives 800,000 times amplification totally which means 118 gains. The accuracy of measurements depends on sensitivity of the recording system and aracteristics of the U gauge, and the later has a linear relationship as in Fig. 3 even der low load. Thus, the sensitivity of the recording system is comparatively reliable, and makes possible to measure flow velocity of 5 cm/sec within errors of less than 1 %, using e above amplifier system that operates an ink-oscillograph with full scale of 20 mm at 200 input, if the possible reading on the recording paper is as small as 0.5 mm. The time lag tween the current meter and the recording system was scarcely noticed after many checks. e results obtained with this whole system were good.

) Wave height meter.

The water level meter of resistance type was used in this experiment.

(5) Wave used for experimental runs.

Three kinds of experimental waves were chosen among a series of waves. The wave lengths were 4.46, 2.84 and 2.08 m and the heights 4.62, 6.02 and 6.81 cm when transformed to the deep water waves.

(6) Observation points.

Current velocities for above three waves were measured at points from ① to ⑦ shown in Fig. 1. The point ① locates in the region where the shallow water wave (h/L = 1/10 - 1/2. where L is the wave length at the water depth h) develops and ②, in the transitional region where h/L = 1/10, and ③ - ④, near the breaking points, ⑤ - ⑦ , in the region where the up-and backrushes prevail after breaking.

3. Analysis of experimental results and its consideration

(1) Variations in maximum velocities of water particle in vertical direction.

In classical treatment for engineering uses, wave heights, lengths, and celerities have been only subjected for theoretical and experimental studies on characteristics of waves in shallow waters and surf zone that might be of most important factors on the movement of sand drift. Although many studies on the variations in maximum velocities of water particles with the change of wave characteristics in surf zone, based on the wave theory in shallow water, have been made, it is impossible to discuss the movement of sand drift unless the water particle movement by wave action is studied, since the movement of sand drift is essentially a dynamic process in behaviour. From this stand point of view, the authors have made an experimental research on the changes in maximum horizontal velocities of water particles and compared the results with the varieties of wave characteristics which have been studied by many engineers.

With the use of the knowledge on shallow water wave theory, the horizontal component of particle velocity is expressible as

$$U = A \sin 2\pi \left(x/L - t/T \right) \qquad \cdots\cdots\cdots (2)$$

where

$$A = (\pi H/T) \cosh(2\pi z/L) / \sinh(2\pi h/L); \qquad \cdots\cdots\cdots (3)$$

derived by the theories of Airy's small amplitude wave and trochoidal wave. H,T,z, and L are wave height, period, distance from bottom, and wave length, respectively.

For h/L < 1/25, the waves are classified as long wave or solitary wave, and the maximum velocity of water particle is given by

$$U_{s\,max} = \sqrt{g(h+H)} \cdot H/(h+H) \qquad \cdots\cdots\cdots (4)$$

The wave characteristics, comparing the above theoretical values and experimental ones obtained in the experimental runs, will be treated.

Fig. 6 shows the variations in maximum horizontal velocities of water particles at us points in Fig. 1 in the vertical tion, and z/h is taken in ordinate he ratio of water particle velocity at height z to bottom velocity u_{bmax} scissa. The solid line in the figure e theoretical curve computed from the y of small amplitude wave and trocho- wave as in Eq. (4). All the measured es are the velocity of water particles rds shore.

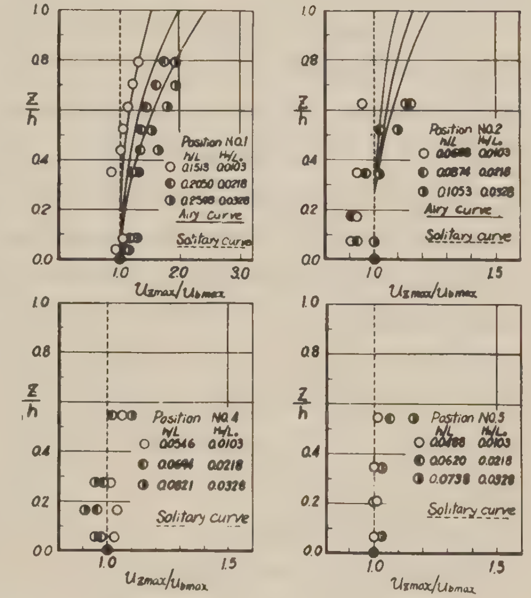

Fig. 6 Relation between u_{zmax}/u_{bmax} and z/h

It is seen in this figure that at rvation points where the relative depth, h/L, of incoming wave is in range of 1/10～1/2 the experimental es are rather agreed with results in shallow water wave theory curve, ite of various values in steepness. eans that the motion of water particles e indicated by the theory of shallow water wave, even when the wave configuration of waves characterized by small values of steepness in this range is smaller than that ng and solitary waves. At the observation point ②, however, where the wave characteris- are in the range of h/L = 1/25～1/10, experimental results do not agree with the curve allow water wave theory, and the waves becomes similar to the long waves in behaviours the velocity profile in waves becomes uniform. Nevertheless, the experimental curve ates a poor correlationship with the curve derived by solitary wave theory. From these ences, it will be concluded the motion of water particle due to the waves in this region ot be treated by both theories expressed by Eqs. (2) and (4).

Furthermore in shallower regions, no appreciable changes in water particle velocities bserved in the direction of water depth. At the point ⑤ however, where the water is shallow after passing breaking point, velocities near surface are greater than those bottom for waves with large steepness, whereas the velocity profile in waves with steepness, is largely characterized by the uniform distribution.

This evidence will result from the characteristics of breaking of waves. For large ness of waves, the breaking of waves is characterized by the formation of surface r with white bubbles known as the spilling, and consequently the particle velocity rds shore is larger in the upper layer than that in the lower layer. On the other hand, mall steepness, the wave breaks suddenly as plunging breaker, it maintains the characteristics of long waves and therefore the velocity change is not appreciable.

Fig. 7 shows the relationship between the vertical distribution of maximum velocities of water particles taking z/h in ordinate and the ratio of u_{zmax} to u_{smax} obtained from Eq. (4 in abscissa. This figure indicates the evidence noticed in Fig. 6 by slopes of empirical curves obtained by the experimental values. In the figure the solid line is the onshore one In the foregoing discussion, the comparison of the theoretical values in small amplitude wav theory expressed by Eqs. (2) and (3) to experimental values is not referred, but it can be revealed that the experimental value exceeds the theoretical value at all points. The onsho velocity is closely approximated by the value in solitary wave theory in the range from shor side of transition region to near breaking point, as in the point ④. This is verified by the results of field observation which the Beach Erosion Board has performed at water depths of 5∼15 ft.[7)]

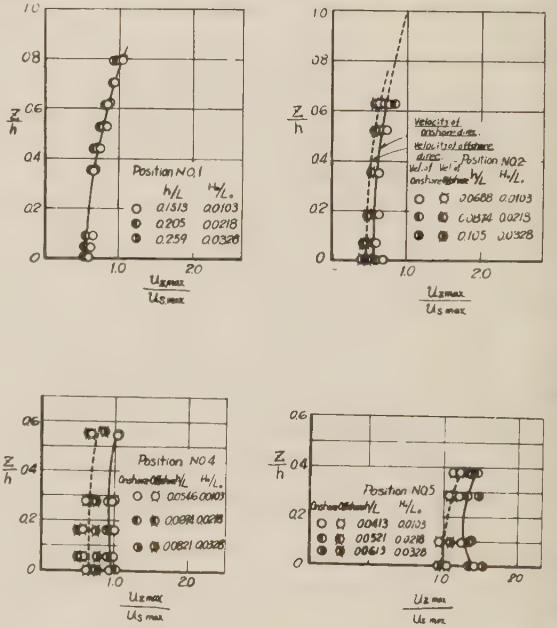

Fig. 7 Relation between u_{zmax}/u_{smax} and z/h.

Fig. 8 is the relationship between the dimensionless locations expressed by h/L_0 in abscissa and the ratio of maximum measured velocity of water particles at bottom, u_{bmax} to theoretical particle velocity by the solitary wave theory, u_{smax}. The breaking line is also shown in the figure for reference. It is seen that velocities at bottom approach gradually to those of long waves of finite amplitude and the coincidence of both values in velocity is obtained at the point a little near shore line from breaking point.

(2) Variations in maximum velocities of water particles by locations.

The fundamental ideas on sorting of sand due to wave action and the theory of critical wave steepness on equilibrium slopes of beach are mainly based on the variations of maximum velocity of water particles along the beach profile and of mass transport velocity of waves. Using these ideas, a graphical representation

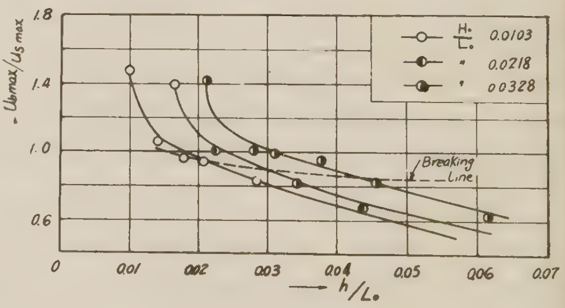

Fig. 8 Variation of u_{bmax}/u_{smax} at various locations

e relationship between the relative water depth h/L_0 expressed in the abscissa and the of maximum velocities of on- and offshore currents (u_{1zmax} and u_{2zmax}, respectively) to aximum bottom velocity u_{bomax} at a point of h = 50 cm in ordinate, (the maximum onshore m velocity and the maximum offshore bottom velocity are almost equal in their absolute s at a point of h = 50 cm.) is seen in Fig. 9. In the figure, the left one indicates elocity variations at bottom (z = 0), and the right one those at z = 2.2 cm. Generally, considered that larger sizes of sediment particles must be deposited near shore line the increase of difference between the maximum velocity of onshore current and the um velocity of offshore current.

As seen in 9, the dif- ce between /u_{bomax} and /u_{bomax} is near the ing point, endent of the ness. Fre- ly observed ring the observation diment at al coasts that verage diameter of particles at bottom are the largest at points near breaking point he sizes of particle become smaller in the offshore. This fact will result from the tion in velocities shown in Fig. 9. For the waves with large steepness (H_0/L_0=0.0328), e region of shore side from breaking point, the difference between u_{1zmax}/u_{2zmax} and /u_{bomax} at z = 2.2 cm is much greater than that at z = 0 cm, but for the waves with steepness (h/L_0 = 0.0218, and 0.0103), the difference between u_{1zmax}/u_{bomax} and u_{2zmax}/u_{bomax} = 2.2 cm and that at z = 0 cm are almost equal.

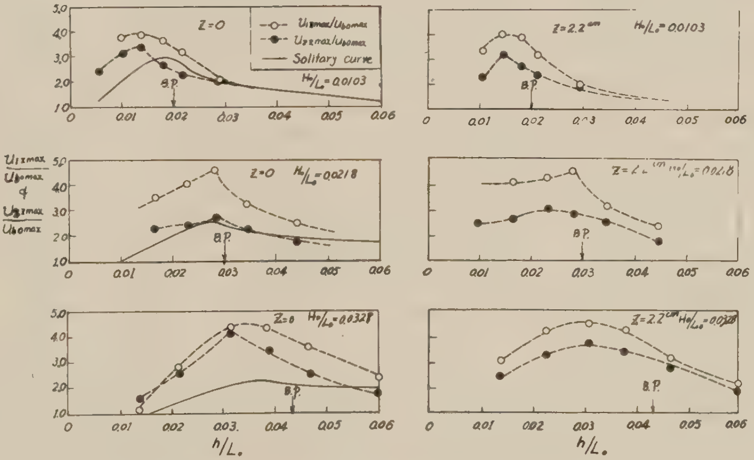

Fig. 9 Variation of maximum water particle velocity at various locations

From above descriptions and the distributions of mass transport velocity, the influence ich will be stated in (4) of this chapter, it is possible to clarify the difference in cteristics of current velocity with the changes in waves characteristics. The details be discussed in (4) of this chapter.

Variations of water particle velocity in course of time.

the previous sections (1) and (2), variations of maximum velocity of water particles e vertical direction at various locations are clarified and the sorting action of sand drift can be discussed using the results obtained. As stated in the introduction, however, the change of particle velocity in the course of time, namely the acceleration of water particles, must be completely treated to establish the dynamic relationship of forces like drag and resitive forces to sand drifts.

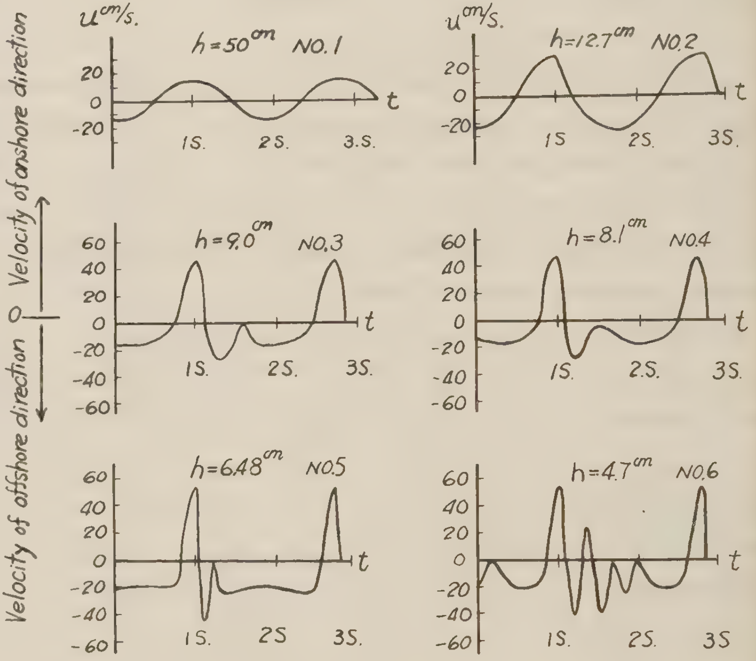

Fig. 10 Water particle velocity in the course of time

In Fig. 10, the time changes of water particle velocity at bottom of observation points are indicated for the wave with steepness of $H_0/L_0=0.0103$, and the velocity change in the onshore direction is given in the upper domain above abscissa and that in the offshore direction below abscissa. Evidently seen in this figure, within the range of shallow water waves, the onshore velocity possesses its maximum value at the crest of wave, whereas the offshore velocity its maximum value at the trough, forming a sinusoidal variation. This curve is not completly sinusoidal and the slightly large value on onshore side is indicated. The fact corresponds to the bottom velocity difference betwe on- and offshore currents in the wave theory of Stokes, which is indicated in Eq. (5).

$$\Delta u = 3C\cdot\left(\frac{\pi H}{L}\right)^2 \frac{\coth(2\pi h/L)\{\coth(2\pi h/L)-1\}}{\sinh(4\pi h/L)} \qquad \cdots\cdots\cdots (5)$$

The ratio of the maximum bottom velocity of onshore current u_{1max} to that of offshore current u_{2max} expressed by Eq. (6) is compared with the experimental results and illustrate in Fig. 11.

$$\begin{matrix} u_{1max}, \\ u_{2max}, \end{matrix} = C\left[\frac{\pi H}{L}\,\frac{1}{\sinh(2\pi h/L)} \pm \frac{3}{2}\cdot\left(\frac{\pi H}{L}\right)^2 \frac{\coth(2\pi h/L)\{\coth^2(2\pi h/L)-1\}}{\sinh(4\pi h/L)}\right]; \quad \cdots (6)$$

where C is the cerelity of wave.

As seen in Fig. 10, the wave is transformed gradually asymmetric in its shape when progressing to the shore line. The theoretical velocity given by Eqs. (2), (3) and (6) can be applied only to the shallow water waves in the range of h/L = 1/10~1/2. Since the celeration of onshore current increases as it moves om transition region to shore, whereas the acceleraon of offshore current becomes comparatively smaller, is impossible to analyze the motion of water particle this region, under the assumption that the particle tion is sinusoidal.

The depth-wise distribution of acceleration is rticularly considered to be one of significant factors at indicate the movement of sand drift. Therefore, e further theoretical and experimental studies to tablish this relationship are distinctively needed.

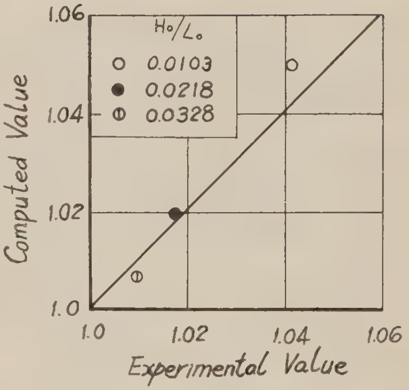

Fig. 11 Comparison of observed data with computed results on u_{1max}/u_{2max}

) Mass transport velocities.

The variations of water particle velocities described in section (1), (2) and (3) have important influence on the instant motion of sand particles, and especially it is easily derstood that the water mass movement in one period will take an important part for analysis net sand transport in the same duration. Eagleson, Dean, and Paralta[3] have derived the lation between net velocity of sand movement and water mass transport velocity.

As the first step for this purpose, the distribution of mass transport velocities in ter of 50 cm uniform depth in which the waves are characterized as shallow water wave, will treated by the use of experimental data and theoretical results of Hamada, Sato, and nguett-Higgins.[8] The theory of Hamada is derived by an extension of Stokes' theory in shallow water and the resulting equation is indicated in Eq. (7). Eq. (8) is derived by Sato, and . (9) is the solution of boundary layer equation for velocity of mass transport obtained der the condition that the surface undulation is expressible as Eq. (10).

Hamada's Solution: $$\bar{U}(z)=k^2\left(\frac{H}{2}\right)^2\cdot C\cdot(\cos kh/\sinh^2 kh)\cdot\sinh kz\cdot\cosh kz; \quad \cdots\cdots (7)$$

Sato's Solution: $$\bar{U}(z)=\left(\frac{1}{2}\right)k^2\left(\frac{H}{2}\right)^2\cdot C\cdot\cosh 2kz/\sinh^2 kh, \quad \cdots\cdots\cdots (8)$$

Longuett-Higgins's Solution: $$\bar{U}(z)=\frac{a^2\sigma\cdot R}{4\sinh^2 kh}\cdot\left[2\cosh 2kz+3+kh\sinh 2kh\cdot\left\{3\left(\frac{z}{h}\right)^2+2\cdot\frac{z}{h}\right\}+3\left(\frac{\sinh 2kh}{2kh}+\frac{3}{2}\right)\left\{\left(\frac{z}{h}\right)^2+\left(\frac{z}{h}\right)\right\}\right], \quad \cdots\cdots\cdots (9)$$

$$\eta=a_1\cos(kx-\sigma t)+a_2\cos(kx-at), \quad \cdots\cdots\cdots (10)$$

ere

$$a=H/2,\quad \sigma=2\pi/T,\quad \bar{U}(z)=(1/T)\cdot\int_t^{t+T}u\,dt \quad \cdots\cdots (11)$$

vertical distributions of mass transport velocities for the offshore waves with the lues of 0.0328 and 0.0103 in steepness at point ① are shown in Fig. 12 and it is seen at Eq. (7) indicates a good agreement with the experimental values for the wave of high steepness (0.0328), whereas Eq. (8) is a better expression for the wave of low steepness (0.0103). Consequently, it will be concluded that for steep waves ($H_0/L_0 = 0.0328$) the mass transport velocity approaches zero at bottom and rapidly increases in the upward direction, whereas for gentle waves ($H_0/L_0 = 0.0103$) the onshore velocity is appreciable in a form of nearly uniform distibution. Therefore, Longuett-Higgins's equation derived under the assumption that the total mass transport is zero at all cross sections and the wave shape is represented as clapotis as seen in Eq. (10) can not agree with the experimental data obtained in the region where the backwash is not predominant.

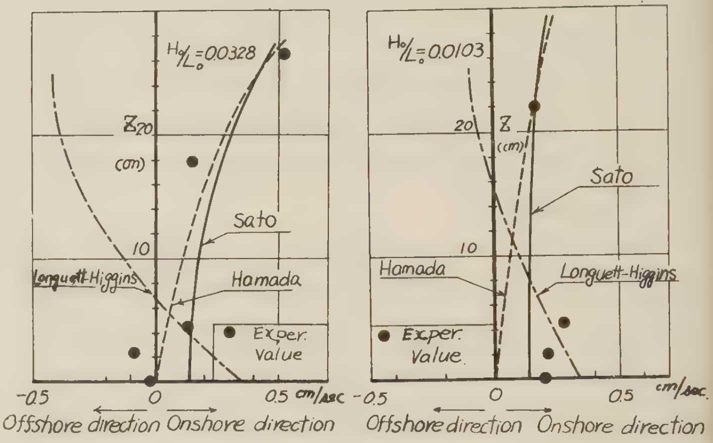

Fig. 12 Variation of mass transport velocity in vertical direction

The depth-wise variations in mass transport velocities at onshore side from the transition region are next concerned. Values of mass transport velocities at bottom in the region where it is pressumed that the influence of undertow after breaking becomes appreciable are zero when calculating by Eq. (7), whereas positive in Eq. (8). These two equations, consequently, are not suitable for computations of net mass transport velocities including the mass transport by the undertow.

Now, assuming that a constant and uniform back current is produced in the whole depth the velocity $\overline{U}_b$ of back current is expressible by the continuity theorem as follows.

$$(1/hL)\int_0^L dx \int_0^h (U+\overline{U}_b)\,dz = 0, \qquad \text{. . . . . (12)}$$

$$\overline{U}_b = (1/h)\int_0^h \overline{U}(z)\,dz = (a^2 k\cdot C/2h)\cdot\coth kh, \qquad \text{. . . . . . . (13)}$$

where $\overline{U}(z)$ is the mass transport velocity expressed by Eq. (8) and $a = H/2$. Fig. 13 shows the comparison of experimental values to computed values by Eq. (8), putting $\overline{U}(z) = \overline{U}_0$ at $z = 0$ and $\overline{U}_0 - \overline{U}_b' = U_c$ and C_0 the wave cerelity in deep water. It is seen that both curves are similar in their behaviours,

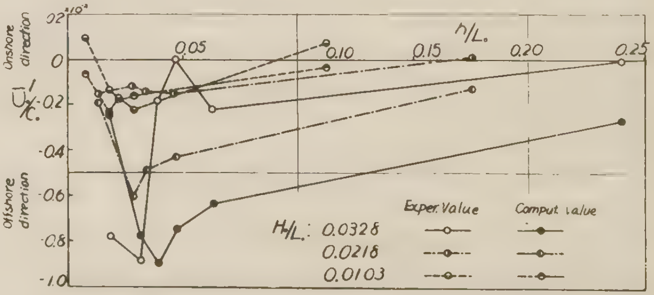

Fig. 13 Variation of mass transport velocity at bottom

therefore it is found that the velocity of undertow shown by Eq. (13) must be included omputation, in order to clarify the flow behaviours in onshore side of breaking point h is largely influenced by the undertow.

The vertical distribution of mass transport velocities at a point, where the influence ndertow becomes appreciable, is expressed as follows, using Eq. (8) and Eq. (13):

$$\bar{U}(z)=\frac{\pi}{4}\left(\frac{H}{L}\right)\left\{2\pi\left(\frac{H}{L}\right)\cdot\frac{\cosh(4\pi z/L)}{\sinh^2(2\pi h/L)}-\frac{H}{h}\coth(2\pi h/L)\right\}\cdot C \quad . . . . . . (14)$$

Fig. 14 indicates the computed values Eq. (14) for the vertical distribution ass transport velocity with the experi- al data, and it is evidently seen that od agreement is obtained.

As the results, the onshore current eds the offshore one at the surface of r, while the latter exceeds the former he bottom, in the shore side of break- point, for all incoming waves. This ence has already noticed in the report ield observation of Eaton, Inman, and n.[9]

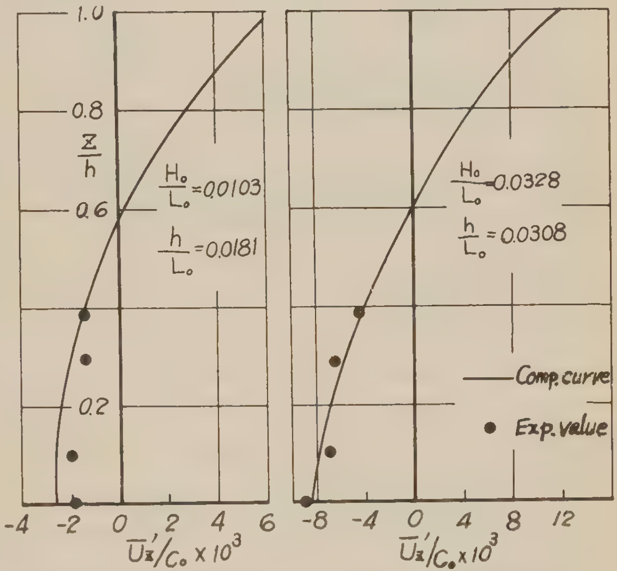

Fig. 14 Vertical distribution of $\bar{U}'(z)/C_0$

The influence of wave characteristics on U'(z) by the use of Eq. (14) is indicated in 15, where values for U'(z) are plotted in solid line for gentle wave of $H_0/L_0=0.0103$ in dotted line for steep wave of $H_0/L_0=0.0328$, when h and H_0 are constant. It is seen his figure that the difference between $\bar{U}'(z)$ at surface and that at bottom is not so inct for gentle wave, while for steep wave, there exist remarkable onshore currents at ace and offshore currents at bottom. The states of currents, therefore, are mainly in- nced by the steepness of breakers, and it will be the basis of Hayami's idea on critical steepness. The water depth z, at which $\bar{U}'(z)$ transforms from positive to negative , it computed by Eq. (15):

$$\cosh 2kz_0=(1/2kh)\cdot\sinh 2kh, \quad . . . . (15)$$

Consequently, z/h is little influenced by h/L and 0.56∼0.60 for all values of H_0/L_0 as in Fig. 15.

In the present chapter, the behaviours of water particle in wave motion, being mainly ential on the movement of sand, have been discussed. The movement of sand particles on

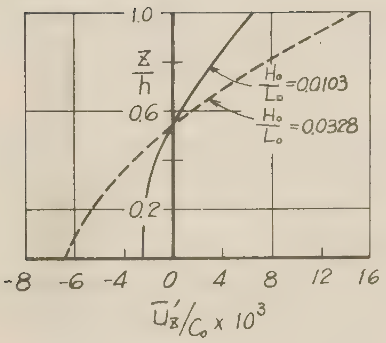

Fig. 15 Effects of H_0/L_0 on $U'(z)$ in case of constant H_0 and h

beach bottom will be treated by means of the preceding concept of mass transport velocity in wave motion. The experimental investigation described in the foregoing, however, is still preliminary, and the complete clarification of the hydraulic behaviour in wave motion is not made. After the real success of the present experimental study is obtained, the dynamic relationship of sand movements in terms of the introduction of mass transport velocity will be certainly established.

However, the engineering need arising from the rapid progress of coastal works urges also to make a relationship of sand movement in dimensional or empirical fashions, so that the transportation of sand drift will be concerned in the following, as an attempt being derived under the assumption that the movement of sand drifts in wave motion will be similar as that in open channel flows.

4. Remarks on mechanisms of sand drift motion

The evaluation of u_c in waves which are mainly characterized by the acceleration term has not been made at all. Hence, the emperical relationships between the critical frictional velocity u_c* and $\sqrt{sgD}$ in open channel flows will be used for the reciprocal movement of sand drifts in wave motion as engineering approximation. Referring to the study on the critical condition of sand drifts by Shinohara, Tsubaki and Yoshitaka,[11] the mean value of ratio of u_c* to $\sqrt{sgD}$ is approximately 0.235, and the ratio of representative flow velocity acting on sands to the critical frictional velocity is 8.5. Therefore the following equation is obtained;

$$u_c/\sqrt{sgD} = 1.85, \qquad \cdots\cdots\cdots \quad (16)$$

where s: specific weight of sand in water, g: acceleration of gravity, D: diameter of sand particles.

Table 1 describes the values of critical flow velocity for various sizes of sand grains.

D(mm)	u_c(cm/s)
0.1	7.4
0.3	12.8
0.5	16.5
1.0	23.4
2.0	33.0
4.0	46.7

Table 1 Critical velocities for particular sizes of sand grains

When the water particle velocity caused by the wave action exceeds the critical velocity, the sand initiates to move. In the behaviour of sand movement, of essential significance is that the relationship between the amount of sand drift and the motion of water particle must be established. However, no studies on the amount sediment transport in unsteady

ave been made and futhermore
erical formulas also have been
l in explicit forms. Therefore,
umption is made here that the
cal relation for sediment
ort in rivers applicable to
ow in wave motions, and thus
llowing equation is used for
tion of the amount of sand

$$q_B/u^*D = A(u^{*2} - u_c^{*2}) \quad . . . (17)$$

q_B is the amount of sediment
ort per unit time, u* is
tional to u as stated before,
s a numerical constant and approximately unity by experimental data, when $(u^{*2} - u_c^{*2})$
umed not to be large[10]. Eq. (17) can therefore be rewritten as follows, for a partic-
ize of particles.

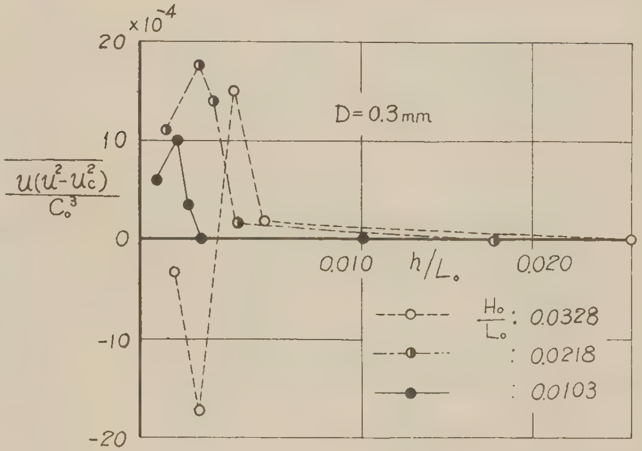

Fig. 16 Relation of $\overline{u(u^2 - u_c^2)}/C_o^3$, h/L_o and H_o/L_o in case of D = 0.3 mm

$$q_B \propto u(u^2 - u_c^2), \quad . . . . (18)$$

enoting the average amount of drifting sand in one period by $\overline{q_B}$, it can be expressed

$$\overline{q_B} = (1/T)\int_t^{t+T} q_B\, dt \propto \overline{u(u^2 - u_c^2)}, \quad . . . . (19)$$

e average amount of sand drift at a point can be estimated, if $\overline{u(u^2 - u_c^2)}$ are obtained
ious locations along the beach profile as shown in Figs. 16 and 17, which indicate the
ental results for D = 0.3 mm and 0.5 mm, respectively.

e experimental wave steepnesses
e 0.0328, 0.0218 and 0.0103.
. 16 and 17, the positive slope
es the process of deposition,
he negative one that of erosion,
the sand ridge will develop at
where the sign of slope
rms from positive to negative.
e discrimination between depos-
nd erosion regions in the beach
is therefore made by the use of
6 and 17, and it is indicated in

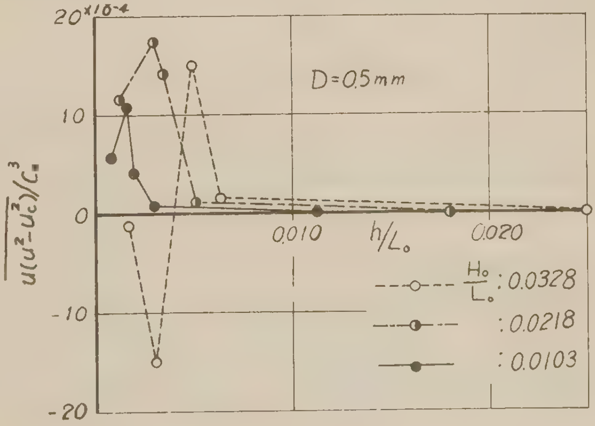

Fig. 17 Relation between $\overline{u(u^2 - u_c^2)}/C_o^3$ h/L_o and H_o/L_o in case of D = 0.5 mm

Fig. 18 for the case of D = 0.5 mm. As seen in Figs. 16 and 17, the sand ridge is developed only by the steep wave of $H_o/L_o = 0.0328$ and its location is in the region of $h/L_o = 0.03 \sim 0.05$. On the other hand, when the incoming waves are gentle ($H_o/L_o = 0.0218$ or 0.0103), the sand ridge can not develop, despite of all particle materials in size, and furthermore the sand moves towards the shore line, which may explain the gradual progression of shore line. The location of sand ridge formed and the beach deformation estimated by the dynamic relationship of particle movement in waves can be verified by the experimental results of equilibrium beach profile obtained before, as seen in Fig. 19.

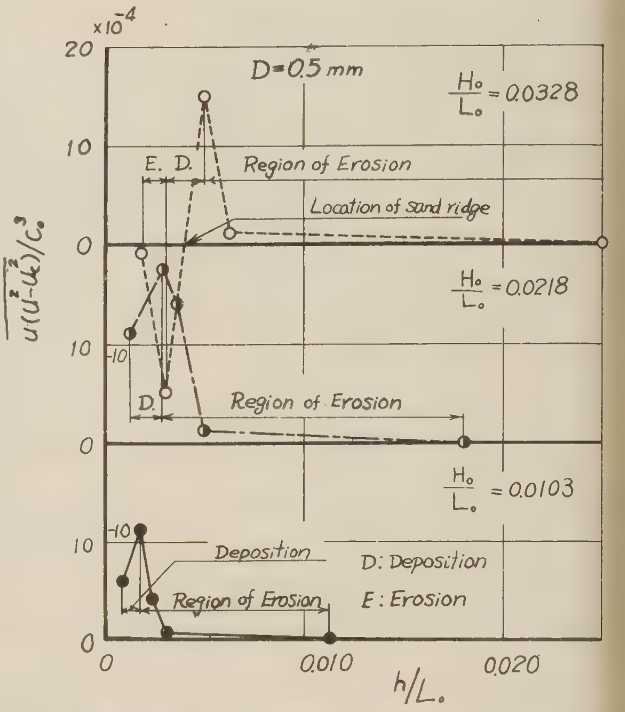

Fig. 18 Beach process estimated by the variation of $u(u^2 - u_c^2)/C_o^3$ at various locations in case of D = 0.5 mm.

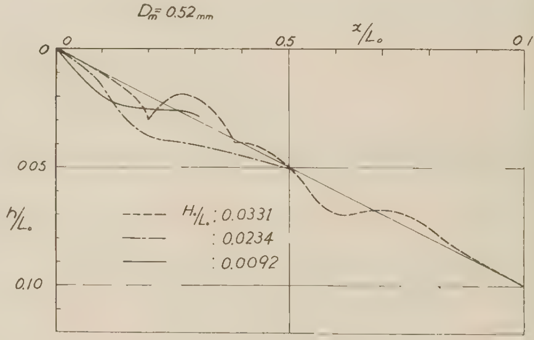

Fig. 19 Equilibrium beach slope for D = 0.5 mm

Adding to the above study, the estimation of beach process in deposition and erosion is described in Fig. 20, under the assumption that the amount of sand drift is proportional to the effective water particle velocity $(u - u_c)$, in which

$$\overline{(u-u_c)} = (1/T)\int_t^{t+T}(u-u_c)\,dt \quad \cdot\cdot \quad (20)$$

In Figs. 18 and 20, it is seen all curves for beach process are similar in both cases. The available formula for estimation of the amount of sand drift is not obtai up to the present time. However, the mechanisms of beach deformation only studied in conne tion with the steepness for deep water waves can be sufficiently explained by means of the idea of water particle velocity subtracted by the critical velocity u_c which is mainly influential on the movement of sand particles.

nclusions

ne velocities of water particles in off- and onshore regions, surf zone and shore side aking point were measured with the use of the current meter of unbonded gauge type to igate the mass transport velocity of

The actual behaviour of undertow in ore side of breaking point was also ied. Although the mass transport ty is mainly influential on the nt of sand drifts, the present study reliminary project of the whole pro- n the dynamic establishment of move- f sand drift can not reveal the basic c principle, so that the authors n attempt to estimate the beach ation in similar forms of bed load ons in alluvial channels, with results larification in beach deformation s.

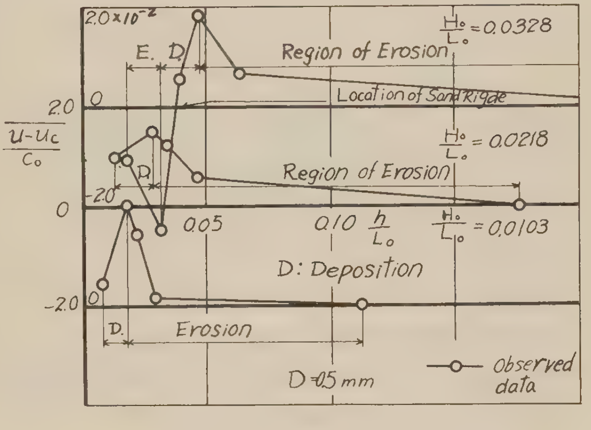

Fig. 20 Beach process estimated by the variation of $\overline{(u-u_c)}/C_0$ at various locations in case of D = 0.5 mm

ne authors intend to obtain the comprehensive solutions for mechanisms of shore line n by analyzing further the complicated behaviours of time variation of water particle ties in the onshore side of transition region where the sand drift movement becomes e, of the critical flow velocity of sand particle in fluid characterized by continuous preciable change in accelerations, and of the amount of sand drift transported.

t is a pleasure to record here the authors' gratitude to Assist. Professors Y. Iwagaki, ihara, and Y. Iwasa as well as Mr. J. Yamaguchi, for their very useful suggestions, isms, and cooperations.

Reference

agaki, Y. and Sawaragi, T.: Experimental study on the equilibrium slopes of beaches d sand movement by breaker; Trans. of Coastal Engineering in Japan, J.S.C.E., Vol. 1, 59 pp. 75~84.

pen, A.T., and Eagleson, P.S.: A study of sediment sorting by waves shoaling on a ain beach; M.I.T. Hydrody. Lab. Tech. Report No. 18, 1955, pp. 1~83

gleson P.S., Dean R. G., and Peralta, L.A.: The mechanics of the motion of discrete herical bottom sediment particles due to shoaling waves: M.I.T. Hydrody. Lab. Tech. port No. 26, 1957.

4) Kalkanis, G.: Turbulent flow near an oscillating wall; Beach Erosion Board, Tec. Memo. No. 97, 1957, pp. 1~37.

5) Ishihara, T., Sawaragi, T., and Amano, T.: Fundamental studies on the dynamics of san Drift, 1st Rep. Proc. of 5th Conference of Coastal Engineering in Japan, 1958, pp. 65~ 71 (in Japanese).

6) Hayami, S.: Types of breakers, wave steepness and beach slope; Trans. of Coastal Engineering in Japan, J.S.C.E., Vol. 1, 1959, pp. 21~24.

7) Inman, D. L. and Nasu, N.: Oribital velocity associated with wave action near the breaker zone; Beach Erosion Board, Tech. Memo. No. 79, 1956.

8) Longuett-Higgins, M. S.: Mass Transport in Water Waves; Proc. Roy. Soc. A., Vol. 245, 1953, pp. 66~581.

9) Inman, D. L., and Quinn, W. H.: Currents in the Surf Zone; Proc. of 2nd Conference of Coastal Engineering, Nov. 1951, pp. 24~36.

10) Hom-ma, M., and Ishihara, T.: Applied Hydraulics, Maruzen, Tokyo, Vol. 2-1, 1958, pp. 27~34, (in Japanese).

11) Shinohara, K., Tsubaki, T. and Yoshitaka, M.: Sand Transport along a Model Sandy Beach by Wave Action; Trans. of Coastal Engineering in Japan, J.S.C.E., Vol. 1, 1959 pp. 111~130.

FIELD INVESTIGATION OF SUSPENDED SEDIMENT BY THE USE OF BAMBOO SAMPLERS

Hisoa Fukushima, Dr. Science
Professor of Hokkaido University, Sapporo

Masakazu Kashiwamura,
Lecturer of Hokkaido University, Sapporo

Introduction

In 1957 and 1958 the present authors investigated the suspended littoral drift at makomai, where the industrial harbor is now under construction. The city is located on e southern coast of Hokkaido as shown in Fig. 1. The suspended sediment in the nearshore ea was captured by bamboo samplers which have been employed the authors in past several years for the investigation of nd movement along the coast of Hokkaido.1)2)

A certain number of bamboo poles were vertically set in e sea for a few days. They were drawn up carefully, so at the sediments captured in the bamboo samplers would not ow out from holes. Samples of sediments were then packed polyethylene sacks. The sediment was desiccated, and ighed in the laboratory.

The time intervals of setting were as follows:

1957; from 10.00~12.00 A.M. Aug. 2 to 2.10~12.00 A.M.
Aug. 7 (120 hours)

1958; from 10.00~11.30 A.M. Aug. 27 to 12.00 A.M.~2.00 P.M.
Aug. 29 (50 hours)

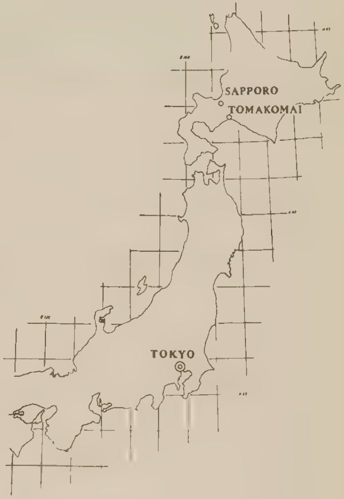

Fig. 1

e distribution of samplers are shown in Fig. 2. The mean tidal range in this area is

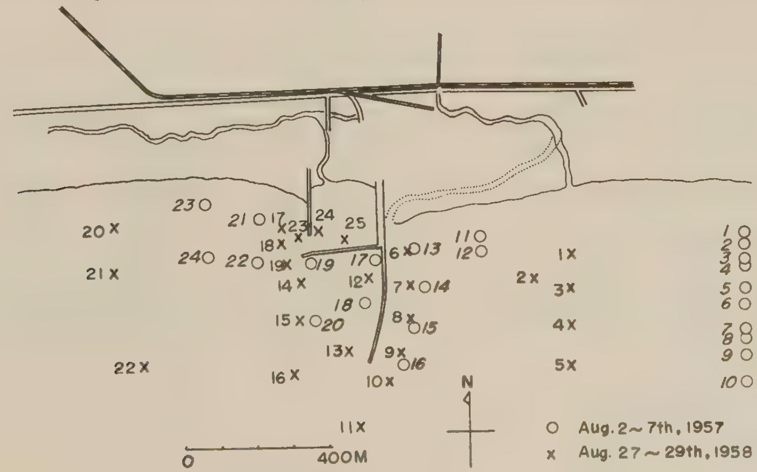

Fig. 2

about 1 meter. During the each interval of observations, the wave heights were respectively 0.8 m~0.4 m (1957) and 1.0 m~0.3 m (1958).

2. Vertical distribution of suspended sediment.

As yet few investigations have been made about the vertical and lateral distributions of the suspended sediment in the nearshore area.[2] Some examples of the vertical distributions of the mass of the sediment load captured by samplers are shown in Fig. 3. The relation between the mass and the height of hole from the sea bed is plotted on semi-log sheets.

In most cases each curve has a bending point which shows that there exists a 'Sprungsschicht' of suspended sediment about 1 m above the sea bed. In the upper layer the increase of the mass per 1 m (height) is much less than in the lower layer. The absolute value of the mass is also larger in the lower layer. Some curves, however, show that the suspended sediment is somewhat decreased near the surface. Perhaps on account of tidal range and wave motion of the surface water, holes at the upper part of the sampler can not always capture the suspended material. Furthermore, they are sometimes exposed to the air and lose the material which is once captured by bamboo poles.

Grain-size analysis was made by sieving the samples in order to study the size distribution of the captured sediment. As will be seen in Fig. 3, the suspended sediment in each depth contains various grades of size in a similar proportion. This fact is nothing but a feasible support of the actual existence of the double layer.

The vertical distribution of mass thus obtained are classified into the following four types which are shown in Fig. 4.

Type I. This type of distribution is understood to be the typical one which appears in natural sandy coasts. The double layer, mentioned above, can be seen in this type of distribution. The slopes of the curve are 0.23 and 7.60 per meter of the depth in the upper and lower layer, respectively. Sometimes the mass decreased suddenly at the surface in the upper layer.

Type II. This type appears at the corner where a sandy coast and a breakwater meet together. As the energy of waves concentrates here, the turbulence of sea water is quite

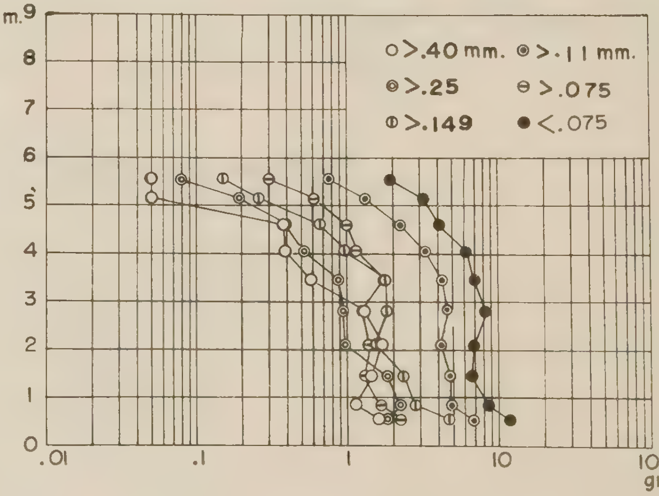

Fig. 3

arkable and the curves of the er layers are steeper than in case of type I. The curve of er layers is somewhat convexed the right showing that the sedi- t load is poured into the corner ough the samll river indicated in . 2.

Distribution curves in this trict show larger values as com- ed with type I. If an observation made at several points between sampler of No. 1 and the shore- e, the curves in this zone must be ilar to the distribtuion of type II.

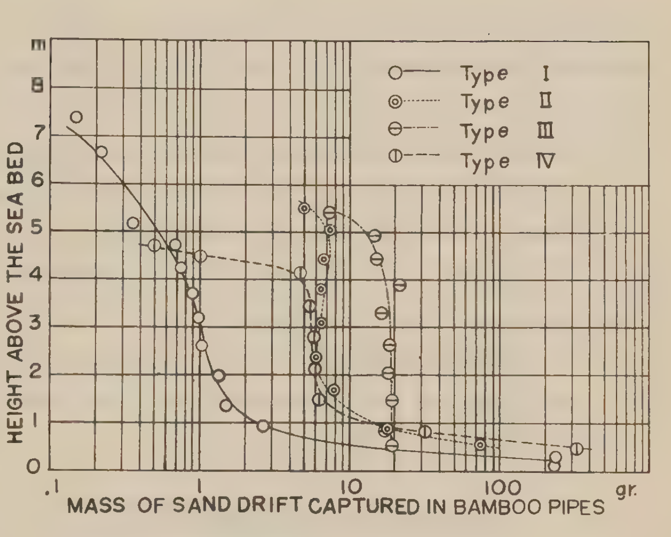

Fig. 4

Type III. Five curves observed at points of No. 16∼No. 20 belong to the distribution type III. They do not have the lower concentrated layer. These points are located at corner formed by breakwater as shown in Fig. 2. As compared with the other types of same depth, it may be understood that the concentrated load in the lower layer of the III is protected from the disturbance in the more shallow zone along the shoreline.

Type IV. The absolute amount of mass captured is generally less than in the other es. The upper part is somewhat vertical. The development of the lower layer can be as in type I.

Points of the observation where these curves were obtained, are located at the west of the harbor. The coast in this area is now being eroded gradually.

According to G. E. Vincent it is reported that, an entrainment current which transports sediment load develops along the direction of waves.[3] Shinohara and others noticed in ir experiment of suspended pulverized coal that a thin layer was moved by waves with a ep slope of vertical concentration in the immediate vicinity of the bed.[4] They called layer as 'transition zone'. In the case of sand, this layer was not observed. In the d observation which was carried out by the present authors, the velocity and the direc- of the bottom current could not be determined. Therefore, it is still questionable the lower layer of heavy concentration represents the entrainment current proposed by ent.

Lateral distribution and profile.

The integration of the suspended load from the bed to the surface were obtained for each point. The results in Fig. 5 shows the lateral distribution of the logarithm of these total mass captured in a day. The total amount of the sediment at each point decreases geometrically with the distance from the shoreline. The total amount of the mass in one point depends almost upon the mass in the lower layer excepting points No. 16 ~ No. 19. In this meaning, Fig. 5 represents the degree of development of the lower layer. By using the curve of type I, the equi-concentration curves of suspended load along the profile, i.e. normally to the shoreline, are obtained in Fig. 6. The depth was observed by lead sounding. Profile obtained in 1957 clearly shows the relation between the sand ridge and the concentration. Inside the ridge, the concentration increases rapidly to the shore. The ridge was not remarkable in the profile observed in 1958, because points of

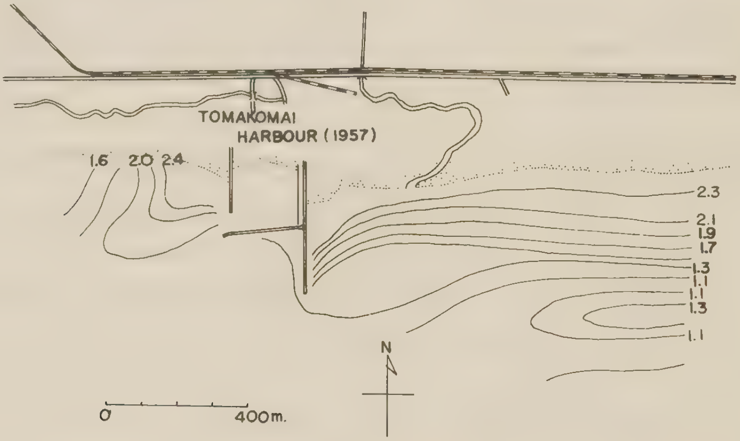

Fig. 5

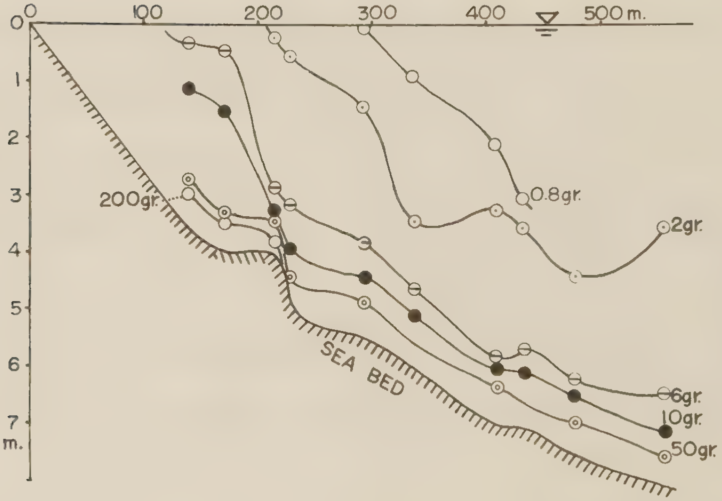

Fig. 6

observation were selected much nearer to the harbor and the number of points was only half of the ones in 1957. In 1958 the observation of the lower layer was not successful.

The authors are very much indebted to the stuff members of the Laboratory of Applied Physics, Faculty of Engineering, Hokkaido University.

References

1) Ikeda, Y., T. Soeya and Y. Mizoguchi (952) : Drifting Sand in the Sea, Journal of the Faculty of Science, Hokkaido Univ. Ser. II, Vol. IV, No. 2.

2) Fukushima, H. and Y. Mizoguchi (1958) : Field Investigation of Suspended Littoral Drift, Coast. Eng. in Japan, Vol. 1.

3) Vincent, G. E. (1958) : Contribution to the study of Sediment Transport on Horizontal Bed due to Wave Action, Proc. 6th Conf. Coast. Eng.

4) Shinohara, K., T. Tsubaki, M. Yoshitaka, and C. Agemori (1958) : Sand Transport along a Model Sandy Beach by Wave Action, Rep. Res. Inst. for App. Phys. Vol. VI, No. 21, Kyushu Univ., Fukuoka, Japan.

THE MEASUREMENT OF LITTORAL DRIFT AT SHORELINE HARBORS

— Result of Field Experiments —

Naofumi Shiraishi, Dr. Eng.
Chief of Niigata Harbor Construction Office,
Transportation Ministry

1. Introduction

Primary considerations of a harbor engineer in planning harbors on sandy coasts are usually the following:

a. A well planned harbor on a sandy coast should require little or no maintenance. Therefore, the first consideration is how to plan a harbor relatively free from excessive deposits of silt (accretion) thereby resulting in a low maintenance cost of the harbor.

b. A harbor well protected from drifting sands is apt to create a problem for ships entering and leaving the harbor. Hence, a compromise will have to be made to satisfy the two conflicting problems.

c. The bigger the harbor is, the more it becomes subject to accretion and erosion of the adjacent coast-line. It is often the case that the land value of such coasts are often high in comparison to the scale of the harbor. Therefore, consideration must be given to the use of accreted lands and the counter-action of erosion in the planning of the harbor facilities. The size of the harbor most suitable to meet these conditions must be considered.

The problems confronting a harbor engineer are conflicting in nature, but must be solved in a rational manner. In order to solve these requirements, the following data should be looked into for present-day coastal engineering:

(1) Predominant direction and quantity of littoral drift.
(2) Dimension and frequency of prevailing waves.
(3) Relation between water depth and drift amount.
(4) Optimum side slopes and the advancing and retreating of the shoreline.
(5) Design and engineering data of adjacent and other harbors.

Item (1) is sufficient to solve item (a), i.e. to decide the location and direction of breakwaters and port entrance, and then to work out the amount necessary to be dredged within the port.

Item (2) is a fundamental consideration in planning navigable channels, and for estimating wave movements within the harbor. Item (1) of course must be considered for selecting the disposal areas of the dredged material.

Item (3) must be considered in order to determine where maximum drift will occur along the coast-line, thereby permitting selection of the harbor entrance so that there will be a minimum of drift into the harbor and shoaling of channels outside the port.

Item (4) must be considered in order to estimate the scale of accretion on the front, and amount of erosion at the rear of drifting sand around a breakwater during certain economic years. This consideration must be made in addition to Items (1), (2), and (3).

Item (5) will be a compilation of data and past experience.

2. Geographical survey

This section is devoted to study of deriving at a method of judging the phenomena of drifting from geological and topographical viewpoint. Needless to say there is a tremendous amount of energy dissipated on coast lines, and the yearly amount of wave energy spent on a simple coast line facing the open sea for a coastline of 1 km is 10^{21} erg, comparable to the energy of typhoon which is on the order to^{23} to 10^{25} erg. Littoral drifts have gross movement in addition to the irregular effects of the winds and waves, and it is not an easy task to make analysis from short-term observations of data.

Common methods currently adopted in determining experimentally the direction of drifting sand from geology and topography are the survey of transformation of shore patterns in the vicinity of headlands and inlets, the measrurment of sand size distribution of bed materials or classification of ores, etc.

The author has made a study of the Yufutsu Plain (the backyard of Tomakomai harbor), from the time of its formation from the point of geomorphology and then assumed the condition of the littoral drift around this area.

The island of Hokkaido is considered to consist of two parts; the Ishikari-Chitose-Yufutsu line was a strait having changed into land during a geological year; this land is called the Yufutsu and Ishikari plains. A hill zone north of the Yufutsu Plain was formed from a land-rise, but the birth of Yufutsu Plain itself, involving vast marsh lands and composed of sand only is considered the result of littoral drift.

An aero-photograph shows big arc lines of old sand-hills, and that is the chief basis for assuming the above process. Furthermore, earthen-wares and shells dug out from shell mounds around the Yufutsu Plain serve to prove that the back arch line of sandhills, that is, the old coastline is of about 4,000 years old. (Different kinds of shells are known to live according to the amount of salt in the sea. Therefore, it is easy to determine from the location of where the shell was dug out whether it was sea-bottom or land before.) It is concluded that 4,000 years ago littoral drifts caused by the Hidaka River deposited in the so-called "Yufutsu Bay", shoaled and made narrow there, advancing the shore-line with some parts of bogs left, and then about 300 years ago they formed same shore-line as

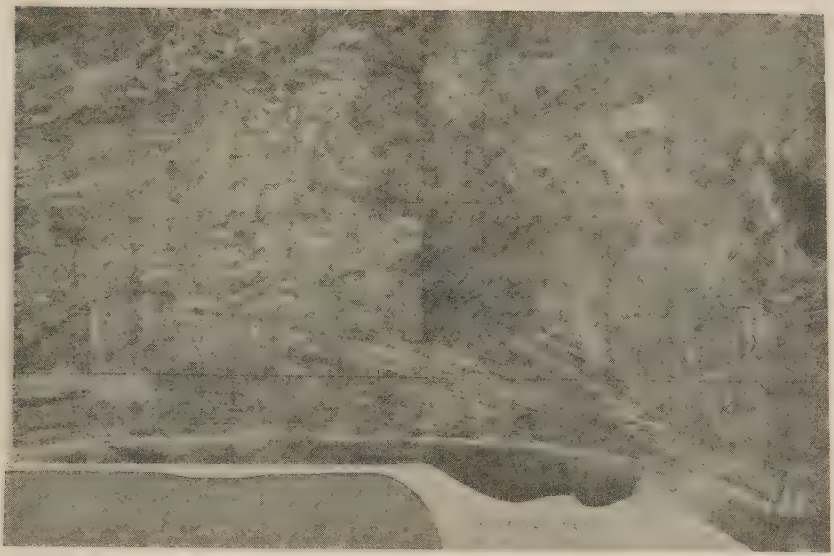

Photo-1

e present one. For this reason we can find a layer of volcanic ashes caused by eruptions 7 and 289 years ago. (The age of a layer of volcanic ashes may be exactly presumed by easuring radioactivity of an isotope C-14 from grasses in the layer.) In this way, the thor has tried to develop his opinion of drifting sand under the following assumptions:

(i) The accretion of littoral drift around the Mukawa-Noboribetsu low surf zone, in- uding the Yufutsu Plain, began 4,000 years ago.

(ii) The amount of littoral drift has been constant for 4,000 years.

(iii) There has been no change in sea level.

(iv) The present shoreline was formed about 300 years ago, and no change has taken ace after that time.

(v) For this period all drifts along the shore less than 5 meters in depth were im- unded and accreted.

According to the above conditions, about 45,000 cubic meters per year of drifting nds along the Tomakomai coast are estimated. This figure is considered to be fairly ac- rate, judging from the amount of 14,000 cubic meters of annual mean sediment at the up- ast side of Tomakomai Harbor, which has been calculated from sounding survey maps for 4 ars. The prevailing direction of drifting sands along the shoreline is from East to st, since estuaries in this area are all facing West.[3]

Measurement of forces moving sand

) Wind: It is not easy to make long-period observations of the waves having the closest nnection with drifting sands. It is, therefore, convenient to study the wind which is

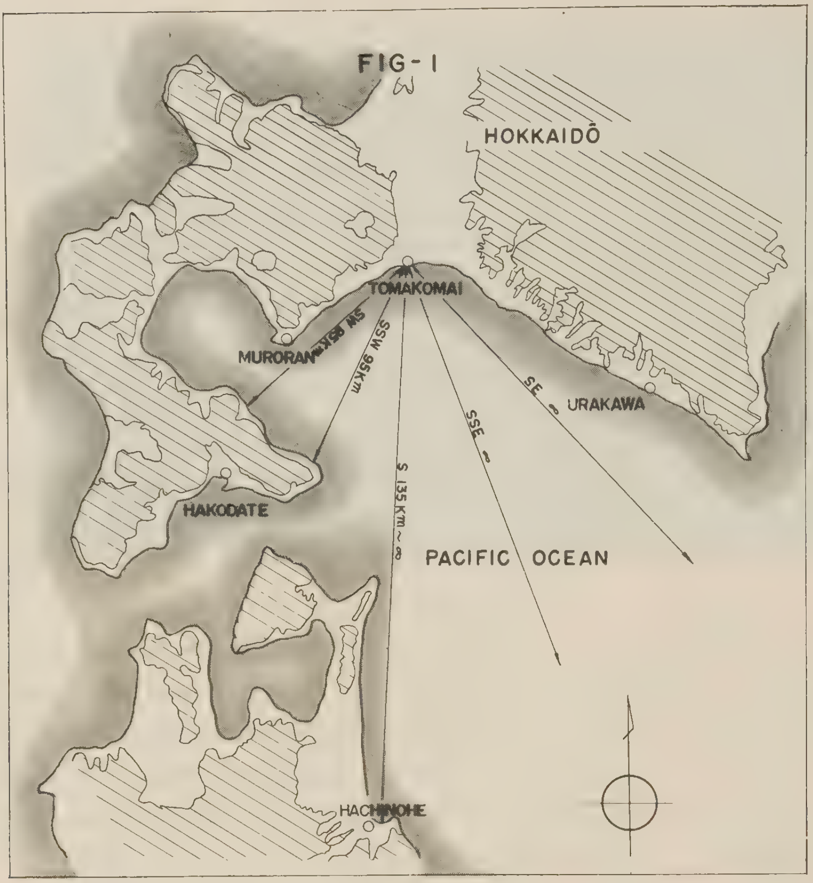

FIG-1

most closely related to the wave, and relatively easy to make recording of such wind readings. Winds, on the other hand, are greatly influenced by nature and due consideration must be allowed.

Let us now look into the case of Tomakomai Harbor. There are 4 observatories called Hachinohe, Muroran, Tomakomai and Urakawa, surrounding the off-sea side of the harbor. First, the wind data at the above observatories were obtained, and then a wind velocity frequency diagram, a wind direction frequency diagram and a velocity-direction distribution diagrams for more than 5 m/sec, 10 m/sec and 15 m/sec were figured respectively for one year. Next, a study of wind characteristics for each season was made from the 28-year data at each observatory. With these characteristics, a trial was made to see how strong winds influenced the tendency topographically. As a result of this study, in judging the wind off the Tomakomai coast, the record of Urakawa Observatory will have to be used for Westerly wind directions, Hachinohe for North-Esterly, Muroran for South-Westerly, and Tomakomai for South-South-Easterly winds. The results coincide with the forecast made from the point of topography.

Next we ascertained that the 10-year records the Tomakomai Observatory had no re- kable change for a period of 1 year and then worked out the maximum wind velocity, and maximum duration time in each direction for 2 years. Thus we arrived at the conclu- n that all winds without S-SE direction were not relied upon, and that the wind off akomai Harbor was predominantly from the East in the summer. In this way we could o presume the prevailing direction of drifting sands.4)5)6)

The effect of waves: In order to solve sedimentary movement, it is necessary to erstand statistically sea roughness, instead of accurate observation of each wave. refore, we will have to deal statistically with the results of a short -time continu- observation, or a regular intermittent survey, and then have to summarize the results o a whole-year sea roughness.

Being engaged in the planning of Tomakomai Harbor which is situated on a sandy coast, author found out that a wave recorder operating at a depth of 9 meters one year, from e 1, 1955 to May 31, 1956, gave the statistical distribution of wave height and period the form of log-normal curve.7) Probability diagrams of wave height and wave period are wn in Fig-2 and Fig-3 respectively.

The equation of probability density of each wave height and wave period are as follows:

(a) Wave Height:

$$y = 1/(\sqrt{2\pi} \times 0{,}2844)\exp - (\log x - 1.760)^2/(2 \times 0{,}2844)$$

FIG. 2 PROBABILITY DIAGRAM OF WAVE HEIGHT

AT TOMAKOMAI HARBOR
FROM 8:00 TO 16:00 EVERY DAY
NO. OF RECORDS 718 NO. OF MISS RECORDS 14

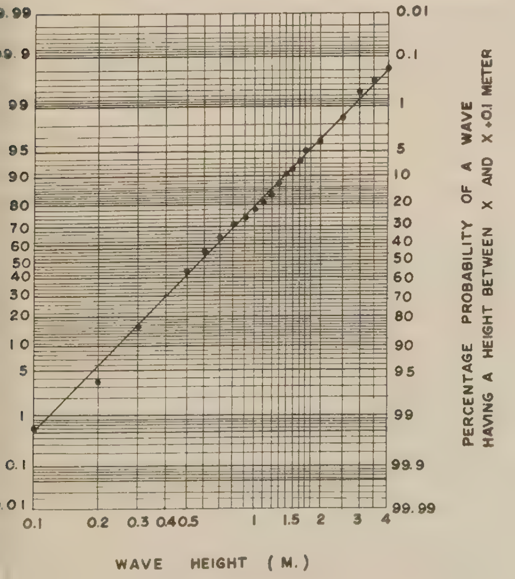

FIG. 3 PROBABILITY DIAGRAM OF WAVE PERIOD

NO. OF RECORDS: (I) 592 (II) 156
NO. OF MISS RECORDS 17
NO. OF RECORDS UNDECIDED 23

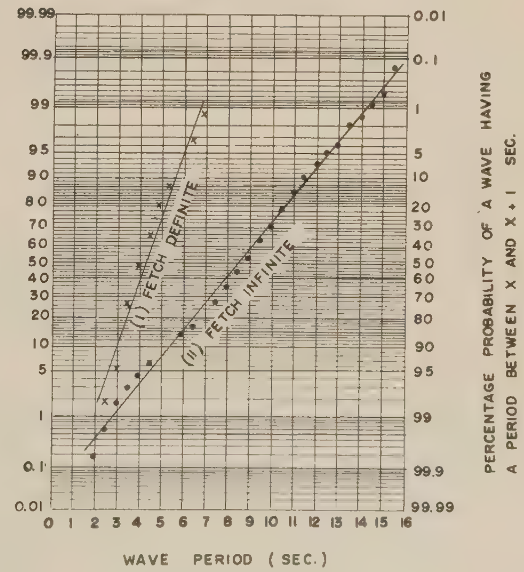

(b) Wave Period:

(i) For fetch infinite direction

$$y = 1/(\sqrt{2\pi} \times 2.425) \exp - (x - 8.627)^2/(2 \times 2.425)$$

(ii) For fetch definite direction

$$y = 1/(2\pi - 0.005) \exp - (x - 4.169)^2/(2 \times 1.005)$$

where

y = Probability density

x = Significant wave height and wave period in each equation

In this way, the probable percentage for waves of more than 4 meters high plotted against time is 0.15 %, for 4 to 1.2 meters - 13 %, and for 1.2 to 0.4 meters - 58%. As for wave period, there can be divided into two groups of 4.17 sec and 8.63 sec and the occurrence probability complies with the law of log-normal distribution, being a function of driving distance. The same can be said for wave energy occurrence probability. For the present time observations have been made regularly twice a day for period of one year. In order to study littoral drift, not only should further precise values of various statistics be made, but also more frequent measurements be made, i.e. 3 or 6 times regularly daily for a few years period, are needed.

As shown from the above, the effect of waves on a shoreline, and furthermore by calculating the wave energy in each direction and summarizing as shown in Fig.4, the prevailing direction and the scale of littoral drift can be predicted. This information has

FIG. 4 THE HISTOGRAM OF WHOLE ENERGY OF OFFSHORE WAVE IN EACH WAVE DIRECTION FOR EACH MONTH SEPARATELY (JUNE '55 ~ MAY '56)

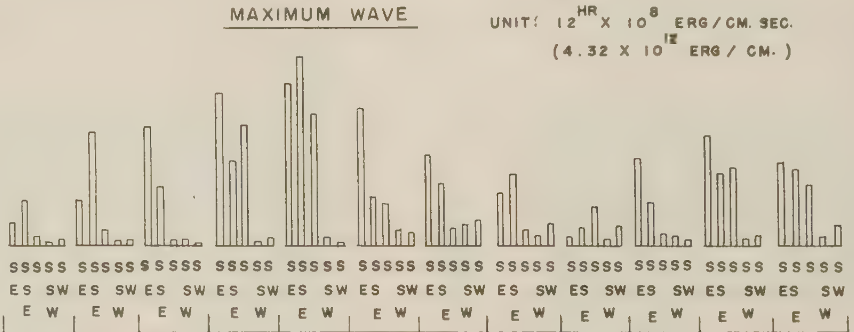

	JUNE '55	JULY	AUG.	SEPT.	OCT.	NOV.	DEC	JAN. '56	FEB.	MAR.	APR.	MAY
S E	54.6	102.7	414.0	556.8	594.2	513.1	330.2	197.7	16.0	330.4	404.6	295.2
S SE	157.5	423.0	200.4	312.2	714.8	160.7	230.2	264.4	49.5	127.9	302.4	275.8
S	19.6	25.0	5.2	427.5	485.2	153.2	49.1	49.5	124.5	10.9	264.0	220.8
S SW	2.4	8.2	9.1	0	23.2	39.4	55.1	25.0	2.7	1.9	5.8	8.0
S W	10.3	4.2	0	9.2	8.1	26.1	84.2	61.5	47.4	2.0	21.4	54.4

valuable in determining the normal line for planning the breakwaters against the ef- ts of sand and waves.

The effects of currents: In general currents along a coastline can be divided into al current, ocean current, density current and wave flow. The first three currents are general constant and are not of a great magnitude for each given area, with a few ex- tions. Currents caused by waves have a tendency to alter its direction and velocity ending on the condition of the wave. The current having the greatest effect upon lit- al drift is this one caused by waves, and is generally called "littoral current". Hence study of currents is very complicated, and in many cases records obtained after pains- ing effort must be discarded as unreliable. Though many formulas have been published calculating coastal currents based on winds and waves, none seems to be adoptable. le 1. shows a wave-current relationship at Tomakomai area. Since the coastline at akomai runs in a East-to West direction and faces South, littoral currents caused by es from ESE - SSE and S - WSW are driven from West and East respectively. According to table, littoral currents in a stormy weather, which has the greatest effect on sand fting are entirely controlled by waves; and the bigger the angle between a wave direc- n and the shoreline, and also higher the wave, the stronger the littoral current.

Measurement of slopes of sea bed: In order to predict the process of accretion or sion caused by breakwaters, it is of importance to know the slope in equilibrium of the st line. Roughly speaking, a bed slope can be given as a function of wave elements and in diameters of the bed sands. Consequently, at coasts where neither waves nor bed

TABLE - I

WAVE HT.	DIRECTION OF L.C.	DIRECTION OF WAVE														TOTAL	
		ESE		SE		SSE		S		SSW		SW		WSW			
		OCCUR.	%	OCCUR.	%	OCCUR.	%	OCCUR.	%	OCCUR.	%	OCCUR.	%	OCCUR.	%	OCCUR.	%
OVER 2 M.	E			6	85	6	100	2	25							14	67
	STAN.															0	0
	W			1	15			6	75							7	33
1.95 M. ~ 1.50 M.	E			14	87	4	67	1	20							19	68
	STAN.															0	0
	W			2	13	2	33	4	80			1	100			9	32
1.50 ~ 1.00	E			54	95	28	74	1	8							83	96
	STAN.					1	1									1	1
	W			3	5	9	24	11	92	3	100	9	100	1	100	3	3
0.95 ~ 0.50	E			53	74	66	74	8	40	9	26	3	71			139	54
	STAN.			3	4	1	2	2	10							6	2
	W			16	22	22	24	10	50	26	74	39	29	1	100	114	44
0.45 ~ 0	E	1	100	36	68	70	49	13	50	5	29	10	21			135	47
	STAN.					1	2									1	2
	W			17	32	70	49	13	50	12	71	37	79			149	52
OTAL	E	1	100	163	79	174	62	25	35	14	25	13	13			392	55
	STAN.			3	2	3	1	2	3	0		0				8	1
	W			39	19	103	37	44	62	41	75	86	87	2	100	313	44

L.C. = LITTORAL CURRENT OCCUR. = OCCURENCES STAN. = STANDING

FIG. 5

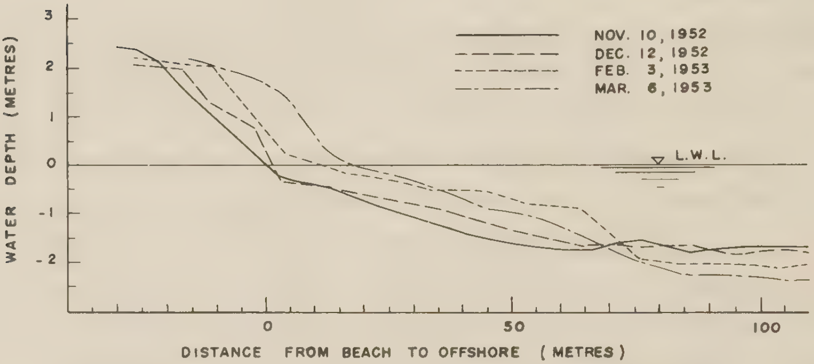

sands change from year to year, this can be performed by measuring the bed slope with extreme care. Especially, it is important to take measurements of accretion and erosion around structures (under construction) than it is on a natural coastline, and taking an average on a yearly basis.

Fig.5 is an example of changes of slopes of an accreted area on the front side of a breakwater under construction at Tomakomai Harbor. The length of the breakwater was approximately 60 meters, and the foreshore slope above low-water-level was almost constant. There was no effect of accretion at distance of 70 meters toward the seaward side of the breakwater. The same tendency can be seen at Irako Harbor (Aichi Prefecture) which is also located on a littoral coast.

5. Measurement of littoral drift with isotopic tracers:

There are many methods of measuring littoral drift, and one method tried by the suthor with the use of radio-isotopes is described herein.7), 8), 9), 10), 11), 12), 14)

This method consists principally of the following; prepare homogeneous radioactive glass beads having the same specific gravity, and the same size distribution as that of the sea bed sand, and measuring the effects of coastal currents, waves, etc. with radioactive tracers after placing the glass beads on the sea bottom. Actual results of these measurements made at Tomakomai Harbor by the author were published in the "Dock and Harbor Authority"9) and will not be repeated here. Similar measurements have been made in England at the Thames Estuary, Poole Harbor on Norfolk coast, and also at Kaike Coast Tottori Prefecture, Irako Harbor Aichi Prefecture in Japan.

The radio-isotopes used in Japan were Zn-65 (Kaike Coast and Tomakomai Harbor), and Co-60 (Tomakomai and Irako Harbors), that used in England was Sc-46. Sc-46 excells in gamma-ray flux density and sensitivity to counters, but has the disadvantage of shorter life, being 85 days. If an atomic pile is available, Sc-46 would be the best medium to

It would be advisable to make the diameter of the glass beads uniform and approxi- the majority of the diameter of the sand granules of the bed sand, thereby simplify- analysis of the test results. The grain size distribution of the radioactive glass s was made the same as the bed sand for the experiment at Poole Harbor, as in the case omakomai, but according to regulations of the Radiation Hazard Division of the Harwell ratory, those beads with over 0.1 micro-curies per grain (or over 0.25 mm dia.) were ved. The glass beads used at Tomakomai were less than 0.2 micro-curies, and so there no radiation harzards. Care must be taken to place the glass beads on the sea bed in ng with the bed sand. In the experiment at Poole in England, the glass beads were drop- from a height of 8 ft (depth of water 19 ft) and it was found that the glass beads were ersed by the ocean current and making a movement different from the bed sand, that from second time they made it a practice to release the glass beads on the sea bottom. At e glass beads in the amount of 1.75 curies per observation were used and it is claimed they were able to make continuous readings for a period of 4 months even during the hest winter months. On Norfolk Coast in England it is claimed that they were able to continuous readings for 3 successive months at a depth of 5 meters. At Tomakomai it possible to take readings for a month and a half for a amount as small as 2 to 30 milli- es. It seems that the radiation counters of Japan are just as effective as those of and. It goes without saying that the efficiency of the radiation counters must be ed before use. This includes the directional ability, dead-time, absorption and back- tering of the sea water and bed sand of the detecter. Fig.6 gives the radiation ab- tion of the gamma-counter for cosmic ray measurements, which shows that the count of 10,000 counts falling off to 10 counts at a distance of 70 cm. It can be deduced this that the radiation count is limited to immediately in the vicinity of the radiation ter.

It can be easily assumed that some of the oactive glass beads will become buried by r sand. A great un-evenness in the sea bottom tend to make useless qualitative analysis. he present time the only way to offset any irregularity is by taking samples of the and experimenting in the laboratory. At komai, it is not believed that any covering of 10 cm took place, and exact results are not n at this time. However the results show that etrimental effects took place on account of

FIG. 6 ABSORPTION OF GAMMA-RAYS BY SATURATED SAND, DRY SAND AND SEA WATER

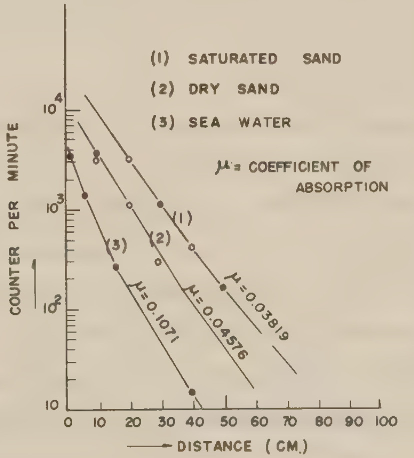

covering up of the glass beads. The resluts of the experiment at Tomakomai can be summed up as follows:

(a) At depths of 3 to 4 meters, and near the shoreline, the movement of bed sand was so great as to not be able to give relationship of the wave to drift. Improvements must be made in the method of measurement.

(b) At depths of 6 meters, no perceptible movement of bed sand is noticeable against waves of 1 meter in height, and comparatively small granules move for waves of 1 to 2 meters in height, and largest of sand granules move against waves over 2.5 meter in height. The sand and waves move in the same direction, with the amount of bed sand moved in proportion to that of the wave energy imposed upon the sand.

(c) At depths of 9 meters, bed sand movement is not noticed for wave heights of 2 meters and under. Any movement of bed sand is subject to the ocean current. The bed sand showed some movement against waves over 2.5 meters in height, but the direction of the movement did not agree with the wave, and the direction of the ocean current had a marked influence on the direction.

(d) Bed sands near underwater structures (breakwaters) are controlled by waves rather than by littoral currents caused by the structures themselves.

(e) In summary, it can be said that the movement of bed sands is more influenced by waves than by littoral currents.

Measurements have been underway since January 1958, by radio-isotopes at Irako Harbor in order to study the shoaling process caused by littoral drift. To date the following has been disclosed[15]:

The grain size of sand and the regional conditions of external forces has allowed us to determine whether the sand movement is of the creeping type or the suspending type. Fig. 7 gives the two modes of dispersion of radioactive sand. The contour lines in the figure indicate zones in which equal numbers of radioactive impulses were received. The resulting diagram thus gives the dispersal of active sand around the initial injection point.

6. Items of measurement of littoral drift and harbor plannings

(1) Items to investigate: In making preliminary studies of harbor planning, the first consideration is to make a geological survey, and then make a rough determination of the items given in the introduction 1. and consider these items in the light of observations of the phenomena taking place on the coastline at present.

In making studies of the wind, it is of prime importance to obtain wind data from observatories located in spots where they can accurately catch wind date creating waves affecting the proposed harbor construction site. Many cases are cited where due to insufficient wind data littoral direction has been misjudged. We believe that next to geological

FIG. 7

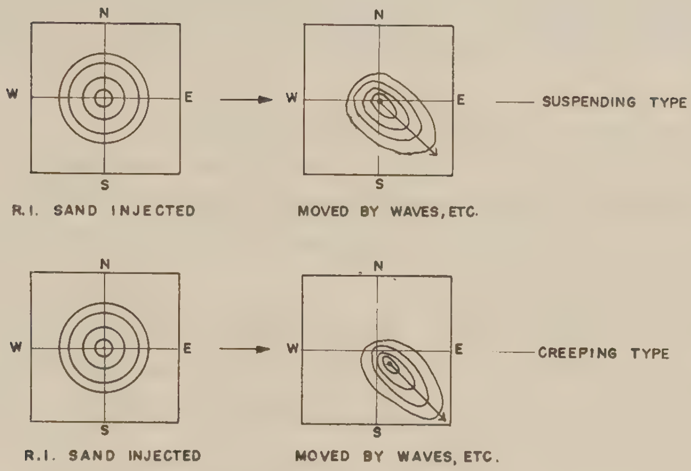

nsiderations, wind study should be placed topmost in making coastline studies.

After preliminary studies are made, the next step is to make full scale studies. At is stage the most important factor is the study of waves. Since littoral drift is inuenced mostly by wave energy, it is of utmost importance to know the elements of the ves and the density of occurence. Though automatic wave recorders are still to be rfected, the only way to study waves is survey waves from high places, or by making a fraction diagram each time. It seems that a study of currents is a waste effort as far littoral drift is concerned. In general, the changes in ocean currents are as large as the coastal currents and tidal currents for prospective harbor sites. Hence, a one- e observation will not yield satisfactory results. Since currents are combined of wave vements (mainly ocean currents) and irregular coastal currents, the changes in currents e unstable as the winds. Since satisfactory recordings cannot be made of currents this dy is not recommended too highly in making harbor studies.

The measurement of bed materials is significant in relation to bed slopes in equilibum, especially predicting the slope due to accretion and erosion after completion of eakwaters. It is important to measure the slope of accreted deposits while the construcon of underwater structures is underway. This study will not have to bid during rough ather and if geological surveys have been conducted, the slopes during rough weather can determined. Since it is not easy to study the bed bottom during rough weather, such dies are not necessary beyond the immediate vicinity of the structures.

Measuring with isotopic tracers has only begun recently and has given engineers a big erest because they can make a direct measurement of drifts for a long term. Direction, tance, or velocity, except for amount of radioactive sand will be clearly recorded even if some were to be covered up. As to the amount moved, we have to expect for a pattern experiment. Anyway various records of measurement of coastal phenomena will not be useful unless they are arranged at least to show annual tendency. A statistical arrangement is a key point.

(2) Harbor planning: Any good survey of a natural coast line will not give an exact knowledge about the processes of accretion, erosion and shoaling after building-up of a harbor. It is, therefore, necessary to look into examples of harbor construction in the world and to produce a key plan.13) Then construction can be started in a "try and check" way rather than in an "all-over" way.

Drifting sand will come in a harbor on a sandy coast, however it may be built with reasonable planning. But if its entrance does not face the prevailing way of drifts, it will be pretty free from shoaling. On the other hand, the site of the entrance is mostly decided by the site of wharfs or the scale of ships coming in and out rather than by considering the depth where there is little drifting sand.

In deciding the position and direction of the entrance, it is of value to estimate what the filling pattern of deposits might be expected at a proposed nearly barrier. Fig.8 is an example simply sketched of Tomakomai Harbor. The assumptions are: The edge line AB of the deposit area is perpendicular to the direction of prevailing wave; the contour line of 9-meter depth at the tip of a breakwater is same even after the completion; the bed slope of AC is to be 1/20, the maximum slope of deposit area of the present breakwater. These assumptions are generally common except for the bed slope. If the entrance is sited near A point, shoaling will take place. To draw a figure like this the above-mentioned items of measurement are needed.

In this way, the selection of the alignment of a breakwater will be soon given from view-point of sailing routes, tranquility within harbor and siting of wharfs.

The way of thinking above has come from the painstaking study on relationship among

FIG. 8 PATTERN OF DEPOSIT AT TOMAKOMAI PORT

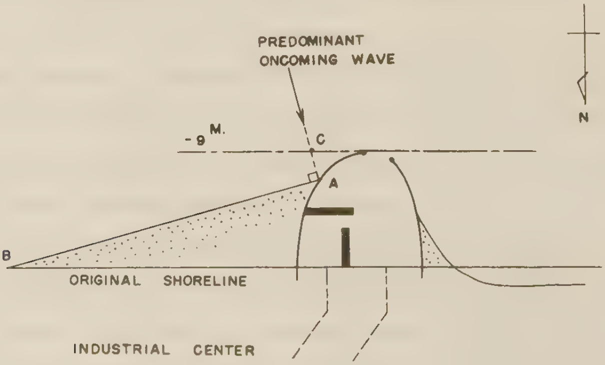

stal engineering, field experiments and plannings, while the author has been engaged in ld work. It will be fortunate if this may be a help to those engineers facing the same blems. As for many actual explanations omitted above, please refer to the following ers.

References

1) Shiraishi, N. : An example of method of geographical survey of sandy coast, 12th Annual Meeting, Japan Society of Civil Engineers, June, 1957.

2) Hata, M. : A Life of a Lade.

3) Mashima, Y. : On estuaries at Tomakomai Coast, No.5 Report of Civil Engineering Laboratory, March, 1952.

4) Mashima, Y. : Littoral current at Tomakomai Coast, No.5 Report of Civil Engineering Laboratory, March, 1952.

5) Mashima, Y. : Littoral current and maximum wave height at a harbor, Journal of J.S.C.E.,1954.

6) Tomakomai Municipal Office : Report of Survey of Tomakomai Coast.

7) Inose, S., S. Sato, N. Shiraishi : Drifting sand at Tomakomai Harbor, Preceedings of Coastal Engineering, J.S.C.E., 1956.

8) Inose, S., M. Kato, S. Sato and N. Shiraishi : The field experiment of littoral drift using radioactive glass sand, Proc. of the International Conference on the Peaceful Uses of Atomic Energy in Geneva, Vol. 15, Aug. 1955.

9) Inose, S., N. Shiraishi : The measurement of littoral drift by radio-isotopes, Dock and Harbor Authority, Jan. 1956.

10) Allen, F. H., J. Grindley : Radioactive tracers in Thames Estuary -- Report on an Enperiment Carried out in 1955, Dock and Harbor Authority, 1957.

11) Allen, F. H., J. Grindley : Detection of offshore beach movements with radioactive tracer -- Pilot Experiment at Poole -- Hydraulic Research, 1956.

12) Shiraishi, N. : Study on movements of littoral drift, Journal of Industry of Atomic Energy, Daily Industrial Press, Oct., 1955.

13) Johnson, J. W. : Littoral drift problem at shore line harbors, Journal of the Waterways and Harbors Division, Proceedings of the A.S.C.E., Vol. 83, 1957.

14) Reid, W. J. : Coastal experiments with radioactive tracers -- Recent work on the coast of Norfolk, Dock and Harbor Authority, July, 1958.

15) Aichi Prf. Office : On littoral drift at Irako Habor, Report on Coastal Survey of Atsumi Peninsula, March, 1958.

SHAPES OF SHORE STRUCTURES (DIKES) AND ITS DAMPING EFFECT FOR WAVE FORCES

– Especially on wave run-up and wave pressure –

Juichi Kato

Section of Shore Reclamation, Kyushu Agricultural Experiment Station

This paper represents a summary of studies on rational dike design for the wave mping effect of various dike forms, especially on wave run-up and wave pressure.

Up to now a number of studies have been presented on the several problems regarding is theme, for instance, on wave run-up, overtopping, wave forces and others. The author kes especially into account of the partial clapotis which varies in accordance with the apes of dikes and further considers on the wave run-up in company with wave pressure king note of the real state of locations synthetically.

I. Laboratory Equipments and Procedures.

Experiments were performed in a wave tank, glazed on both sides, 1 meter wide, 25 ters long, and 1.20 meters high. The model waves generated by a ballistic pendulum, d the wave pressured were measures by micro-wave pressure gauge (magetic strain type) d were recorded by electromagnetic oscillograph with six elements at the same time connuously.

In this study, 35 kinds of the dike models as shown in Fig. 1 that were picked out om about 300 sections all over the country were used and were grouped under three types. for the model waves, in order to generate the deep water wave and the shallow water ve, the angle of the pendulum swing were changed into seven kinds. That is to say, the lues of h_o/L on Coyer1) were changed from 0.04 to 0.05. The range of shallowness, h_f/L_o from 0.00 to 0.30 and the range of steepness, H_f/L_0 is o.0054~0.072, where h_f is the pth of water at the toe of the structure, L is the wave length, H is the wave height and ffix o shows the value in deep water depth. Furthermore, the wave height, lwngth and riod at several points in the wave tank, the height of wave run-up and spray, wave presre at the surface of dike, several dimensions of breaker, ratio of reflection and the her dimensions were measured.

Moreover, the certifications of the model waves, the movements of water molecules in veral cases and the characteristics of breaker in case of non-structure were examined in tail.

II. Wave up-rush on dikes.

Let us show the situations of wave up-rush on dikes that were grouped into three pes as mentioned in the previous chapter.

(1) Cross Section of Dike Form, Group I (Fig.1 - 1~25).

Cross Section of Dike Form, Group I is called the Upright Type, which is widely used as general shore structures in all countries.

a) It is a well known practice to discriminate between the Clapotis Type and Breaking Impact Type in the incident wave on the mechanism of wave run-up on dike form, Group I. The author, however, thinks that it is rational to divide further the Breaking Impact Type into Breaking Point Impact Type, Heighest Point Impact Type, Dropping Point Impact Type, etc. These types of incident impact mechanism are consistently mentioned in this paper.

b) Cross Section of Dike Form, Group I, is of various kinds because of the variety in the slope and the form of riprap. Therefore, the wave up-rush on dikes also changes correspondingly. However, it is thought that dike form may be subdivided from the mechanism of incidence and impact of the wave into two types, i.e., the cross section which is composed of lines having pretty abrupt change and the cross section composed of smooth curves. These types give very different influence to the incident wave. Generally, on the former, the breaker is apt to occur and the spray flies high; on the latter, it is just the reverse. An example is shown in III, (1).

(2) Cross Section of Dike Form, Group II (Fig.1 - 26~32).

The dike with gentle slope, (smaller than about 45 degrees) on which the rate of reflection is small is called Group II.

The incident situation for this type of dike is different from that for the dike form, Group I. That is, the advancing wave falls on the returning wave, and the actions of plunging and knocking repeated on the sloping wall of structure uniformly. On the dike form, Group II, the mechanism of incident wave to the slope is constant even if the incident wave is clapotis or breaker type, and it may be generally presented for this group that the incident situation is regulated by the gentle slope.

Furthermore, on the mixed form of dike, Group I and Group II, it is shown in III, (4).

(3) Cross Section of Dike Form, Group III (Fig.1 - 33~35).

Dike forms belonging to Group III are made with the aim to attain the rational cross section of dike by the results of the above two experiments.

The form of this Group has a large step, and the length of step and the water depth on the step must be determined so that dropping point of breaker may occur on the step. The mechanism of an incident situation for Group III should be regulated like in Group II, that is, double breakers occur at the end of the large step and it progresses and falls down in front of the vertical wall. Thus, the up-rush and wave forces on the dike wall is very small.

After all, it is due to the difference of the rate of reflection. The situation of up-rush and incident wave should vary with the dike form. In the following apter, the character of the artial clapotis regarding the ate of reflection, and the relation between the up-rush and he wave forces are analized.

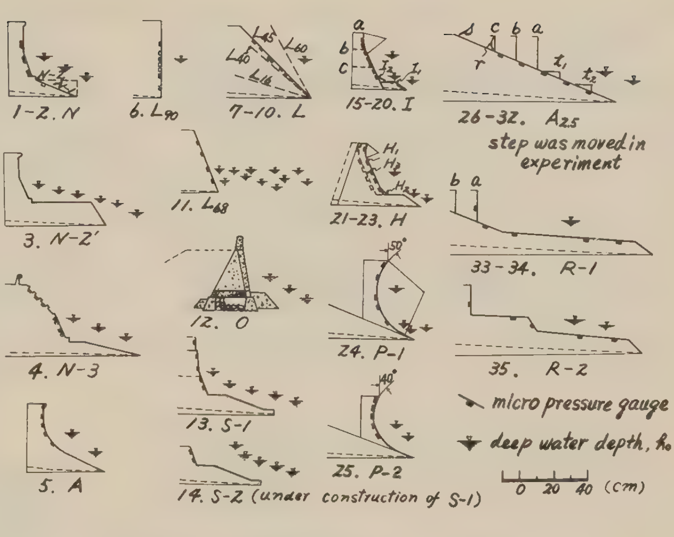

Fig. 1 KINDS OF DIKE MODEL

III. Height of Wave Run-up.

The characteristics of ncident wave is one of the important elements which deterine the wave run-up. In this tudy, the following relations f the character of incident aves are examined: i) the elation between the wave form nd the breaking depth, .e., $H_b/L_b \sim h_b/L_b$, H_0/L_0 h_b/L_0 and $a_{/b}/H_b \sim h_b/L_b$ ii) the relation beween the steepness and he breaking conditions, i.e., $h_b/H_b \sim H_b/L_b$, $_b/H_0 \sim H_0/L_0$ and $H_b/H_0 \sim$ $_0/L_0$, where $a_/$ is the eight from the still ater to the wave crest nd suffix b represents he values at the breakng point, iii) the elation between the ater depth and the ave height, the wave rest height above stil ater level in the reaker zone and its ength, i.e., the length f breaker zone is a istance from the startng point to the droping point of breaker.

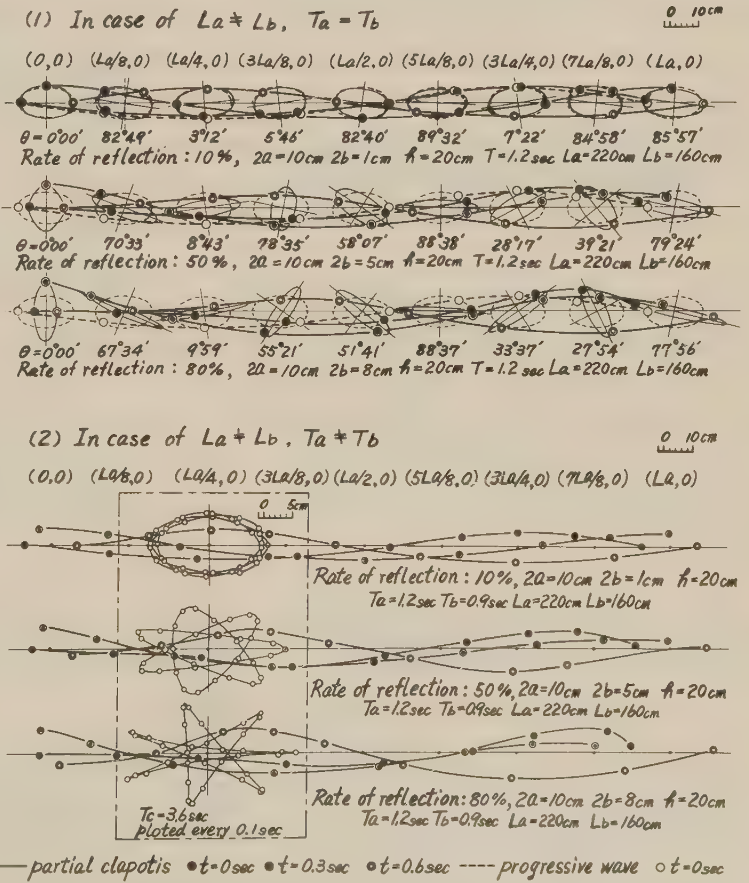

Fig. 2 LOCI OF WATER PARTICLE MOTION IN PARTIAL CLAPOTIS (at surface)

(see Fig.4 - (6)) In this report, however, these relations are omitted.

Next, the rate of wave reflection which is closely related with the wave run-up was examined. A part of the results obtained is shown in Fig.2. The rate of wave reflection was calculated by Healy's method.2) Moreover, Fig.3, obtained by using the Healy's method shows the state of the wave reflection in each case.

The wave run-up is shown according to Dr. Ishihara's method3). Furthermore, the relation between a_u/H_0 and H_0/L_0 with shallowness as a parameter, where a_u is the height from still water to the maximum point of up-rush, and others were examined. The characteristics of the dike form were generalized. This report treats only on the relation between a_u/H_0 and h_f/L_0.

(1) Cross Section of Dike Form, Group I.

The state of the wave run-up in each group is shown in the following three dimensions: i) the limit of the overtopping of wave on a levee (sign ——), a_{uw}, ii) the limit of the fairly overtopping of sprays on a levee (sign ----), $a_{u\beta}$, iii) the limit of the highest overtopping of sprays on a levee (sign —·—), $a_{u\gamma}$. Furthermore, B.P., i.e., the breaker point (sign ○) and M.P., i.e., the maximum point (sign △) are expressed in every steepness, H_0/L_0 as shown in Fig.4.

Though the dikes in Fig.4 (1) and (2), which are very general, are very alike in form, the wave run-up on them presents very different values because the dike wall in (1) is composed of broken lines and it is interposed by curved line (2).

To mention briefly about Fig.4, the following data on a_{uw}/H_0 and $a_{u\beta}/H_0$ or $a_{u\gamma}/H_0$ are picked out: i) though spray on N - 1 (I - 2) is higher than on A (P - 1), the values of a_{uw} on the former are smaller than on the latter, ii) the values of shallowness at B.P. and M.P. are very different, iii) the same as in ii) is presented for shallowness of the peaks in a_{uw}- curves and $a_{u\beta}$ or $a_{u\gamma}$- curves, iv) the parapet whose cross section is composed of curves is very effective.

Moreover, the curves (sign -- --) shown within Fig.4 - A that were calculated by Stoker's impact wave theory, are not a little different from the curves of the wave run-up on the dike A.

As for the dike under the construction, its stability for the wave pressure was investigated using three kinds of the reduced scale, 1/10～1/30. But it is omitted here.

(2) Cross Section of Dike Form, Group II.

The curves in Fig.4 (3～4) show the wave run-up on various kinds of 1 : 2.5 slope which belongs to gentle slope type, where $A_{2.5}$- s is a dike with a sigle slope 1 : 2.5 and $A_{2.5}$- a, $A_{2.5}$- b and $A_{2.5}$- c are dikes with vertical wall of same level height on the slope 1 : 2.5 of $A_{2.5}$- s dike at the different positions respectively.

As for $A_{2.5}$- s the same results as by Dr. Satô4)and 5) were obtained. The value of a shows the maximum point of the wave run-up. How does the dike form with the ver-

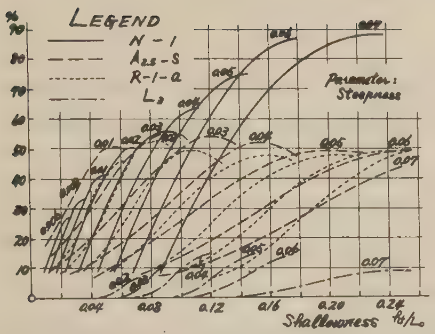

Fig. 3 RATES OF WAVE REFLECTION

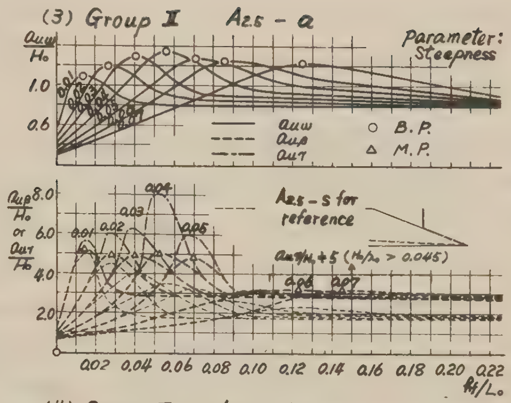

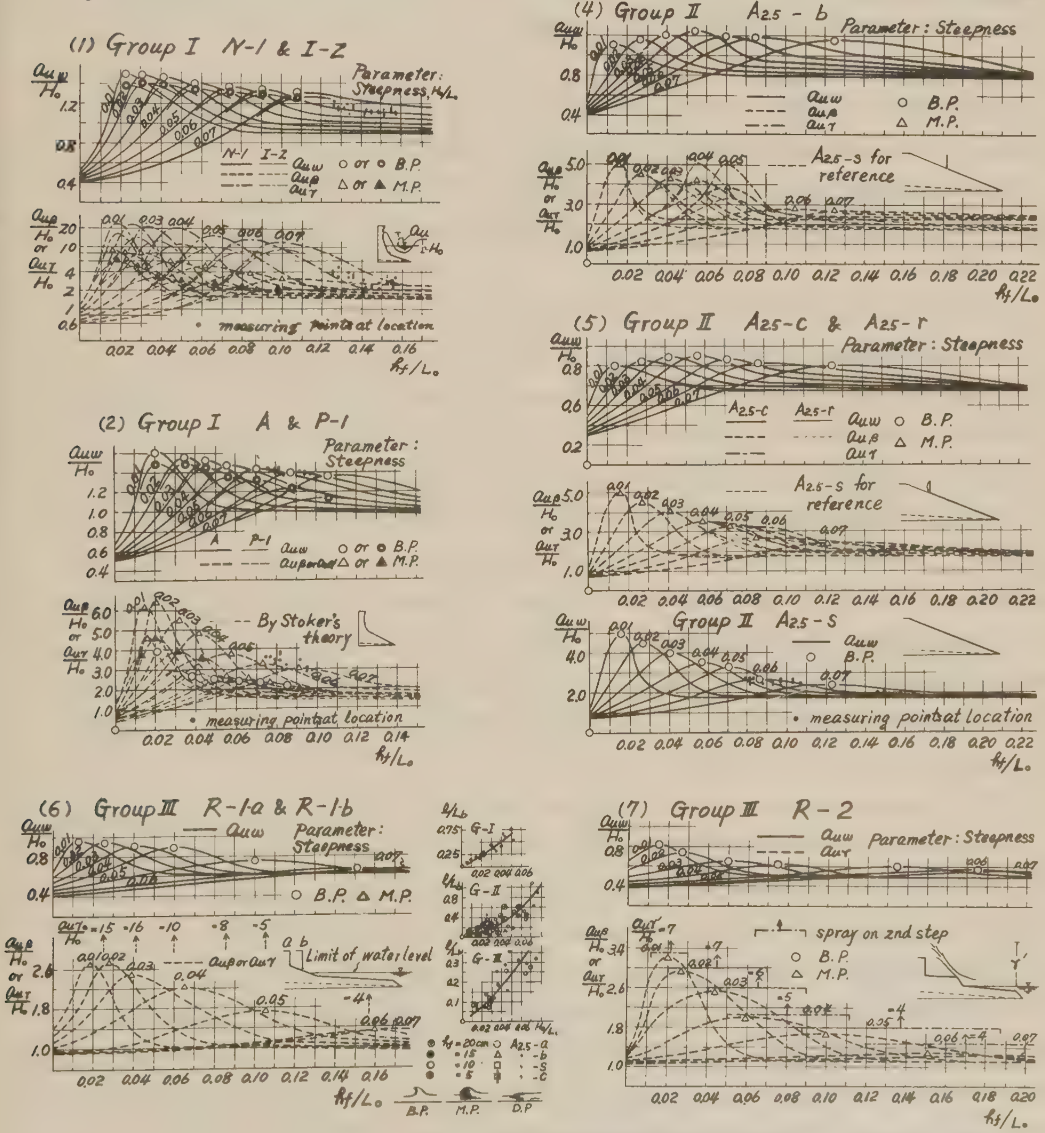

Fig. 4 HEIGHTS OF WAVE RUN-UP

tical wall on the slope influence the wave run-up ? Now let us compare this result with those in $A_{2.5}$ - a, $A_{2.5}$ - b and $A_{2.5}$ - c, etc.

The data obtained from these curves are the following: i) the maximum peak of curves occurs on the curve of $H_0/L_0 = 0.04$, ii) as the value of shallowness becomes greater, the influence of the upright wall appears, iii) as the upright wall moves backward such as $A_{2.5}$ - b, $A_{2.5}$ - c, $a_{u\beta}/H_0$ curves tend to approach the run-up in $A_{2.5}$ - s. So it may be assumed that the curve in $A_{2.5}$ - s corresponds with $a_{u\beta}/H_0$ curve in other cross sections. Thereupon the a_{uw}/H_0 curves in the $A_{2.5}$ - s cross section were decided according to the appearances of the plunging waves on the slopes. Consequently, it was judged that these curves are approximarely equal to the a_{uw}/H_0 curves in $A_{2.5}$ - c. In each graph the curves in $A_{2.5}$ - s are shown with smaller broken lines for reference.

Here, special mention is given to the fact that as the rate of reflection becomes larger, B.P. occurs after M.P. (the same is true in Group III).

From these results, many useful data in practice can be obtained. For instance, it is desirable that the form of cross section with broken lines, such as a berm, is avoided.

(3) Cross Section of Dike Form, Group III.

As for this type, even the largest value of $a_{u\gamma}/H_0$ is only about three. The dike in this Group has a pretty similar character to that of Group II. Furthermore, as if there is little difference between the cross section R - 1 - a and R - 1 - b.

The arrow marks in R - 1 graph show an example of the height of spray, γ_0 , when breakers fall on the dike wall in case of large h and the breaker impacted on the upright wall. As in this case the appearance of the run-up is like that of Group I, the property of Group III vanishes. The length of breaker zone, l, can be obtained from the same graph. And the arrow marks in R - 2 show the height of spray, γ', when the breaker impacted on the slope of the second step. The selection of the stair having one step or two steps must be decided from the construction for the foundation and the waves.

(4) General Cross Section of the Dike Form (On Use of Single Slope Method).

In regard to the representative dikes as mentioned above, the wave run-up was analized from the data of the experiment. But, how can this problem be solved considering the general dike containing the dikes in Group I, II, and III ? It is convenient if the height of the wave run-up can be estimated by other methods.

On this problem, Saville[6)] reports an interesting result by the Single Slope Method - " when incident wave becomes a breaker, the height of wave run-up on general composed structures is equal to the height of wave run-up on a single slope which is drawn from the breaking point to the maximum point of wave run-up. "

So, the author examined the results of the experiment by this method and the re-

ts were as expected. Here, the author expanded the method and arrived at the fol-
ing conclusion:

" The height of wave run-up on dike can be replaced by the height of the wave
-up on a single slope which is drawn from the breaking point in case of the break-
incident wave or from the point of L/2 length from the dike in case of clapotis
ident wave, to the maximum point of wave run-up. "

Fig.5 shows the up-rush on a single slope. Then, according to Fig.5, using
Single Slope Method, the up-rush on optional dikes such as Group I, II, and III,
., can be estimated. Fig.6 obtained by the same method for dike form as shown
ve illustrates an example showing its accuracy.

IV. Intensity of the Wave Forces.

To study on the effect of wave damping for several dike forms, the intensity of
e forces should also be considered taking into account the wave run-up simultane-
ly. Many people have studied on the wave force, nevertheless, up to now, there
but a few practical methods available. On the wave pressures, the theory of
tial clapotis is not established, so the important relations remain obscure as the
lowing: i) How is the problem of wave reflection related to the wave pressure ?
) How is the wave pressure of its medium type in incidence between clapotis and
aker which takes place frequently in the actual wave be calculated ? iii) How is
relation between the various mechanisms and the wave pressure treated ? In this
ort the rational formula based upon the numerous results of the experiment is in-
ed.

(1) Results Obtained.

The following relations were considered from the results of wave experiments:
The vertical maximum wave pressure distribution. ii) Relation between P_{max}/W_0
H_0. iii) P_{max}/W_0 and H_0/L_0. iv) P_{max}/W_0 and $C^2/2g$. v) P_{max}/W_0 and T (where P_{max}
maximum wave pressure, C is the velocity of the wave, T is the period of the wave).
re, only remarkable data are enumerated. They are:

On the breaker: i) In this experiment, there was no occurrence of the phe-
enon reported by Minikin[7) that the crest of the wave engulfs the air and dashes a-
nst the dike wall compressing the air horizintally. But it is considered that
phenomenon, for the crest of the wave to engulf, may occur occasionally only when
ure progressive wave with small value of steepness dashes against Group I dike
se riprap is composed of broken line in its cross section. So it is thought that
occurrence of such phenomenon as Minikin reported is possible actually by the in-
ference of the waves themselves. ii) The actual wave pressure is accompanied by
oscillation owing to the complex reflected wave. iii) The maximum pressure dis-
bution diagrams in Group II and III have a definite trend clearer than in Group I.
) The relations between P_{max} and H_0, H_0/L_0 and $C^2/2g$ have a definite tendency on the

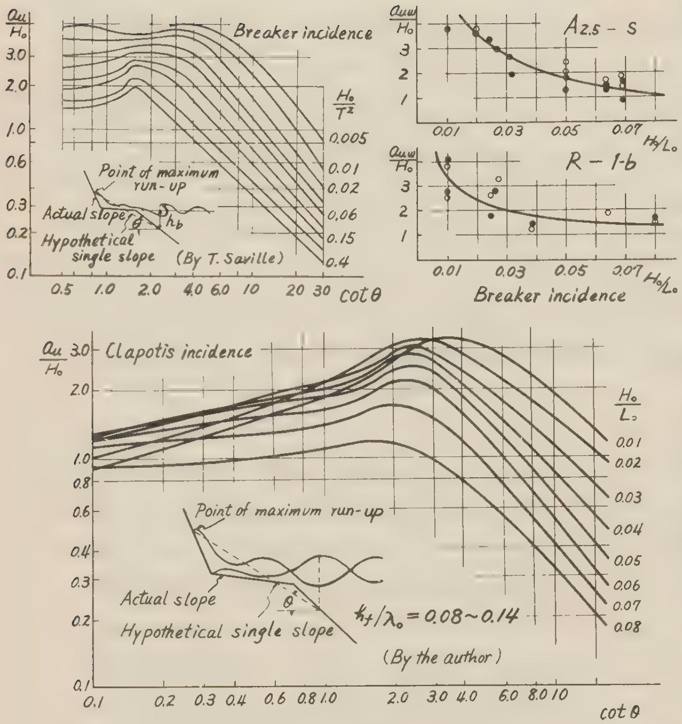

Fig. 5 RUN-UP ON SINGLE SLOPES

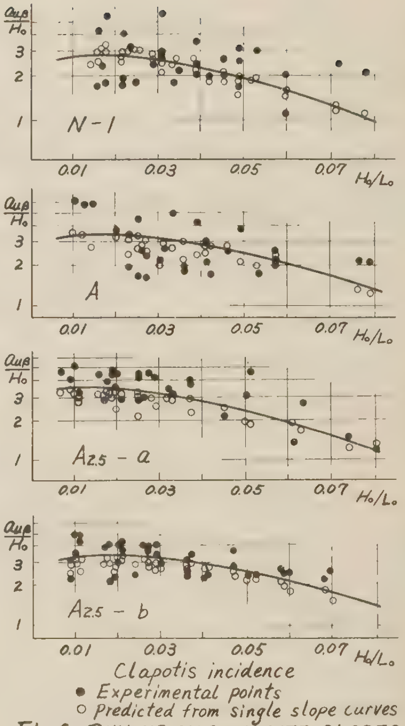

Fig. 6 RUN-UP ON COMPOSITE SLOPES

TABLE OF μ

H_0/L_0	0.01	0.02	0.03	0.04	0.05	0.06	0.07
N-1				←16.001→		←12.637→	
N-2				←4.649→		←2.610→	
N-3				←4.934→			←2.101→
A		←28.743→	←15.343→		←5.061→		
$L_{0.4}$	←98.708→		←46.219→			←7.035→	
S-1	←65.689→		←43.799→		←16.393→		
S-2		←96.607→	←34.823→		←13.274→		
$A_{2.5}$-S		←19.576→			←3.502→		
R-1-b	←26.643→	←12.923→			←4.138→		

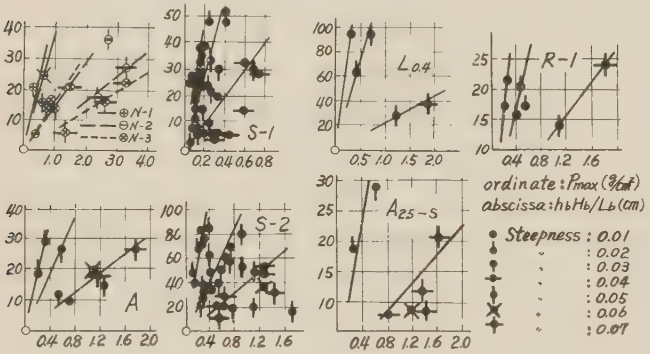

Fig 7 RELATION BETWEEN P_{max} AND $h_b H_b/L_b$

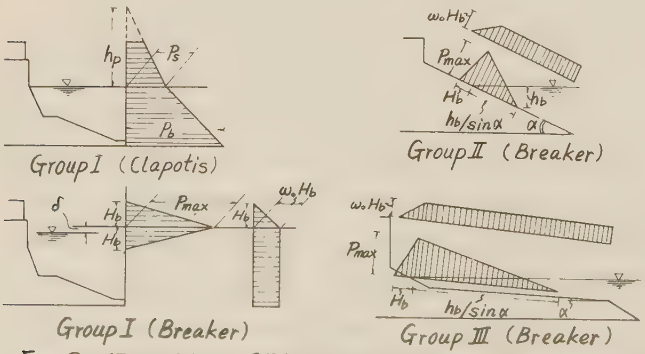

Fig. 8 VERTICAL DISTRIBUTIONS OF WAVE PRESSURE

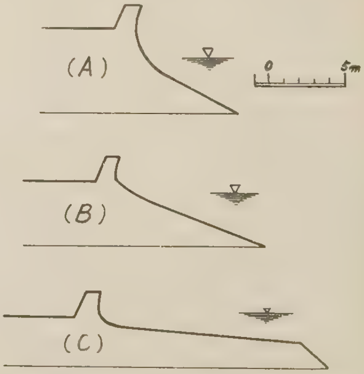

Fig. 9 RATIONAL CROSS SECTIONS OF SHORE DIKE

nd of incident mechanism respectively. These results up to now are not very r. v) Both the positive and the negative force in the impact on the dike step Group II and III interact frequently at the same time. Therefore, the attention have to be paid to the construction of dike.

Next, on the clapotis: vi) With regard to the vertical maximum pressure dis-bution for Group I, the maximum value of wave pressure is larger than the theoreti-value computed by Sainflou's formula.

After all, it can be concluded that the typical continuous or non-continuous or lsive periodical fluctuation as reported by Larras[9] or by Sainflou[8] does not occur wave pressure diagram.

(2) The Formula for the Maximum Pressure of Breaker on Dikes.

As the mechanism of breakers is very complicated, it is difficult to solve prob-s on the breakers directly from the standpoint of hydrodynamics. However, accord- to numerous pressure data obtained by this experiment, all situations of breaker act may be able to consider as the phenomenon that a jet dashes, in spite of the ious incident situations (i.e., in spite of the various dike forms). So, con-ering this phenomenon as a jet flow in the same way as Dr. Nagai's method[10], the fficient of the maximum pressure formula is determined experimentally in each im- situation of every cross section of dike:

That is

1. $P_{max} = \rho C^2$ where ρ is density of water.

This formula shows the pressure of a jet flow which dashes against a vertical . However, as the motion of the water particle which varies according to the e form is very complex, P_{max} is shown by the equation containing the coefficient, μ ermined in accordance to each dike form. That is

2. $P_{max} = \rho C_0 \mu' C^2$ where C_0 is constant.

Now, the first approximate value of the theory of shallow water is shown as lows

3. $ka = \tanh kh$ where a is the half wave height and k is $\frac{2\pi}{L}$.

4. $L = 2\pi a / \tanh kh$

If the wave length at the water depth $h_i\,[= f(H_i)]$ where the incident wave is nsformed (mainly, it is the water depth at the toe of the dike) is shown with L_b, coefficient of dike form is given by the formula

5. $\mu' = \dfrac{2\pi a}{\tanh kh} \Big/ L_b$

Then, if $C_0 \mu'$ is replaced by μ, P_{max} is given by the formula

6. $\underline{\underline{P_{max} / W_0 = \mu \pi h_b H_b / L_b}}$ where C is $\sqrt{g h_b}$ and $2a$ is equal to $H_b\,(\fallingdotseq h_b)$.

This formula is the general form of the computational equation for intensity of the maximum pressure of breakers. In Fig.7 the incident situations are classified in each group of dike according to the experimental data, and the relation between P_{max} and $h_b H_b/L_b$ is shown. The values of μ can be decided from Fig.7. Each line in Fig.7 is shown according to the classification of the incident situations corresponding with the range of steepness to each shallowness which is obvious in Fig.4.

Furthermore, according to this experiment, the distribution of wave pressure in each case can be decided by using equation 6. as shown in Fig.8.

V. Rational Cross Section of Dike.

From the above-mentioned, we know that the wave action on dikes varies with the remarkable change of condition in the locations. For instance, first of all, the depth of water at the toe of the structure, wave shape, interference of wave itself, and moreover, wind force, etc., and that at the same time, these elements are affected by the various forms of dike cross section. So, we have to design dikes taking into consideration that the form of dike must be selected so that it can be expressed in the most advantageous terms.

That is, the wave energy must be dissipated not by shore structures directly, but by the transformation of wave according to the shape of dike, i.e., by making the breaker waste its energy on account of the turbulence. So, it is necessary to make the dike in such a way that its cross section promotes the formation of breaker and its turbulent energy exhausted just in front of the dike wall. Moreover, the shape of the dike is influenced largely by the condition of the location, for instance, geographical features, foundation of site, etc. So, we have to decide the rational cross section of dike from all angles. Thus, we are made to realize that not only one rational shape of dike can be brought into existence in the future. Cross sections of dikes from Group I to III have merits as well as demerits, and we must choose the most profitable shape of dike according to circumstances.

From this, we can gain three types of the rational cross sections of dike as shown in Fig.9.

Let us make note on Fig.9: i) The surface wall of the dike in (A), (B) and (C) type is constructed smoothly by curves so that the slope composed of riprap at the dike's toe may not change abruptly, and the dike itself may do the duty of a parapet in order to control spray as much as possible. ii) The three dike forms (A), (B), and (C) are successively lower in height and longer in width in case of constant depth of water at the toe of the dike. Fig.9 is shown as the example with water depth of 3.6 meters at the toe of the structure, the wave height of 2 meters, the wave length of 50 meters and steepness of 0.04. iii) The characteristic of type (A) is that the cost of embankment is the cheapest among the three, and the experience of construction is abundant now-a-days, although in general, its wave run-up and wave pressure are the est. So the banking of type (A) is unsuitable in the site where the foundation oft and the change of water level is very large and where typhoons often occur. the other hand, type (B) and (C) are very suitable for wave forces, but the cost mbankment is not at all cheap. So these two types are unfit in ordinary founda- and where the change of water level is small. iv) The problem on the general truction, the form of rear part of dike and the others (including the problem of eability and drainage, etc.) is omitted in this paper.

The author would like to reiterate that this is only an example for the princi- of dike form and the dimensions of these types are changeable adequately in accord- with the circumstances.

In this paper, the author shows the characters of incident wave to shore struc- s and of wave run-up and wave pressure in every case. Here we can derive a prin- e of practical dike design. As mentioned in the preface, this is only a summary he study, so the author would like that Reference 11) in which this theme is dis- ed in detail be read. Moreover, in this study, each problem is considered only he situation of no wind at two dimensions, so the studies in which the case of que incidence and problem of diffraction and reflection of wave and wind forces, will be taken into account are expected in the future.

The author wishes to express his indebtedness to Prof. Toyoichi Takatsuki and . Prof. Toshio Sawata of Kyôto Univ., who kindly sent useful assistance and advice im. Moreover, the author takes this opportunity in thanking Prof. Tôjirô Ishihara Prof. Yûichi Iwagaki of Kyôto Univ. for the privilege of copying several litera- s and very helpful suggestions and criticisms.

References

Lt. C. B. Coyer
A Multi-Purpose Wave Generator
Proc. Minnesota Intern. Hydraulics Convention, 1953, pp. 281 ~ 291

John J. Healy
Wave Damping Effect of Beaches
Proc. Minnesota Intern. Hydraulics Convention, 1953, pp. 213 ~ 220

3) Tôjirô ISHIHARA, Yûichi IWAGAKI, Yûta SUZUKI
On the Design of Shore Dike - Specially its effective height
2nd Conf. Coast. Eng'g. Japan, 1955, pp. 57 ~ 70

4) Seiichi SATÔ, Tsutomu KISHI
Experimental Study of Wave Run-up on Sea Wall and Shore Slope
3rd Conf. Coast. Eng'g., Japan, 1956, pp. 127 ~ 137

5) Japanese Society of Civil Engineers
The Collection of Hydraulic Formulas
4th Part " Harbors ", pp. 247 ~ 248

6) T. Saville
Wave Run-up on Composite Slopes
Coast. Eng'g., Vol. 6, 1958, pp. 691 ~ 699

7) R. R. Minikin
Winds, Waves and Maritime Structures, 1950, p. 31

8) M. Sainflou
Essai sur les diques maritimes verticales
Annales des Ponts et Chaussees, IV, 1928

9) M. J. Larras
Le deferlement des lames sur les jeticales
Annales des Ponts et Chaussées, Mai, 1937

10) Sôshichirô NAGAI, Isao YAKUWA
The Pressure of Breaker on the Break Water
4th Conf. Coast. Eng'g., Japan, 1957, pp. 3 ~ 14

11) Jûichi KATÔ
Studies on Dike Design for Shore Reclamation - Consideration from the standpoint of hydraulics
Report of Shore Reclamation Section, 67th Report, 1959, pp. 1 ~ 475

THE EFFECTS OF COASTAL STRUCTURES ON THE LITTORAL SAND DRIFTS

Shohei Adachi, Member of J.S.C.E.
Assistant Professor, Disaster Prevention Research Institute, Kyoto University

Toru Sawaragi, Member of J.S.C.E.
Research Assistant, Dept. of Civil Engineering, Kyoto University

Akio Ogo, Member of J.S.C.E.
Technical Official, Harbour Bureau, Ministry of Transportation

ynopsis: This report concerns with the estimation of the shore line deformation of sand eaches by the variation of longshore current velocity along the shore line, when the ffshore breakwater is constructed. The development and final stable forms of tombolos esulting from the construction of offshore breakwater are experimentally analyzed in erms of the influences of length of breakwater, water depth at which the breakwater is onstructed, and steepness of deep water waves.

Furthermore referring to these basic experimental results, the deformation of shore ines at Miyazu Coast, Kyoto Prefecture, is estimated, when the offshore breakwater is lanned.

. Introduction

Among many types of shore deformations in beach processes caused by sand drifts, the each deformation in short duration results mainly from the movement of sand drifts in the irection of beach profile, whereas that in long duration such as a year, several years or ore, is commonly influenced by the littoral sand drifts with some exception in several ases of specific coastatal features. When coastal structures like jetties, breakwaters, ffshore breakwaters and sea dikes are planned, most significant is that the future shore eatures after completion of coastal structures must be estimated as possible as accurately o insure the control of the beach deformation against the wave action. Problems, therefore, oncerned with the effects of coastal structures on the littoral sand drifts become important o secure the hydraulic performances in beach protection, though each of coastal structures s distinctively different.

Many studies1)~4) have been made for the effects of shore structures on the deformation f shore line. These studies, however, treat mostly with the performances of jetties, beach roins, or levees on the beach process, whereas the influences of offshore breakwaters and ea dikes on the beach deformation have scarcely been studied. Offshore breakwaters are frequently used as a mean for protecting anchorages and beaches, and their effects on the littoral sand drifts are of quite importance.

For clarification of the effect of offshore breakwater on sand drifts, the following subjects must be studied: (1) duration and amount of littoral sand drifts, and (2) zone of movement of drifts. The relation between the amount of littoral sand drifts and the velocity of longshore current, which is the most important factor to the movement of sand drifts, has not been established, and therefore past studies made by the authors were only to estimate qualitatively the deformation of coastal features from the velocity distribution of longshore currents.

In this report, first is ascertained from the experiments conducted in the model basin that the method of estimation of the deformation process in the coastal features by the velocity distribution of longshore current is available for engineering needs and an analysis of the effects of offshore breakwater length, water depth at the breakwater and steepness of deep water wave on the formation of tombolos and its stable shapes is presented. Furthermore, with results of experimental data and the littoral distribution of the amounts of littoral sand drifts computed from wave energy, the deformation process at Miyazu Coast and its final feature are estimated, when the offshore breakwaters are constructed.

2. Transformation of wave heights by refraction and diffraction

When the waves come obliquely from offshore with a definite angle, they are gradually refracted by the topographical features. If there exists an offshore breakwater near the coast, the refracted waves are also influenced by the diffraction due to the structure and thus the wave height, the incidental angle and the breaking depth in sheltered area are appreciably changed. The same diffracted behaviours in wave characters are evidently seen, when the waves come normally to the structures. The estimation of changes in wave characteristics by refraction and diffraction is of basic importance to calculate the wave energy and the velocity of longshore current in the direction of shore line, therefore the change in characteristics of breaker refracted and diffracted by offshore breakwaters must be revealed for clear estimation of beach deformations in sheltered area. Letting the equivalent wave height to deep water wave (not refracted and diffracted) denote by H'_0 the following expressions are obtained.

$$\frac{H}{H'_0} = f\left(\frac{h}{L_0}\right), \qquad \frac{H_b}{H'_0} = f'\left(\frac{h_b}{L_0}\right) \tag{1}$$

where H is the wave height at the depth h, L the length of deep water wave, H_b the breaker height and h_b the breaking depth.

The relationship between H and H_b is expressed as follows, when the incoming waves are racted and diffracted,

$$\frac{H}{H} = Kf\left(\frac{h}{L_o}\right) \quad , \quad \frac{H_b}{H} = K'_b \quad , \tag{2}$$

re K is a coefficient of refraction at water depth h, and K'_b a coefficient of diffracn at breaking point. The ratio of H_b to H_o is then,

$$\frac{H_b}{H_o} = KK'_b\left(\frac{h}{L_o}\right) = KK'_b\left\{f\left(\frac{h}{L_o}\right)/f'\left(\frac{h_b}{L_o}\right)\right\}, \tag{3}$$

inserting Eq. (1) into Eq. (3), the equivalent wave height to deep water is expressed

$$H'_o = KK'_b\left\{f\left(\frac{h}{L_o}\right)/f'\left(\frac{h_b}{L_o}\right)\right\} H_o \tag{4}$$

ce K K'_b and f' in Eqs. (3) and (4) are evidently functions of water depth, H_b/H_o can not obtained only when H_o/L_o is given. The relations of H_o/L_o and h_b/L_o to K K'_b for particr waves of definite period must be evaluated in the region where the waves are diffracted, can be calculated by the following procedures.

(1) Assume the wave period T or deep water wave length L_o, and breaking water depth h_b.

(2) Obtain H'_o/L_o, H_o/H'_o $f'(h_b/L_o)$ for particular waves and particular breaking depths, and $H/H'_o = f(h/L_o)$ for the water depth at both ends of offshore breakwater.

(3) Compute the coefficients of refraction and diffraction for h_b assumed in (1), by the following method.

(4) Using the values obtained in (2) and (3), compute the steepness of deep water wave by the following equation of (5) for given values of h_b,

$$\frac{H_o}{L_o} = \frac{H'_o}{L_o}\,\frac{1}{KK'_b}\left\{f'\left(\frac{h_b}{L_o}\right)/f\left(\frac{h}{L_o}\right)\right\} \tag{5}$$

The coefficients of refraction and diffraction in (3) are obtained with the use of raction and diffraction diagrams. If the beach is constant grade and thus all contours parallel, the refraction coefficient can be obtained by the law of Snell, without using refraction diagram. Denoting the angle between the crest line of waves and the contour e at the water depth h by α , and the angle between the crest line of deep water wave the contour line by α_o, the following relations are obtained;

$$\frac{\sin\alpha}{\sin\alpha_o} = \frac{c}{c_o} = \tan h\,\frac{2\pi h}{L_o}\ , \tag{6}$$

$$K = \left(\frac{S_o}{S}\right)^{\frac{1}{2}} = \left(\frac{\cos\alpha}{\cos\alpha_o}\right)^{\frac{1}{2}} \tag{7}$$

re S is the distance between two orthogonals of wave crest line at waterdepth h, and fix o indicates the one for deep water. With the use of these equations, K is calated for definite values of α_o and h/L_o at all points. Fig. 1 indicates the relationp of these three variables, α_o, h/L_o and K. For the diffraction, J. W. Johnson[6] has calculated the changes of wave heights and phases from three to 360 wave lengths and J.W. Dunham also from one to 6 wave lengths, when the waves come perpendicularly to an infinite peninsula.

Offshore breakwaters are commonly constructed within the distance of several wave length from coast, so that the detailed computation for wave diffraction within the distance of two wave lengths was made by the use of Sommerfeld's[8] exact solution.

Fig. 2 is the diffraction diagram obtained by the calculated results, and also the experimental ones in wave height in a form of the ratio between the wave height in the sheltered area and that at the offshore side of breakwater are indicated by numerical values near small circles. As seen in this figure, a good agreement between computed and experimental values for wave height is obtained.

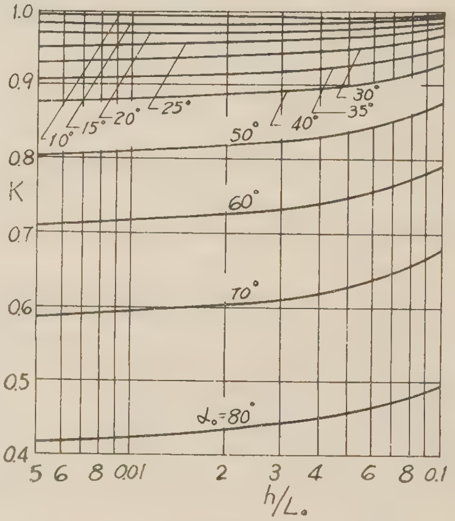

Fig. 1 Relationship between α_0, h/L_0 and K

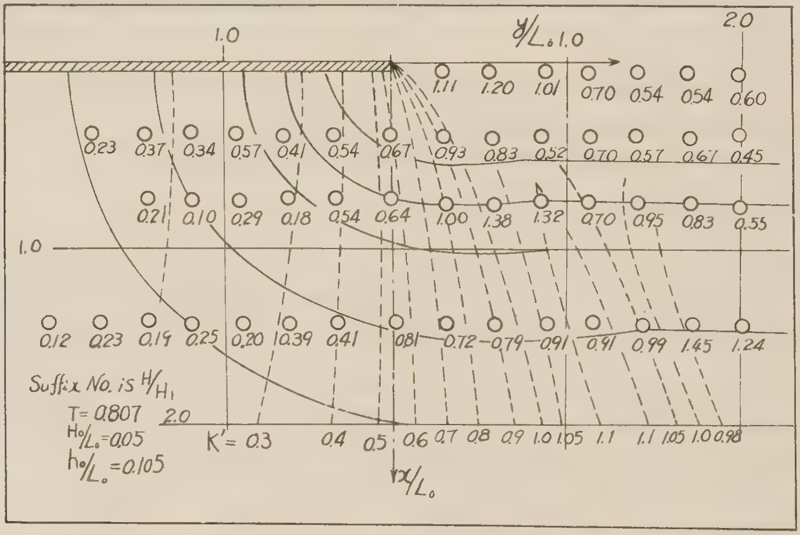

Fig. 2 Refraction diagram in the case of $y/L < 2.0$

3. Beaches deformation in sheltered area and formation and development of tombolos

The velocity of longshore current can be obtained by the height of breaker and the incident angle. In the past, beaches in sheltered area were presumed to be eroded if the locity of longshore current increases in the direction of running current and deposited the velocity decreases.

In this chapter, the validity of the preceding method of estimation for beach deforma-ion by the velocity distribution of longshore currents will be concerned, and the formation tombolos and its development as results of beach deformations are also investigated.

1) Velocity distribution of longshore current and deformation of beaches
in sheltered area.

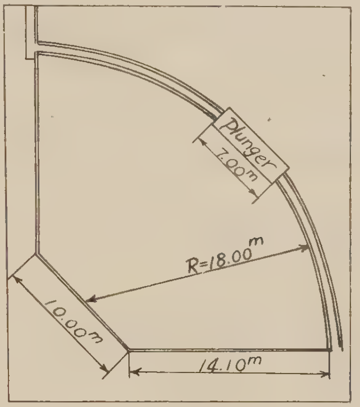

Fig. 3 Plane of the model basin of fun shape

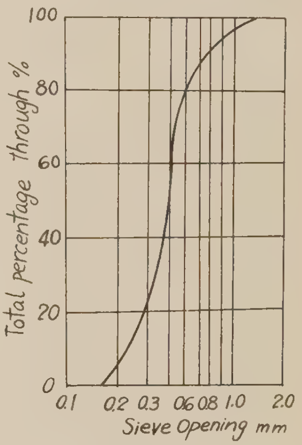

Fig. 4 Sieve analysis curve of used sands

The model basin of fun shape shown in Fig. 3 was used for various runs of experiments o that incident angles of aves can be changed. The elationship between the elocity distribution of ongshore current and the eformation of beaches was xperimentally studied, when he offshore breakwater was laced in the straight shore f constant bottom grade. urrent meters of propellar ype were used for velocity easurements of longshore current and the records ere made by the electrical devices.

The mean diameter of sands used is 0.42 mm, he sorting coefficient $\sqrt{d_{75}/d_{25}}$ is 1.26, the pecific weight is 2.66, and the grains of sands re approximately uniform having the grain size f sieve analysis curve as seen in Fig. 4. xperimental waves generated with angles of 30° nd 40° from shore line. The offshore breakwaters ere placed at angles (θ) of 0°, 30° and 40° from hore line for all waves.

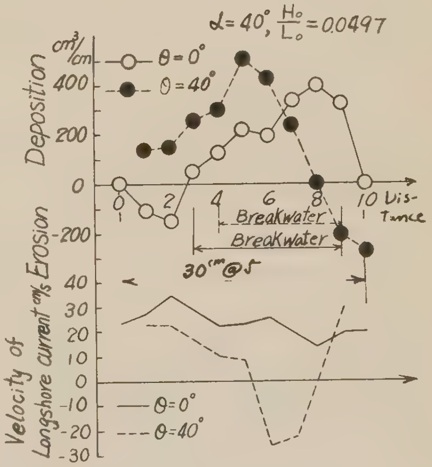

Fig. 5 Velocity distribution of longshore current and experimental results of beach process in the case of = 40°

Fig. 5 indicates the relation between the mount of sand transported per unit width in various sections of sheltered area and the velocity istribution of longshore current along a line 20 m apart from the original shore line. It is vident that the wave height decreases gradually in the inner part of sheltered area with results of decreases in longshore current velocity as estimated by the description in (2). In Fig. 5 which indicate the case of $\alpha = 40^\circ$ positive and negative signs in the velocity of longshore current indicates the components along the shore line in the progressive direction of waves and in the reverse direction, respectively, and θ denotes the angle between the offshore breakwater and the shore line. It is seen in this figure that the positive slope in curves of the velocity of longshore current indicates the possibility of erosion, and conversely the negative slope indicates that of deposition in both cases of $\theta = 0^\circ$ and 40°. The eroded area and deposited area, however, are largely influenced by the angle between breakwater and shore line. For $\theta = 0$, the erosion occurs at the frontal side of breakwater facing the progression of waves and the maximum deposition is seen near the other side. On the contrary, when the breakwater is placed at $\theta = 40^\circ$ and parallel to the crest line of incident waves, the maximum deposition occurs at the former side, whereas the erosion is seen at the latter side, and it indicates the opposite tendency to the case of $\theta = 0^\circ$.

It will be, therefore, evident that the offshore breakwaters constructed at a definite angle to the shore line and resulted in the beach deformation, give much influence to the final tongue-like shape of tombolo which is a result of beach progress due to erosion and deposition. It will be concluded that the future beach deformation can be forecasted for engineering purpose, if the velocity distribution of longshore current is estimated.

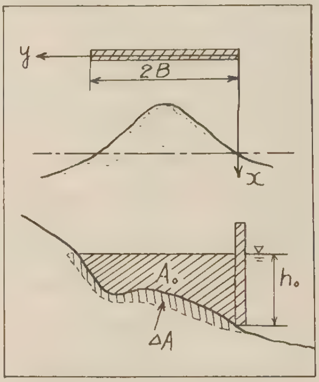

Fig. 6 Representation of symbols used in the study

(2) On the formation and development of tombolos.

The formation and development of tombolos have been briefly described in (1), by means of the diffraction phenomena of waves. In this section, influences of the steepness of deep water wave, the length of offshore breakwater, the water depth at the location of breakwater to the formation and development of tombolos are concerned, and furthermore, the final establishment of tombolo also is treated by the experimental results for $\alpha = 0^\circ$ and $\theta = 0^\circ$.

i) Influence of length of offshore breakwaters:

Before the analysis is concerned, symbols in the study are explained in Fig. 6, h_0 is the water depth at the location of offshore breakwater, and H_1 the wave height at the front side of offshore breakwater. The influence of the length of offshore breakwater was investigated in the four cases of $B/L_0 = 3.00$, 1.00, 0.50 and 0.25 under the definite condition of $H_0/L_0 = 0.05$, $h/L = 0.05$ and $T = 0.807$ sec. The experimental runs revealed that the change of amount V_b of deposited sand in the sheltered area behind the breakwater with time.

ii) Influence of location of offshore breakwater:

As seen in diffraction diagram of Chapter 2, the equivalent deep water wave steepness aries gradually with distance between the offshore breakwater and the beach line. The ave height H after diffraction is given by

$$\frac{H}{H_1} = K' \cos 2\pi \left(\frac{t}{T} - \mu \right), \tag{8}$$

here K' denotes the coefficient of diffraction at water depth h, μ the phase coefficient, the time, and T the period of wave.

The rate of sand drift by longshore currents parallel to the shore line at x/L_0 from he offshore breakwater is empirically expressed by the following equation derived rom the field observation at California oasts[9] and Miyazu coasts as well as exerimental results.

$$q_y = k E_i^m \tag{9}$$

here E_i is the energy of waves in the irection of shore line and k and m are onstant. Since E_i and $\cos\psi$ are,

$$\left. \begin{aligned} E_i &\propto H^2 L_0 \cos\psi, \\ \cos\psi &\propto \left(-\frac{\partial\mu}{\partial y}\right) \end{aligned} \right\} \tag{10}$$

here ψ denotes the angle between the hore line and the progressive direction f diffracted wave.

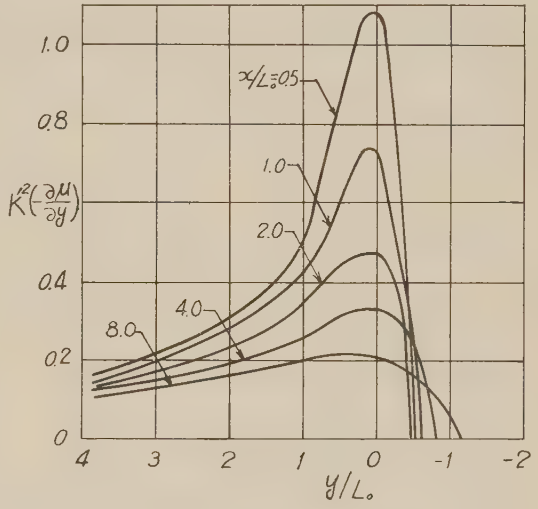

Fig. 7 Relation between $K'^2(-\partial\mu/\partial y)$ y/L_0 and x/L_0

When the incoming waves have the same characteristics, Eq. (9) is rewritten as follows,

$$q_y \propto \left\{ K'^2 \cdot \left(-\frac{\partial\mu}{\partial y}\right) \right\}^m, \tag{11}$$

Curves of $K'^2(-\partial\mu/\partial y)$ to y/L_0 are indicated as a parameteric expression of x/L_0 in ig. 7. Curves are steep for small values of x/L_0 and they become gradually flat with the ncrease of x/L_0. Since q_y is related with the $K'^2(-\partial\mu/\partial y)$ through Eq. (11), the heavy rates f sand movements are indicated by steep curves in Fig. 7, and therefore for small values f x/L_0, the transportations of littoral sand drifts, which results in erosion and deposiion, are appreciable.

No large variation in transportation of sand drifts along the beach line is produced y the longshore current, despite of the movement of sand particles, when the offshore breakwater is placed far from the shore line, and the sand drifts are little deposited in the sheltered area. On the contrary, the sand drifts transported decrease rapidly with the increase of y/L_0 in the sheltered area when the offshore breakwater is placed near the shore line, with results of appreciable deposition.

iii) Influence of steepness of deep water wave:

The wave of $H_0/L_0 = 0.05$ in this experimental run is transformed into the wave of equivalent deep water wave steepness $H'_0/L_0 < 0.03$, at which the sands are extremely transported. The wave of $H_0/L_0 = 0.02$ becomes the equivalent deep water wave of $H'_0/L_0 < 0.012$ gives less movement of sands compared with the former case. Therefore it is estimated the rate of deposition is larger in the case of $H_0/L_0 = 0.05$ than in that of 0.02, despite of the value of h_0/L_0. This facts is revealed by Fig. 8, which shows the rate of deposition at various cross sections in sheltered area with the changes of H_0/L_0 and h_0/L_0.

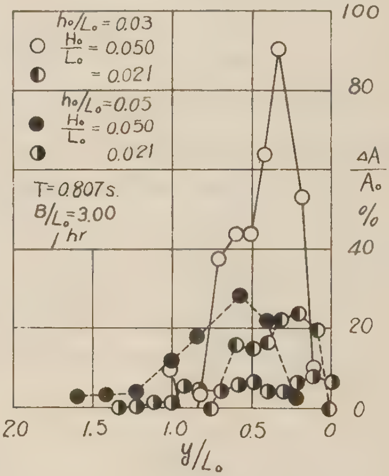

Fig. 8 Variation of rate of deposition by change in H_0/L_0 and h_0/L_0

iv) Final shape:

The formation and development of tombolos have been discussed in i) ~ iii), and in this section, the final shape after establishment of tombolos will be treated. Fig. 9 shows the final shapes of the shore line for various values B/L_0 and it is seen that the resulting beach line is independent of the length of offshore breakwater. When the depth at the location of offshore breakwater is taken as variable, the final features of shore line are of similar shapes, independing on the shallowness, h_0/L_0. The shape of shore line coincides to the crest line of incoming waves after diffraction. Therefore, it is considered the final shape of tombolos will be estimated, when the incident waves come normal to the shore line and no sand drifts along the shore line are produced. Since the shape of tombolos becomes stable when the shore line coincide with the crest line of diffracted waves, there will be some relationship between the depth of water h_0 at the location of offshore breakwater and the distance B' from the intersecting point of tombolo and offshore breakwater to the end of structure. The experimental relationship is indicated in Fig. 10. Thus, with

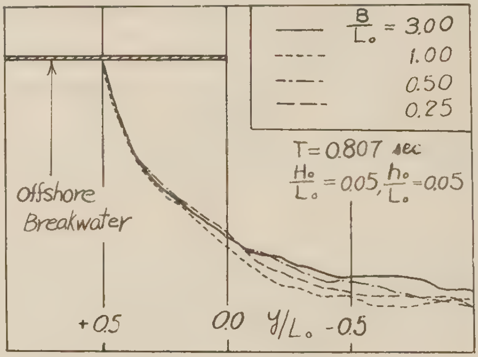

Fig. 9 Final shapes of shore line for variable B/L_0

e use of the diffraction diagram, the future
atures of shore line will be estimated for
ven water waves L_0.

The influence of H_0/L_0 to the final shape
tombolos will be next considered. The
apes of diffraction diagram are not in-
uenced by the values of H_0/L_0, as explained
the theoretical solution on diffraction by
mmerfeld. Although the values of H_0/L_0 in-
luence to the rate of growth of tombolos, its
inal features will be considered not to be
nfluenced by the wave steepness of deep water
aves.

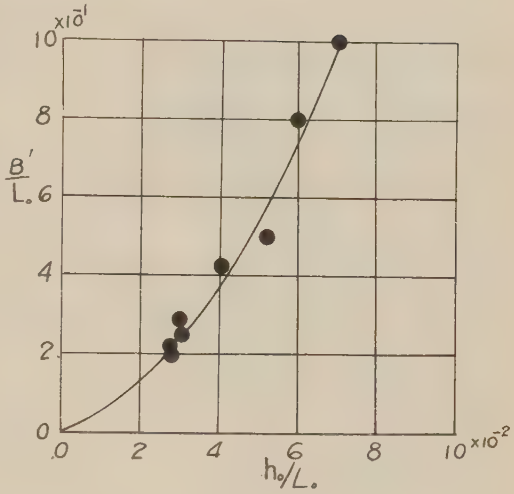

Fig. 10 Relation between B'/L_0 and h_0/L_0

Fig. 11 shows changes in the rate of
eposition at several cross sections in the
heltered area with the change in H_0/L_0 and
he evidence of foregoing description, and
o significant influence of H_0/L_0 to the
inal shape of tombolos will be seen.

The beach deformation in the sheltered
rea by the action of diffracted wave for
= 0 and $\theta = 0$ has been discussed in above
ections. Problems on the final shapes for
≠ 0, $\theta \neq 0$ remain unsolved. Further
asic studies should be made in order to
larify the process of beach deformations in
his case.

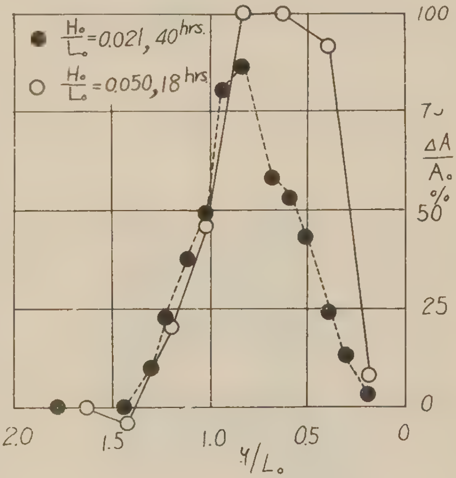

Fig. 11 Changes in rate of deposition at each cross section with change in H_0/L_0

. Estimation of beach process at Miyazu Coast

In this chapter, using the foregoing
asic experimental results, the process of beach deformation by the construction of off-
ore breakwater at Ejiri of Miyazu Coast, Kyoto Prefecture, is revealed. As the first
tep, the authors estimate the beach deformation from the velocity distribution of long-
ore current along shore line and check the estimation by the distribution of amount of
and drifts, along shore line, using the relation between the wave energy and the amount
sand drifts, obtained by the field observations.

Furthermore, the final shapes of shore line in sheltered area resulting from the construction of offshore breakwater will be treated, using the descriptions in Fig. 10 and the diagram of diffraction.

(1) Estimation of beach deformation by the velocity distribution of longshore current.

Miyazu Coast situates in the west coast of Miyazu Bay, the mouth of which opens northeast toward the Japan Sea, and Amanohashidate which is a typical sand spit is in this coast. The bottom grade is nearly constant. The sand drifts in this coast are transported by waves of incident angle 85° to the shore line and moved from north to south.

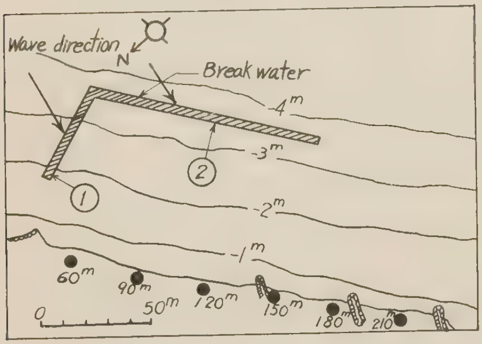

Fig. 12 Location of offshore breakwater at Miyazu Coast

The period of incident wave at Miyazu Coast is estimated 3 7 sec by the analysis of wind velocities and directions.

The offshore breakwater for anchorage shown in Fig. 12 has been planned and constructed partly. Before the velocity of longshore current in the sheltered area by the offshore breakwater is estimated, the variation of breaker height and the breaking angle to the shore line resulting from the refraction and diffraction must be definitely evaluated. Fig. 13 is the relationship of H_o/L_o, h_o/L_o to $K \cdot K'_b$ for Miyazu Coast described in chapter 2 and it is seen in the figure that the breaker height and breaking depth for a particular deep water wave of a definite steepness are variables of locations in the sheltered area. In the figures, the values of y represent the distances along the shore line as in Fig. 13.

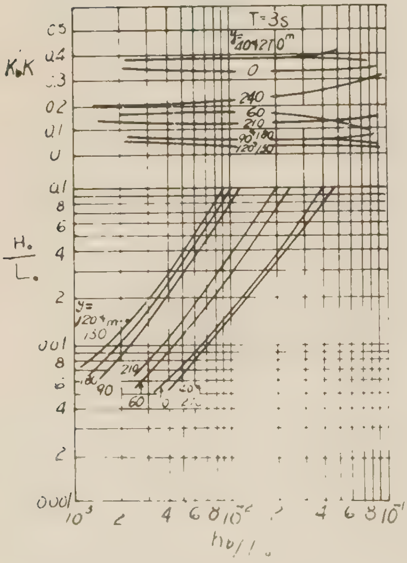

Fig. 13 Relation H_o/L_o, h_o/L_o an $K K'$ at Miyazu Coast in the case of T 3 sec.

The coefficient of friction k_f must be known for computation of longshore velocity. Inman and Quinn[11] proposed the empirical equation of (12), using a large number of data obtained by field observations and experiments,

$$k_f = 0.00404\ V^{-\frac{3}{2}} \quad (\text{m - sec}) \qquad (12)$$
$$= 0.024\ V^{-\frac{3}{2}} \quad (\text{ft - sec}).$$

The calculated velocity by Eq. (12), however, is different from the observed results by the authors o that the authors obtained the value of k_f by the bserved data through the equation of Putnam, Munk nd Traylor[12] on the velocity of longshore current. ig. 14 shows the relationship between k_f and observed velocity of longshore current and the follow ng empirical equation for k_f will be proposed.

$$k_f = 0.0249\,V^{-\frac{3}{2}} \quad (\text{ m - sec }) \\ = 0.1476\,V^{-\frac{3}{2}} \quad (\text{ft - sec }). \qquad (13)$$

sing Eq. (13), the velocity of longshore current t various locations in the sheltered area are calulated for particular waves of definite characterisics in period and steepness, and the results are hown in Fig. 15. The regions of erosion and deposiion estimated by the decrease and increase of longhore current velocities are also indicated in the same figure.

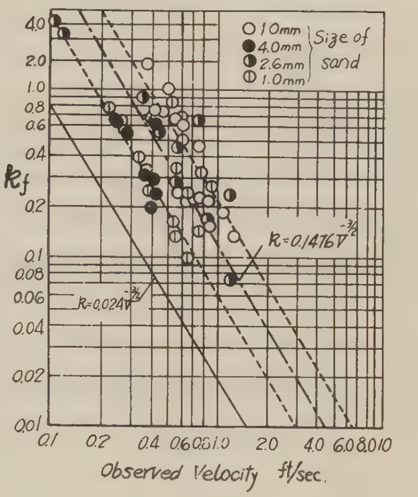

Fig. 14 Relation between coefficient of friction and velocity of longshore

As seen in this figure, when an offshore breakwater is constructed at sandy beach, the and drift is deposited in the inner part of breakwater, whereas the erosion is occurred in he out side of breakwater, independing on the characteristics of incoming waves.

2) Estimation of beach deformation by the distribution of amount of littoral sand drifts.

Fig. 16 indicates the relation between the transmitted energy of breaker per unit length long the beach line expressed by Eq. (14) and the total amount of littoral sand drifts Q_1 n terms of a parametric expression of H'_0/L_0.

$$E_i = \frac{1}{16}\,wH_b^2(L_b/T)\sin 2\alpha_b, \qquad (14)$$

where L_b is the wave length of breaker, w the specific weight of water. Fig. 17 shows the distribution of amount of littoral sand drifts for the wave of T = 5 sec and H_0/L_0 = 0.03, and that of T = 6 sec and H_0/L_0 = 0.02 with use of $K \cdot K'_b$ obtained in (1), E_i in Eq. (14) and Fig. 16. Evidently seen in this figure the prediction of beach features by the distribution of amount of littoral sand drifts is reduced to the same result

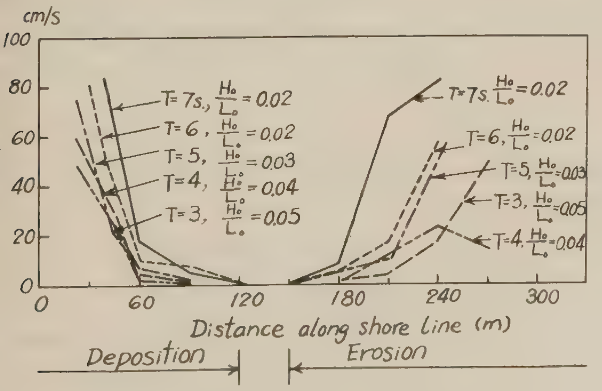

Fig. 15 Distribution of longshore current velocity in sheltering area

estimated by the velocity distribution of longshore current.

(3) Final shape

As shown in Fig. 12, the breakwater is made up with two parts; the one ① runs towards the shore and the another ② runs parallel with the shore line. As regards the part ① of the offshore breakwater, resulting function of the tombolo to the littoral sand drifts becomes the same one as of groin. Then we have only to consider the diffracted wave by the offshore breakwater ② which can also form a tombolo. The final shape of this shore will be able to be estimated, since the final shape of tombolo is not influenced by H_0/L_0 and B/L_0 as described in the previous chapter and is determined only by h_0/L_0.

In the plan on construction works of breakwaters at Miyazu Coast, the depth of breakwater placement is designed to be 3.5 m. The final shape of tombolos therefore is determined only by the wave length L_0. Table 1 indicates the value of B' for

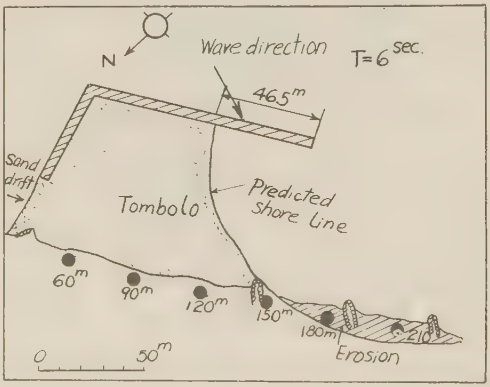

Fig. 18 Final shape of shore line in the case of T = 6 sec

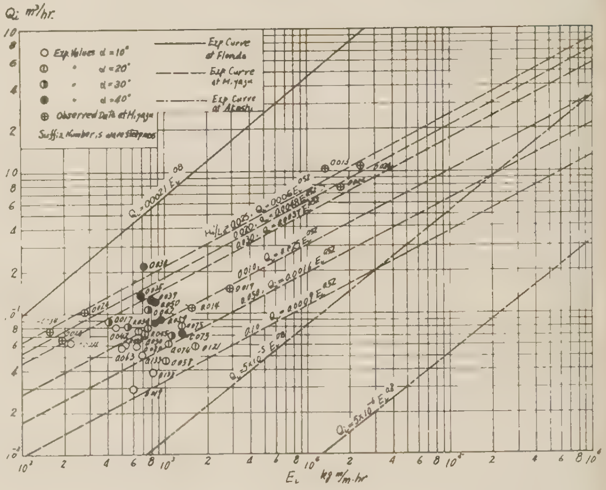

Fig. 16 Relation between E_i and Q_i

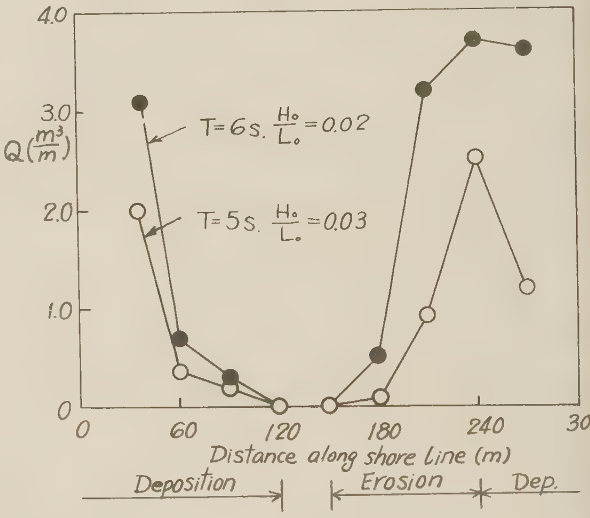

Fig. 17 Distribution of amount of littoral sand drifts in sheltered area

T(s)	B' (m)
5	50.6
6	46.5
7	37.8

Table 1 Values of B'

aves of $5\sim7$ sec. obtained from Fig. 10. The value of B' becomes large with decrease ve length as seen in Table 1 and thus the tombolos hardly when wave length becomes .

'ig. 18 shows the final shape of tombolo for the wave of T = 6 sec. which is most commont yazu Coast. When the offshore breakwater is designed as anchorage, if the depth at the nent of offshore breakwater is constant, the anchored area is determined by the wave i, so that longer breakwaters than those determined by the previous discussion are unsary for coastal design.

As seen in Fig. 18, a good agreement between the final shape predicted by the empirical ionship described in Fig. 11 and the estimated result by the distribution of longshore nt velocity and the distribution of amount of littoral sand drifts is obtained.

onclusion

In this study, the authors proposed the method of estimation for beach deformations by ffshore breakwater by means of the velocity distribution of longshore current, and it erified from the experimental study and the field observations of sand drifts at the . The effects of the breaker length, the water depth at the location of breaker and teepness of deep water waves on the formation and development of tombolos were experiilly investigated, and the final stable shapes of tombolos were also treated. With the f the results obtained, the process in beach deformation at Miyazu Coast was estimated, the offshore breakwater would be constructed.

'urther investigation to obtain the influences of incident wave angle and the location fshore breakwater to the beach deformation by the basic experiments will be extensively ipate.

The authors desire to express their hearty thanks to Prof. Ishihara and Assist. Prof. ci for very valuable advices and suggestions during the work.

References

agai, S. : Studies on Groins (Report 1), Proc. 1st Conf. of Coastal Engr. in Japan, .S.C.E., Vol. 1, 1953, Nov., pp. 99-104

agai, S. : Studies on Groins (Report 2), Proc. 2nd Conf. of Coastal Engr. in Japan, .S.C.E., Vol. 2, 1954, Nov., pp. 107-116

iimano, T., Homma, H., and Horikawa, S. : On the effects of Groins, Proc. 2nd Conf. f Coastal Engr. in Japan, J.S.C.E., Vol. 2 1954, Nov., pp. 49-56

iimano, T., Homma, H., and Horikawa, S. : Experimental studies on the effects of groins, oc. 3rd Conf. of Coastal Engr. in Japan, J.S.C.E., Vol. 3, 1955, Nov., pp. 195-202

shihara, T., Iwagaki, Y., and Murakami, M. : On the Investigation of Beach Erosion along the North Coast of Akashi Strait, Trans. of Coastal Engr. in Japan, Vol. 1, 1958, pp 97-

6) Johnson, J. W., O'Brien, M. P., and Isaacs, J. D. : Graphical Construction of Wave Refraction Diagrams, Hydrographic Office, U. S. Navy, Publ. No. 605.

7) Dunham, J. W. : Refraction and Diffraction Diagrams, Proc. 1st Conf. of Coastal Engr. 1950, pp. 39-49.

8) Sommerfeld : Theorie Mathematique de la Diffraction, Math. Ann., Vol. 47, 1896.

9) Caldwell, J. M. : Wave Action and Sand Movement near Anaheim Bay, Calif., Beach Erosion Board, Tech. Memo., No. 68, 1956.

10) Sawaragi, T., and Murakami, M. : On the Estimation of Amounts of Littoral Sand Transpor Proc. 4th Conf. Coastal Engr. in Japan, Vol. 4, 1956, pp. 41-49.

11) Inmann, D. L., and Quinn, W. H. : Currents in the Surf Zone, Proc. 2nd Conf. on Coastal Engr., 1951, Nov., pp. 24-36.

12) Putman, J. A., Munk, W. H. and Traylor, M. A. : The Prediction of Longshore Currents, Trans. A.G.U. Vol. 30, No. 3, 1949, pp. 337-345.

ARRANGEMENT OF GROINS ON A SANDY BEACH

Shoshichiro Nagai*

It is an important and difficult problem to arrange groins effectively for protection st erosion by wave action on a sandy coast. This paper will present the relation of roins' length, space, and orientation with respect to the shoreline, the direction of propagation, and the breaking point of the breakers. The relationship between wave ness and sand transport, and some results of experiments concerning special types of s are also presented.

Groins, constructed perpendicular to, or at an inclination with the shoreline, have used as one of the most effective measures for coastal protection on a shore which n abundant littoral drift coast. Notwithstanding a few laboratory experiments and investigations with the groins, it has until today been impossible to deal rational- th the length, direction with respect to wave climate, space and arrangement of the s on sea shores. Therefore only practical experience has played an important role in problem.

The writer has been studying since 1954 about the relationship between the length of s, the space between them, the orientation with respect to wave propagation, the type haracteristics of waves, and the longshore currents due to wave breaking in the Field ulic Laboratory of Osaka City University. Only the results of the experiments on s will be described in this paper.

MOTION OF SAND PARTICLES BETWEEN GROINS

Shoshichiro Nagai and Hirokazu Kubo**

Experiments on the motion of sand particles between groins were performed in a fixed to compare with the results of groins in a movable bed. The comparison proved that results were in comparatively good agreement.

Arrangements of groins on a sandy beach were studied for two years, 1954 and 1955,

---

of. of River and Harbor Engr., Faculty of Engr., Osaka City University.
st. of River and Harbor Engr., Faculty of Engr., Osaka City University.

in a basin with a movable bed, and the results were reported in the Proceedings of the American Society of Civil Engineers, Separate Paper 1063, WW 4, September 1956. The experiments dealing with the motion of sand particles between groins were made in a basin with a fixed bed during the period April 1957 to March 1958. This paper presents a comparison of the results of the previous movable bed experiments with the results obtained in the fixed bed experiments.

THE SHOCK PRESSURES EXERTED BY BREAKING WAVES ON BREAKWATERS

Shoshichiro Nagai

Since the prediction of shock-pressures exerted by breaking waves on breakwaters is the most important thing to be known for the design of breakwater, the problem has been studied by a number of harbor engineers and investigators during several decades in nature as well as in model in many parts of the world. But very few informations have been available in regard to both the theory and the practical data obtained by measurements in seas, because of the difficulties in the experiments and actual measurements due to the high intensity and instantaneousness of the shock pressures. Therefore most of structures along a shore and in a sea has hitherto been designed by rule of thumb methods established from the experiences of disastrous damages caused in maritime structures at storms. To the author's knowledge it seems that there exists no generally accepted formula which is available with sufficient confidence to insure that both safe and economical designs are obtained, being established on the basis of a sufficient number of practical or experimental data.

In Japan the Hiroi's formula, $p = 1.5\ w_0 H$, which was established for the pressures of breaking waves on the still water surface by Dr. Isamu Hiroi about forty years ago, has been used till now for the design of maritime structures by the use of a thumb method, in which the pressures of the intensity $p = 1.5\ w\ H$ were assumed to be distributed uniformly on the vertical walls of breakwaters from the top to the bottom for the prediction of the total wave pressure on the unit length of the vertical walls.

In other countries the first information was probably given in 1937 by Mr. Larras, as far as laboratory data were concerned on the time variation of the shock-pressures of breaking waves. Mr. Bagnold reported in 1939 on the shock-pressures exerted on a vertical wall by a single wave driven forward along a level floor. The actual measurements of shock pressures were carried out in 1935 and 1937 on the breakwater in the harbor of Dieppe But this problem was too difficult to be solved by only these few field and laboratory data

The author has been studying on this subject since 1959 and the experiments are still w under way. Two thousands or more tests have been performed of the shock pressures erted by breaking waves on the vertical walls of composite-type breakwaters by the use two or three wave-pressure-gauges, and the behaviours from instant to instant of the eaking waves plunging against the breakwaters, the relationships between the wave pres-res and the configurations of the breaking waves, the motion of the water particles in e breaking waves, etc. were measured by motion of the 16 millimeter high speed movie taken 3000 frames per second in synchronism with the pressure gauges. On the other hand, e mechanics of the shock pressures was also studied theoretically. From the results of e theoretical considerations and the experimental data, the new formulas of the maximum ock pressure as well as the vertical distribution of maximum simultaneous shock pressures ere established for the vertical walls of composite-type breakwaters.

) Proc. of ASCE, Separate Paper 1063, WW 4, Sept. 1956.

) Proc. of ASCE, Separate Paper 1876, WW 5, Dec. 1958.

) to be published recently in the Proc. of ASCE.

AN EXPERIMENTAL STUDY ON THE SUBMERGED BREAKWATER

Masashi Hom-ma, Dr. Engineering
Professor of Civil Engineering, University of Tokyo

Toshitsugu Sakou
Postgraduate Student, University of Tokyo

Introduction

A submerged breakwater is a kind of offshore structures, with its top at or below sea er level, used for the creation of a protected area of waters or for the protection of stal structures and beaches from damage and erosion caused by wave action.

It is considered that the submerged breakwater possesses the following two principal ctions:

(1) to attenuate waves by causing prematured breaking and partial reflection,

(2) to bar a seaward movement of the bed materials in the surf zone.

Up to present there have been a great deal of contributions to the study of these ctions, theoretically and experimentally, from various sources and from various points view. Most of them deal with the effects of the height, shape, width, location, etc. of breakwater on the transformation of waves passing it. Pre-breaking condition of waves adopted for this treatment. On the other hand, the effect on the sand movement and demation of beach due to the existence of the breakwater has not sufficiently been argued . In applying the submerged breakwater to the actual coast, as a means to prevent beach sion, however, this latter function of the breakwater might be of more significance and, the same time, post-breaking condition of waves should be considered as it is oftener ated in the surf zone. Indeed it is our desire to become able to predict the possible nge in beach profiles after the construction of the wall and to estimate the amount of ur around the wall, for design, construction, and maintenance of the submerged breakwater.

Therefore, the aim of this study was to know the basic facts in connection with the dimensional deformation of beach in an experimental wave flume with breakwaters in place especially the depth of scour around the wall placed in the vicinity of the breaking nt.

Equipment and procedures

The wave flume, 17 m long, 0.7 m wide, 0.6 m deep was used, water depth kept at 0.35 m, the beach slope 1/15 was built at one end of the flume. Fig. 1 shows the mechanical ysis of the beach sand used, which was chosen to reproduce actual conditions and to

NO.	T	H_{35}	L_o	H_o	H_o/L_o	d_b	x_b
I	1.80 sec	10.1 cm	506 cm	10.4 cm	0.0205	13.0 cm	195
II	1.40	11.8	300	12.8	0.0427	14.7	220
III	1.15	9.2	206	10.1	0.0490	11.3	170

Table 1

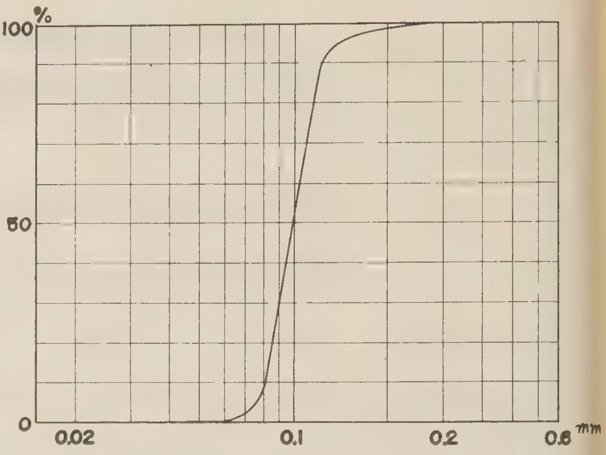

Fig. 1

simplify the analysis by limiting sand size variation to a narrow range.

Table 1 shows the characteristics of the model waves employed. A model breakwater was made up of a concrete block stand and movable wooden blocks which completely intercept the flow of water in sand layers beneath the breakwater.

The model breakwater was placed during each run at breaking point, inshore 1/4 of the distance from the breaking point to the shoreline, and offshore half of the breaking wave length. The ratio of the wall height to the water depth of placing, h/d, was varied 0.5, 0.75 and 1.0 for each run and wall location.

Beach profiles were recorded, for each run, at 15 min., 30 min., 60 min. and 100 min. from the start.

3. Experimental results

Attacked by waves, initial beach slopes began to deform in a way corresponding to individual wave characteristics, wall location and wall height for each run. In a few minutes from the start deformation became visible near the wall, then propagating gradually seaward and shoreward. Sand ripples were found throughout the entire bed except for the nearest vicinity of the wall. Their size, shape or the region they dominated varied for each run and seemed to depend on wall conditions and the duration of the wave attack.

For small value of h/d, trough-like deformation shoreward of the wall was produced but its magnitude was much smaller than troughs formed in case there was no wall in place. It is easily imagined that the breakwater acts as an artificial longshore bar in that case. For larger values of h/d, there existed the region in the shoreward bed of the wall where no visible change or irregularity of bed profiles was observed.

Figs. 2 and 3 show the change of bed profiles with the lapse of time for wall location at breaking point. These figures show that scouring action of waves came to be weak in a relatively short time, and then the change of bed profile spreaded gradually seaward.

Fig. 4 shows the ratio of maximum scour depth of every 5 minutes to that of 100 min.

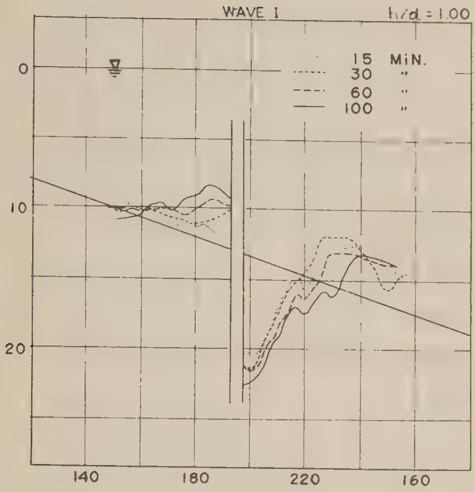

Fig. 2

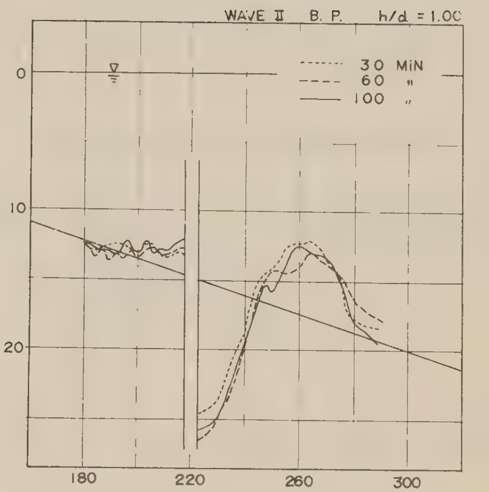

Fig. 3

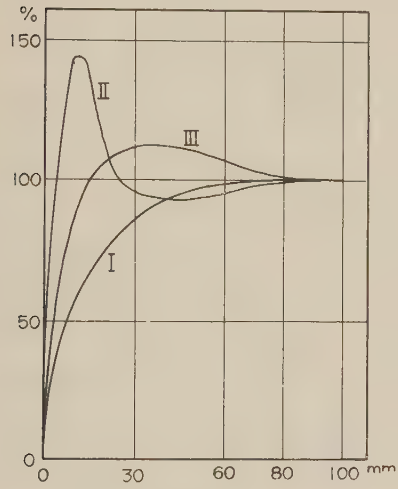

Fig. 4

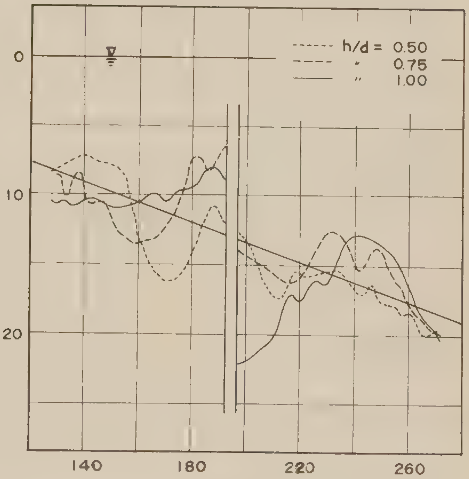

Fig. 5

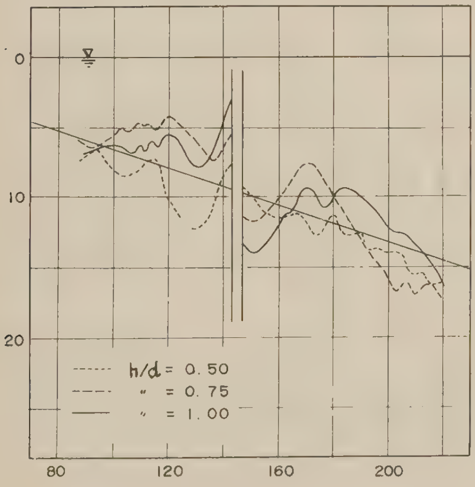

Fig. 6

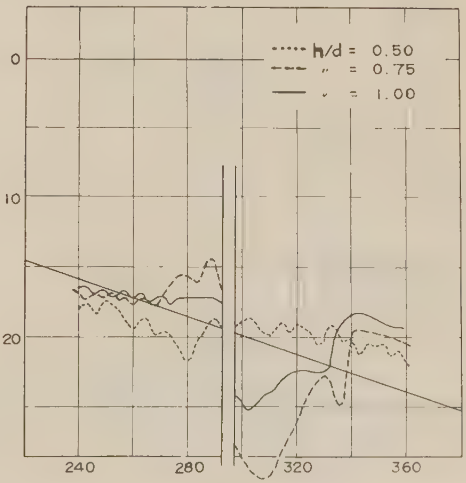

Fig. 7

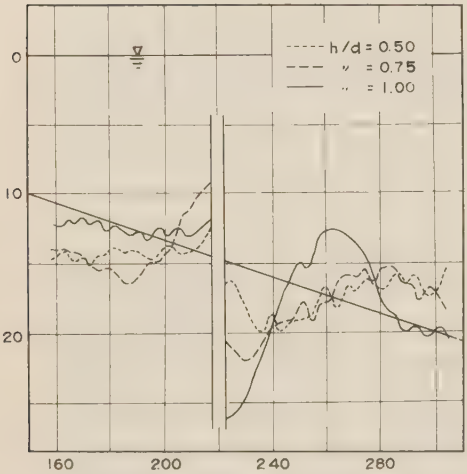

Fig. 8

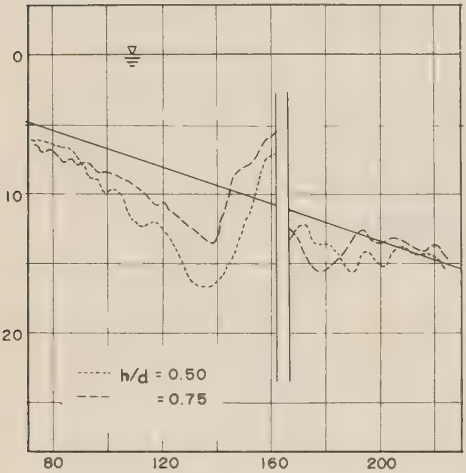

Fig. 9

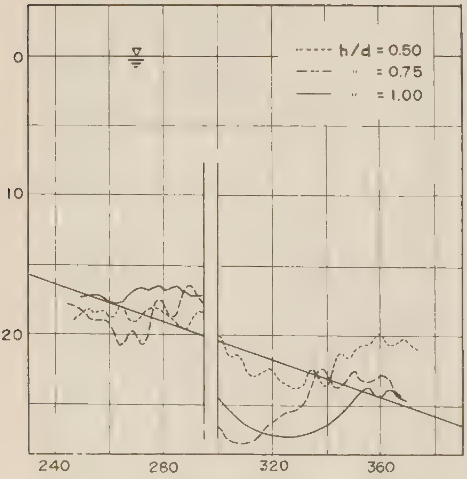

Fig. 10

from the start for that run. In that figure types I, II and III represent breaking point, inshore and offshore locations of the wall, respectively. The depth of wallside scour seaward of the wall seemed to reach a constant value in a comparatively short time.

Figs. 5,6,7,8,9 and 10 show the effects of h/d on profile deformation for each set of wave and wall location after 100 min. from start. Taking Fig. 5, for example, the bed immediately seaward of the wall was scarcely scoured for h/d=0.50 and 0.75, while for h/d = 1.00 the depth of scour reached 70 % of the water depth of the wall location, and the bar formed further seaward grew larger.

Fig. 6 represents the results with the wall in the surf zone, that is, shoreward of the supposed trough position without any wall in place as is shown in Fig. 11. Comparison illustrates the decrease of magnitude of bed deformation due to the existence of the wall. Scour for h/d=1.00 was remarkably deep, but the bottom topography is different from that for h/d=0.5. Breakwaters placed on a sloping beach caused sea level rise shoreward of the wall as they hinder the return flow from the shore. Flow over the wall due to this rise played an important role in scouring shoreward bed, and the types of vortice thus produced were different as is illustrated in Fig. 12. This is the cause of the difference of bed scouring patterns produced by the composite action of waves and overflowing waters.

Fig. 7 is the result with walls offshore of the breaking point. It is noticed that little deformation took place around the wall for h/d = 0.5. That is attributed to the fact that waves broke spillingly over the wall, exerting little force on the bed in the vicinity.

Figs. 8, 9 and 10 show similar results corresponding to each of the examples mentioned above, depending on each wall location.

Figs. 13 and 14 are the graphical presentation of the ratios of the scour depth immediately seaward of the wall to the water depth of the wall position and the maximum scour depth throughout the entire bed to the water depth of the wall location, respectively.

From these figures following facts were summarized;

(1) The ratio is maximum for wall position at breaking point and minimum for offshore wall position.

(2) The ratio increased as h/d increased for breaking point and surf zone wall location. It decreased, however, for offshore wall location with $h/d = 1.00$.

(3) The difference of wave characteristics, as far as Wave I and II concerned, did not affect the result.

Summary 2 above can be considered to be due to the supposed fact that the faculty of causing scour by overflowing water diminished as the height of the wall increased.

Fig. 14 employs $s(\max)$, the maximum scour depth throughout the entire bed, instead of s in Fig. 13. Difference between $s(\max)/d$ and s/d became smaller as h/d increased which varifies the explanation on the mechanism of scouring mentioned above.

Bed immediately shoreward of the wall in Fig. 5 was accreted. Its magnitude increased for large value of h/d. Similar statement can be made for Fig. 6. Fig. 7, on the other hand, shows that there was no change in the bed profile in the shoreward vicinity of the wall. As far as all the experiments conducted here concerned, the bed in the shoreward vicinity of the wall deformed little and was rather accreted.

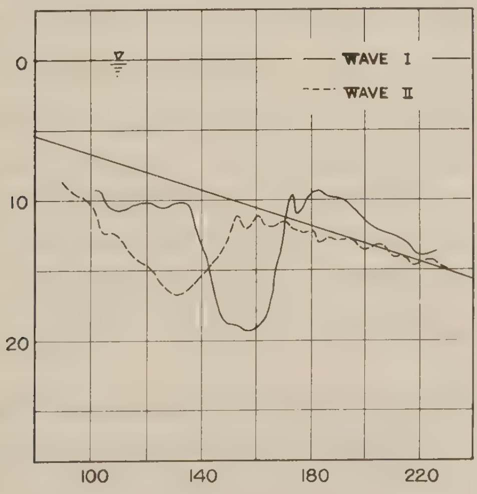

Fig. 11

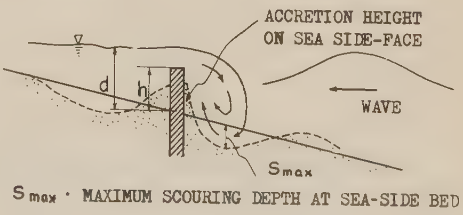

S_{max} · MAXIMUM SCOURING DEPTH AT SEA-SIDE BED

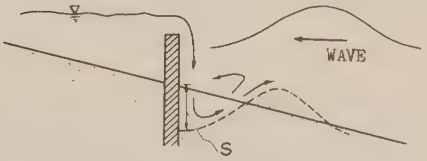

S SCOURING DEPTH ON SEA-SIDE FACE
(= MAXIMUM SCOURING DEPTH AT SEA-SIDE BED)

Fig. 12

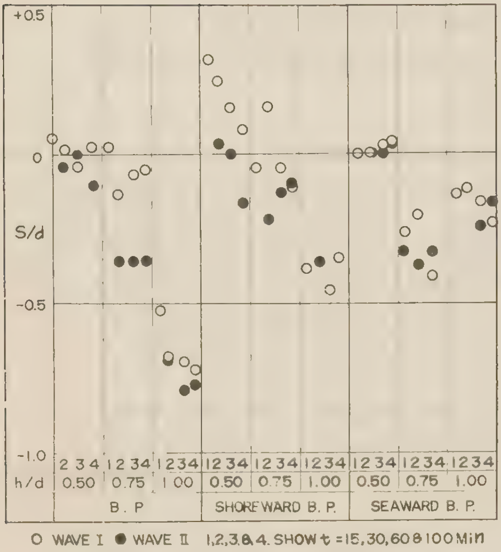

Fig. 13

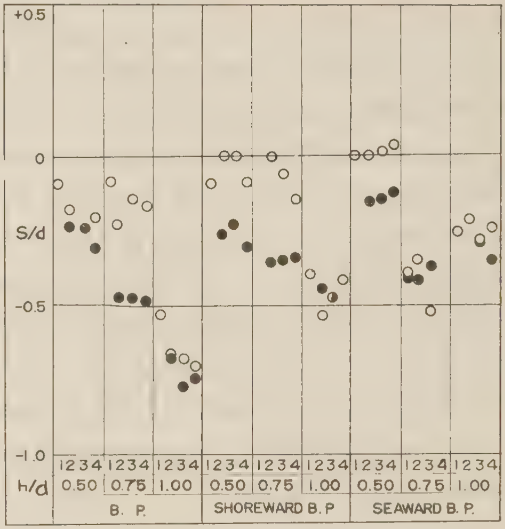

Fig. 14

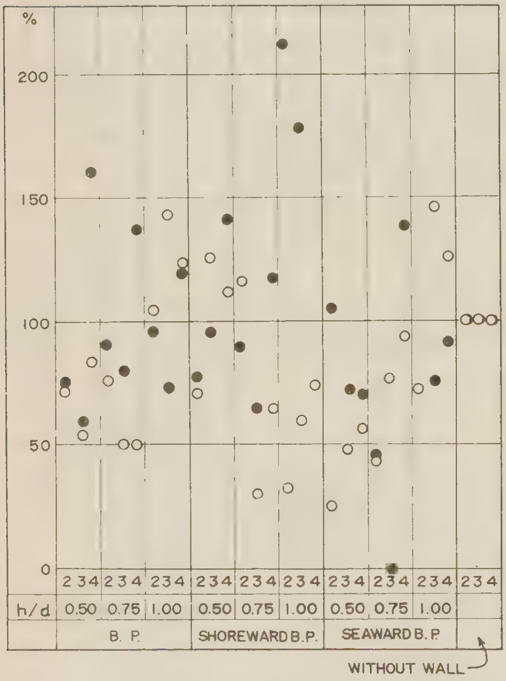

Fig. 15

Trough-like hollows produced shoreward of the wall were much smaller than these with no walls in place. The sectional area of the trough was one third at the largest of that with no wall in place.

It is natural that this magnitude depends on the location and the height of the wall. Troughs were hardly perceivable where walls were placed at breaking point and large h/d. Offshore wall location did not cause depression of the bed near the wall. It moved to the vicinity of the shoreline as secondary for breaking of waves took place there.

Regression of the shoreline from its initial position was observed for any of our experiments. This may possibly be due to the fact that the initial slope was much steeper than that of ordinary existing beach.

Fig. 15 shows the ratio of regression for each run to that of no wall in place. Generally speaking, submerged breakwaters contributed to lessening the recession of the shoreline, but the individual values scattered fairly wide. This may partly be due to sand ples or some irregularity of profiles existing around the shoreline.

One thing to pay attention to is the rise of water level near the shoreline due to the stence of the wall referred in the preceding page, for it makes sea cover more land, thus arging the area eroded by waves. Further study is required in this connection. The bot- slope of actual beach, moreover, is much gentler and often there is a current along the st which may make the application of the experimental results to actual conditions more ficult. Besides, there are other factors such as the concentration of current into the s between or the ends of breakwaters which will be serious to planning and maintenance blems.

Conclusion

(1) In examining the functions of submerged breakwaters, we must take into account their entire effect on beach processes.

(2) Progress of scour with passage of time depends on the location of the wall and the final profile is reached in a relatively short time.

(3) Scour depth vaies widely according as h/d and wall location vary. The deepest relative scour is found for wall location at breaking point and the smallest one for offshore wall location.

(4) Types of correspondence between h/d and the depth of scour for shoreward location differ from those for seaward and breaking point disposition.

(5) Bed in the shoreward vicinity of the wall was never eroded, but rather accreted. This accretion took place rather gradually and indicated the breakwater's function as a sand trap against the seaward movement.

(6) Trough with walls in place were much smaller than those with no wall in place.

(7) Submerged breakwater evidently decreased the regression of the shoreline but we should be careful in its interpretation.

Studies on beach deformation have much difficulties due to variation and complexity factors affecting the phenomena. Construction of an artificial structure will further plicate the matter. It is considered that to further the study purposes the post- aking characteristics of waves, effects of the bed material properites, a seaward low r the wall and change of orbital motion due to the existence of the wall be evaluated e completely. In addition, shape effect of the wall must be examined.

nowledgement

We appreciate the cooperation by Messers H. Tega, K. Akiyama, S. Nunokawa and H. Homma experiment and arrangement of the results. We are also grateful to Mr. K. Horikawa for valuable suggestions.

THE CONSTRUCTION OF A LIGHTED BEACON ON A REEF IN THE OPEN SEA

Yoshio Fujino, Dr. Eng. Director, First Harbor Construction Bureau
Ministry of Transportation

ntroduction

A lighted beacon is one type of aids to navigation erected on isolated shoals or s in the sea. Today, there are 125 lighted beacons along the coasts of Japan, but are located in port and harbor areas, inland seas, or on elevated foundations such mall islands, and it has been considered extremely difficult to construct a lighted on on a reef in the open sea. However, recently, we have succeeded in constructing acon on a reef off the shore of Omaezaki in Shizuoka Prefecture.

The reef, known as "Gozeniwa", is located in the Pacific Ocean three kilometers the shore, measuring 150 m from the east to the west end, and 1,100 m from the north he south end, Though in several sections, the reef stands about one meter above the r level, due to the high wind waves and swells in these waters, it is seldom found e exposed above water.

Past records revealed that very few days of calm weather could be expected to carry onstruction works on the site. Moreover, the completed beacon would be exposed to vigorous force of ocean waves.

These circumstances called for special consideration in determining the type of cture and method of construction.

This paper is a brief account of our study of winds and waves in connection with construction of the lighted beacon and an outline of the design and construction of beacon.

Study of Offshore Waves Generated by Typhoons

In order to determine the maximum height and period of waves in the Gozeniwa waters, erve as a basis for the design and construction of the lighted beacon, we studied wind statistics of outstanding typhoons recorded since the establishment of the zaki Weather Bureau.

Winds of maximum velocity were found among south winds when the center of a typhoon ed the west of Omaezaki in the north or northeast direction.

We studied the records of 583 typhoons which passed this area during the past 67 s up to 1954, we obtained the location of the center of each typhoon when it was at shortest distance from Omaezaki and plotted these positions in quadrants divided by lines perpendicular to each other from east to west and north to south with Omaezaki he center of the axis. We numbered the quadrants clockwise beginning with the heast quadrant as the first quadrant. We obtained the number of typhoons in each quadrant and classified them according to the distance of the center of the typhoon from Omaezaki. Table I gives the frequency of occurrence of these typhoons in the respective quadrant and their distance from Omaezaki.

Table I. Frequency of Occurrence of Typhoons (%)

Distance of center from Omaezaki (Km)	0 - 100	100 - 200	200 - 400	400 - 600	600 - 800	800 - 1000	Total
First Quadrant	1.7	0.7	1.0	0.7	-	-	4.1
Second Quadrant	12.7	10.7	14.1	6.2	2.2	-	45.9
Third Quadrant	1.9	1.9	4.6	4.5	1.4	0.3	14.6
Fourth Quadrant	7.9	7.7	11.3	7.4	1.2	-	35.5

Typhoons which are most disastrous to this area are found among those whose centers approach Omaezaki in the fourth quadrant. Therefore, we studied 18 outstanding tyhpoons which approached Omaezaki in the fourth quadrant since 1891 to obtain their maximum velocity and atmospheric pressure. In ten cases, the velocity exceeded that of typhoon Tess of 1953, and in five cases, the velocity and the center pressure were comparable to those of typhoon Tess. Typhoons of the scale of Tess approached this area five times in 67 years, which corresponds to 1% of the total number of typhoons and the rate of occurrence is once in 14 years.

Observation of waves had been carried on by the Omaezaki Weather Bureau on the shore of Omaezaki from Aug. 1951 to Sept. 1953, and we computed the wave height of offshore waves from the observation data.

Waves of maximum observation values were those generated by typhoon Tess, with a period of 12 seconds.Outstanding typhoons recorded during this period include typhoons Marge, Ruth, Dinah, Jean, and Nina.

We computed the height and period of waves generated by Tess and the other five typhoons according to the Sverdup-Munk method, the results of which are presented in Table 2.

Table 2. Waves of Maximum Dimensions in the Omaezaki Waters

1. Date	Sept. 1934	Oct. 1949	Oct. 1951	Sept. 1953	Sept. 1954
2. Name of Typhoon	Muroto	Patricia	Ruth	Tess	Lorna
3. Maximum Center pressure (mb)	912	940	925	915	950
4. Minimum distance of center from Omaezaki	130	130	170	50	10
5. Direction of maximum wind at Omaezaki	SSW	NNE	SW	SSW	ESE
6. Maximum velocity of wind at Omaezaki (m/sec)	27.9	18.0	23.5	31.6	22.0

Winds which generated maximum waves					
7. Velocity m/sec	25	20	20	23	18
8. Fetch (knot)	450	640	120	230	250
9. Duration (hour)	17	48	10	14	30
10. Distance of decay (knot)	130	620	0	0	50
Waves of maximum dimensions					
11. Wave height of significant waves (m)	8.9	5.7	6.0	9.0	6.0
12. Period of significant waves (sec)	9.9	14.5	6.6	8.0	9.0
13. Travel time	21.18	28.18	15.15	25.21	19.07

When the Bretschneider and Piersen-Neumann-James methods are applied to typhoon Tess, results are as given in Table 3.

e 3. Waves of Maximum Dimensions generated by Typhoon Tess

Basic Theory	Sverdup-Munk	Bretschneider	Piersen-Neumann James
Significant Waves			
Wave height (m)	9.0	9.2	8.4
Wave period (s)	8.0	12.0	4.5 - 12.7

There is a considerable difference among the periods obtained by the three methods, the Bretsneider method seems to be reasonable and the calculated value is in close ement with the period 12 seconds obtained from actual observation.

If we assume the maximum period of waves generated by typhoons to be 12 seconds, we obtain the conditions under which these waves break by applying Iversen's chart, the lt of which is given in Table 4.

e 4. Depth of water and wave height of breakers

Wave height of offshore waves Ho (m)	9	9	9	9	9
Wave period of offshore wave T (sec)	8	10	12	14	16
Wave height of breaker Ho (m)	8.0	7.9	8.3	8.7	8.7
Depth of water hb (m)	13.1	10.3	10.0	10.0	10.8

The waves break in the vicinity of Gozeniwa where the water depth is over 10 m and wave height reaches 80 - 8.7 m. However, as the water depth within the Gozeniwa area is estimated to be 9 m, offshore waves do not directly reach this area. Waves his area would retain the maximum period of offshore waves, but the wave height be limited by the water depth. Table 5 gives the maximum dimensions of waves breaking in waters with depths of 9 m obtained from Iversen's chart. These waves may be considered to be of the maximum height within the reef area.

Table 5. Waves of Maximum Dimensions in Water Depths of 9 m

Water depth hb (m) Period T (sec)	9 8	9 10	9 12	9 14	9 16
Wave height of offshore waves Ho (m)	7.1	7.8	8.0	7.7	7.2
Wave height of breakers Hb (m)	6.2	7.2	7.8	8.0	7.8

III. Investigation of Waves in the Reef Area

In view of the difficulty in analyzing the condition of waves within the Gozeniwa reef area, we made a qualitative analysis of the characteristics of waves generated by typhoons such as Tess which attacked Gozeniwa from the southern areas at 1 P.M. April 18, 1956 by means of aerial photographs. (See Fig. 1)

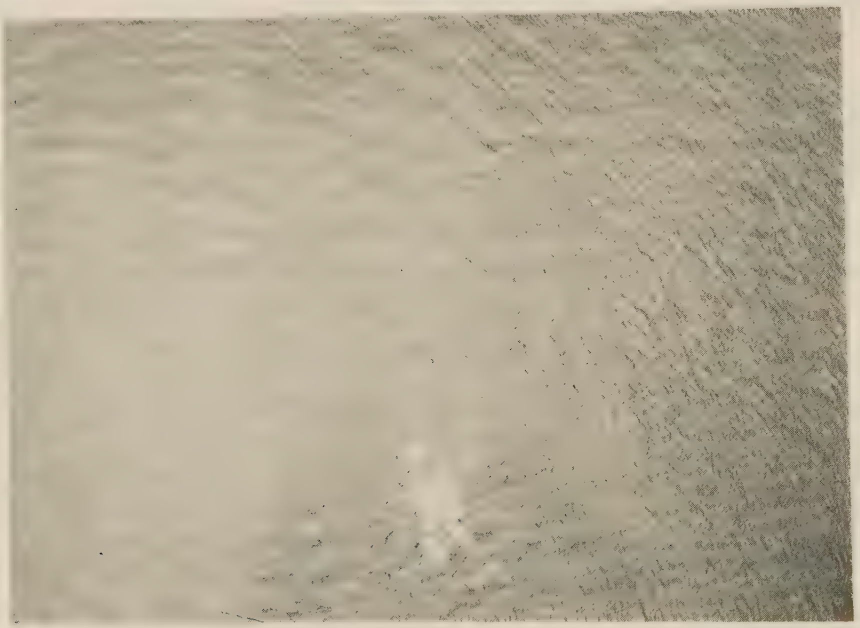

Fig. 1 Aerial Photograph of Waves in the Gozeniwa Waters

The following facts were revealed by the photographs.

(a) Offshore waves from the southern seas interfere with each other before they reach the Gozeniwa reef and no longer possess the form of offshore waves at the northern end of the reef. However, they maintain the wave period of offshore waves.

(b) From the reflection of the sun rays, it may be assumed that the wave height is highest at the southern end and decreases as it travels northward.

(c) Around the northern end of the Gozeniwa reef, there is an interference of waves which may produce choppings.

(d) Therefore it would be advisable to select a locality in the northern part of the reef where the wave force has been reduced as the construction site of the lighted beacon.

. Wave Height and the Design of the Lighted Beacon

The lighted beacon was decided to be constructed on the northern end of the reef in ew of the above factors. The maximum height of waves in this locality depends on the pth of water. However, in this case, we must consider the tidal range and extraordi- ry rise of water as well as the average water depth of the area.

The water depth at this locality is -6 m on the chart and the tidal range is 2.0 m. times of typhoons, assuming that the decrease in atmospheric pressure would be 100 s, and the extraordinary rise of water would be 10 m at the most, the maximum water pth at the site of construction would be 9.0 m.

If we determine the wave period of maximum waves to be 12 seconds according to ble 3, the maximum wave height in this locality would be Hb = 7.8 m. This figure was opted in the design of the substructure of the lighted beacon with due consideration r the interference of waves and choppings generated by typhoons.

Construction Works and Meteorological Conditions

The number of calm days which would be available for construction works on the sea re studied as a basis of determining the design and method of construction.

The standard for determining whether it is possible or not to carry on the operation works on the sea differs greatly according to the type and nature of work and the sign of the structure, and Glenn of America has carried on an investigation in this eld. According to his studies, in regard to works on lighted beacons, generally, wave ights of 2 ft or 0.6 m mark the limiting point of conducting operations on the sea. we compute the wind velocity in this case from a formula for the relationship of wind locity and wave height, V = 3.3 m/sec, belonging to Grade 2 in the wind force order.

We calculated the number of calm days to be expected for construction works on e sea by the following methods.

1. The number of calm days available predicted form the duration of weak winds.

Wind velocity and wave height are decisive factors in determining whether the conditions are suitable for works on the sea or not. However, as data on the wave height at Gozeniwa were not available, we calculated the number of calm days from the duration of weak winds and obtained results as shown in Table 6. Most favourable conditions were found in July and August, but it is extremely difficult to expect calm weather to continue over 48 hours.

Table 6. Duration of Winds below Wind Force Order 2 (3.3 m/sec)

Hours Month	0 - 5	6 - 10	11 - 15	16 - 20	21 - 25	26 - 30	31 - 35	36 - 40	41 - 45	46 -
1	24.8	5.9	1.5	1.0	0.3	0.1	0.3	0.1	-	-
2	32.6	4.3	1.5	0.5	0.3	0.2	-	0.1	-	-
3	34.4	6.8	2.1	0.9	0.1	0.1	-	-	-	-
4	35.9	6.8	3.8	1.8	0.1	0.2	-	0.3	-	-
5	32.4	7.8	4.4	3.3	0.8	0.2	0.1	0.2	0.1	0.1
6	30.7	7.7	3.7	1.8	0.5	0.3	0.1	-	0.1	0.1
7	30.7	7.3	4.3	4.5	0.8	0.3	0.2	0.1	-	-
8	36.0	6.2	6.3	4.7	0.7	-	0.2	0.1	0.1	-
9	37.4	6.7	5.5	2.5	0.7	-	0.1	0.1	-	-
10	37.2	8.4	3.3	0.8	0.5	0.2	-	-	0.1	-
11	35.8	6.5	2.5	1.1	0.2	0.2	-	0.1	-	-
12	23.9	4.2	2.0	0.6	0.2	0.1	0.1	-	-	-

2. The number of calm days available determined from the analysis of wave height and wind velocity.

In order to determine the number of calm days available from the point of wave height as well as wind velocity, we analyzed the statistical data from observations carried on during the past 4 years, at 24 lighthouses throughout the country. We picked out the calm days when the wind waves, swells and wind velocity belonged to Grade 1 or 2 in each water zone and season. On the Pacific coast, the number of calm days when both wave height and wind velocity were in favorable condition was 70% of the number of calm days determined by wind velocity alone.

Hence, with reference to Table 6, we may forecast the number of calm days available for construction works in the Gozeniwa waters.

On the other hand, if it is assumed that a wave height of 0.5 m recorded in the wave observation in the Omaezaki harbor is the maximum limit for the operation of works on sea, the maximum wind velocity in this case would be 7.9 m/sec, slightly stronger than desirable. Calm days with wave heights and wind velocity below these values are given in Table 7. In July, there are the largest number of calm days, the maximum being 10 days, and May, June, September and April follow in order with the number of calm days. In August the number of calm days varies greatly each year due to the attack of typhoons in this month.

Table 7. Number of Days of Calm Seas (Max. wind velocity 7.9 m/s)
(Max. wave height 0.5 m)

Month Year	Jan.	Feb.	March	April	May	June	July	Aug.	Sept.	Oct.	Nov.	Dec.
1951	-	-	-	-	-	-	-	3	5	1	1	4
1952	1	0	1	3	5	4	9	11	8	0	0	1
1953	0	3	2	9	9	10	9	0	6	-	-	-
Average	0.5	1.5	1.5	6.0	7.0	7.0	9.0	3.6	6.3	0.5	0.5	2.5

3. Forecasting the number of calm days from the weather chart.

Selecting cases when favorable wind velocity and wave height continued for more than 48 hours, we studied the pattern of the weather chart in each case and obtained the following conclusions.

(a) Construction works on the sea should be carried on during the period from April to September, of which July will be the most favorable month.

(b) As a rule, favorable weather may be expected when variable high atmospheric pressure or the north Pacific high atmospheric pressure overlies the area.

(c) The cold front extending from the south to north, and high atmospheric pressure traveling at a high velocity are apt to bring unfavorable weather.

. The Substructure of the Gozeniwa Lighted Beacon

The substructure of the lighted beacon to be constructed in the open sea was bound various restrictions from the standpoint of designing and method of construction.

(a) The structure must be of sufficient strength to withstand the vigorous force of ocean waves.

(b) The principal part of the construction works must be carried on at the work base so that works on the sea will be limited and simple.

(c) Works on the spot must be completed in a short period of time.

(d) Each unit of work on the spot must be completed within one round of continuous calm weather, and the completed portion must be able to withstand the attack of minor storms until the next round of continuous calm weather when works will be undertaken again, gradually increasing the stability of the structure with each unit of work.

A braced cylinder type tripod structure as shown in Fig. 2 was adopted as the substructure to meet the above conditions.

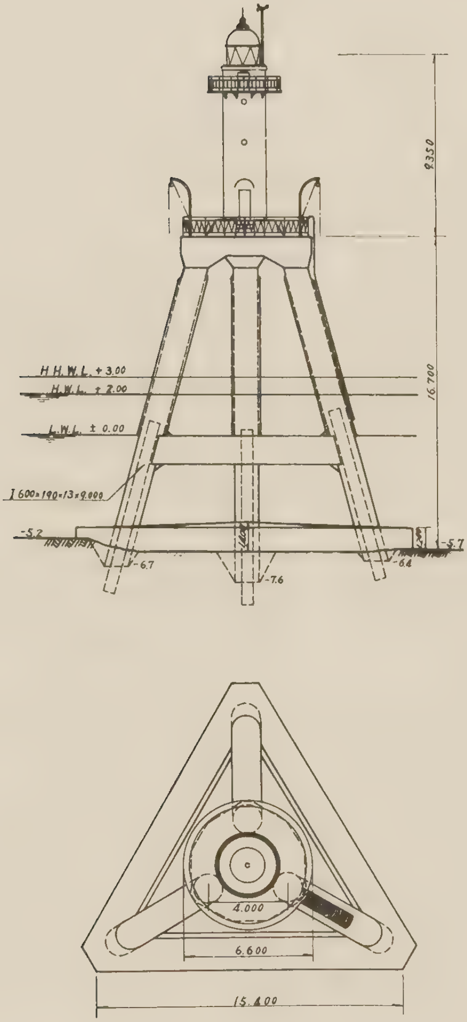

Fig. 2 The Gozeniwa Lighted Beacon

The body, with a platform, was assembled at the base, launched in water and towed e site of construction where it was fixed on the reef 6 m under the water level, rovided to withstand swells of 1 meter.

Then I type steel piles were driven into the reef through the cylinders to stabilize tructure to withstand swells of 2 - 3 meters.

The cylinders were then filled with concrete, and prepact concrete was cast around hree cylinders at the base to form a triangular body, one side of which measures m to a height of 1.8 m, firmly adjoining the structure to the bed rock.

Theories of Wave Pressure exerted on Lighted Beacons

Theories of wave pressure exerted on submarine structures may be divided into two categories, wave pressure on vertical walls, and wave pressure on cylindrical s. Wave pressure exerted on lighted beacons may be classified in the second category.

Theory of wave pressure on cylindrical bodies

Recently, with the development of new theories, various experiments have been conducted on computing the wave force acting on cylindrical bodies in water.

Generally, friction drag F, and inertia drag F_2 act on d_z a portion of a cylindrical body in fliud.

When these two are represented by F.

$$F = F_1 + F_2 = \tfrac{1}{2}\rho C_D D u^2 d_z + CM \rho \frac{\pi D^2}{4} \frac{\partial u}{\partial t} d_z \text{ .... (1)}$$

C_D : drag coefficient

C_M : inertia coefficient

D : diameter of cylindrical body

u : lateral velocity of water particles

ρ : specific weight of water

The coefficients C_D, C_M vary according to the motion of water on the cylinder, and may be considered to be constant for each part of the cylindrical surface.

The maximum moment does not occur at the wave crest but at a point with an angle displacement   from the crest.

$$= \sin^{-1}\left[\frac{\pi}{8} \frac{C_M}{C_D} \frac{D}{H} \frac{\{K_1 - (d + Z) K_4\}}{\{K_2 - (d + Z) K_3\}} \right] \text{ .... (2)}$$

K_1, K_2, K_3, K_4 are functions of Z only.

When the water depth d is relatively small compared to the wave length L, or when the diameter of the cylinder D is small compared to the wave height H, the value of B approaches zero. On the other hand, when d/L and D/H are large values, the value of B approaches 90°. The values of C_D, C_M are determined by the wave curve and moment-time curve.

Experiments of J. R. Morison

Morison erected a cylindrical structure in water and conducted observational experiments on offshore waves, swells starting to break, breakers, and breakers with some foam, and obtained the values of the drag coefficient C_D (See Fig. 3)

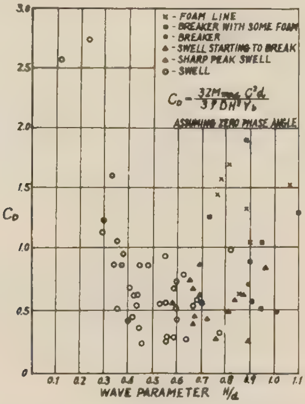

Fig. 3 Variation of C_D in relation to H/d

The experiments were conducted under the following conditions:

$D = 0.3$ ft.

$H = 8 - 13$ ft.

$T = 8 - 12$ sec.

$d = 3 - 5$ ft.

Therefore D/H and d/L were both small values and may be assumed to be almost zero.

Hence $C_M = 0$,

and B was not actually obtained in the experiment.

According to the diagram, the value of C_D is greater in the case of breakers compared to swells, indicating a value close to 1.0. Strictly speaking, this theory is not applicable to breakers, but actually, the results are in close agreement with the general conditions when breakers act on lighted beacons, and it may be considered to be an outstanding experiment in this field.

3. Resistance force of cylindrical bodies in steady flow

Generally, the pressure exerted by waves on cylindrical bodies in steady flow may be represented by the first term in equation (1) from which the drag coefficient C_x may be obtained. C_x is determined by the Reynold number (R_e) only, and it shows a sharp decrease and reaches a transient state when,

$$R_e = 3 - 5 \times 10^5$$

but enters a steady state after it passes this point.

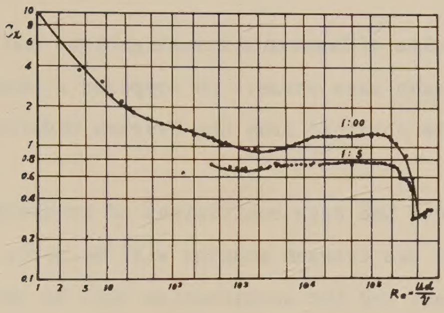

Fig. 4 Drag Coefficient of Cylindrical ·Bodies in Steady Flow

When we compute the value of the Reynold number in the case of J. R. Morison's experiment, the value obtained is within the transient state, and a wide scatter may be observed in the value of C_D.

In the case of lighted beacons, we apply the **formula** $R_e = 10^6 - 10^7$, and the value of C_x may be assumed to be in a steady state.

4. Lateral force exerted by waves on concrete **blocks** on the sea bed.

T. Hamada has conducted **experiments** on the pressure exerted on concrete blocks on the sea bed in shallow water and breaking points.

In the case of swells, the inertia coefficient is of a considerably large value and in the case of breakers, it is 20% - 40% of the drag coefficient. When x is the length of one side of the block,

$$x/H = 0.5 - 1.0$$

However, in the case of lighted beacons, it is generally,

$$D/H = 0.1 - 0.2$$

If a similar experiment were conducted on a lighted beacon, the inertia coefficient would most likely be of a **negligible** value.

5. Computation of the wave force on pier piles

Munk has computed the wave force on a cylindrical pier pile off the shore of Scripps Institute. He has computed the wave pressure exerted by breakers by the solitary wave theory with $C_D = 0.33$.

However this computation involves some questionable points.

(a) As the behavior of breakers differ from steady flow, even when $Re \fallingdotseq 5 \times 10^5$, the drag coefficient should be **greater** than $C_D = 0.33$.

(b) Though $C_D = 0.33$ may be applicable to the drag coefficient at the crest of the waves, as the water particle velocity distribution varies along the vertical surface there is some question in giving a constant value for C_D.

(c) There should be some consideration for the sharp increase in wave height when breakers or waves impinge on the front of the structure.

6. Theory of R.Curtis Cooke

Cooke applied the results of **Iversen's** investigations and proved that the values of C_D and C_M differ for each wave phase. He proposed a common drag coefficient C and proved that C may be obtained from the Iversen Modulus and the Reynolds number.

However, when we compute the drag coefficient of breakers by the solitary wave theory, the value of the Iversen modulus will be zero, as the water particle velocity reaches a maximum, and the acceleration will be zero. Hence the drag coefficient will be determined by the Reynolds number alone.

7. Summary of theories of wave pressure on lighted beacons

From the study of various theories and experiments on wave pressure exerted on cylindrical bodies, we have obtained a satisfactory approximation to the wave pressure exerted by breakers on lighted beacons.

The inertia coefficient may be disregarded. On the other hand, it has been proved through experiments that the vertical distribution of wave **velocity** at the breaking point closely resembles that at the limit of breaking according to the solitary wave theory. R. L. **Wiegel** has also reported similar results from his experiments.

Therefore, the pressure exerted by waves on lighted beacons may be said to be determined by the resistance force of a cylindrical body exposed to the pressure of solitary waves at the limit of breaking.

When the pressure exerted by waves on a lighted beacon is F_o,

$$F_o = \frac{1}{2} \rho C_b \int D u^2 \, dZ$$

With reference to the experiments of J. R. Morison, allowing a sufficient margin for safety, we assumed that,

$$C_D = 1.0$$

in our computation.

VIII. Conclusion

I have presented a brief account of the design and construction of a lighted beacon on an isolated reef in the Pacific Ocean.

However, in regard to the vertical wave pressure exerted by choppings on submarine structures, I have merely presented problems yet to be solved, and there is also much to be explored on theories on wave pressure on cylindrical bodies.

Nevertheless, I hope that our technical approach to the problem of planning and constructing a structure in the open sea, stepping into a hitherto undeveloped field, will serve to promote the development of engineering in this field in the future.